Copyright Warning & Restrictions

The copyright law of the United States (Title 17, United States Code) governs the making of photocopies or other reproductions of copyrighted material.

Under certain conditions specified in the law, libraries and archives are authorized to furnish a photocopy or other reproduction. One of these specified conditions is that the photocopy or reproduction is not to be "used for any purpose other than private study, scholarship, or research." If a, user makes a request for, or later uses, a photocopy or reproduction for purposes in excess of "fair use" that user may be liable for copyright infringement,

This institution reserves the right to refuse to accept a copying order if, in its judgment, fulfillment of the order would involve violation of copyright law.

Please Note: The author retains the copyright while the New Jersey Institute of Technology reserves the right to distribute this thesis or dissertation

Printing note: If you do not wish to print this page, then select "Pages from: first page # to: last page #" on the print dialog screen

ABSTRACT

Vibratory Size Segregation of Particulate Matter

by
Anthony La Rosa

Size segregation imposed by vibration or shaking is an ubiquitous phenomenon whereby a large particle will rise to the top of a bed of smaller spheres upon vibration. Several mechanisms based on computer simulations have been proposed, however a complete theory remains elusive. The objective of this study was to perform experiments to study vibratory segregation of particles for varying size ratios and vibration parameters. More specifically, the rise time of a sphere from the bottom to the top of a vibrated bed was examined. It was found that the rise time decreased with an increase in amplitude for fixed frequencies. In addition, an increase in frequency led to a decrease in rise time for fixed amplitudes. Also, particles of all diameter ratios, including unity, rose to the top of the vibrated bed. Large diameter ratios showed a decrease in rise time when compared to that of smaller diameter ratios. It was found that convective flows within the vibrated system have a strong influence on the rising particles. Based on these findings, conclusions were drawn which lead to a hypothesis explaining the difference in rise time for different diameter ratios in a vibrated bed.

VIBRATORY SIZE SEGREGATION OF PARTICULATE MATTER

by

Anthony La Rosa

A Thesis
Submitted to the Faculty of
New Jersey Institute of Technology
in Partial Fulfillment of the Requirement for the Degree of
Master of Science in Mechanical Engineering

Department of Mechanical Engineering

October 1993

APPROVAL PAGE

VIBRATORY SIZE SEGREGATION OF PARTICULATE MATTER

Anthony La Rosa

Dr. Anthony D. Rosato, Thesis Advisor (date)
Associate Professor of Mechanical Engineering,
New Jersey Institute of Technology

Dr. Rajesh N. Dave, Committee Member (date)
Associate Professor of Mechanical Engineering,
New Jersey Institute of Technology

Dr. Ian S. Fischer, Committee Member (date)
Associate Professor of Mechanical Engineering,
New Jersey Institute of Technology

BIOGRAPHICAL SKETCH

Author: Anthony Joseph La Rosa

Degree: Master of Science in Mechanical Engineering

Date: October 1993

Undergraduate and Graduate Education:

- Master of Science in Mechanical Engineering,
  New Jersey Institute of Technology, Newark, NJ
  1993

- Bachelor of Science in Mechanical Engineering,
  New Jersey Institute of Technology, Newark, NJ
  1992

Major: Mechanical Engineering

This thesis is dedicated to my fiancée Linda for being so patient.

ACKNOWLEDGMENT

I would like to thank Dr. Anthony Rosato for his suggestions and direction pertaining to the topic of this thesis. In addition, I express gratitude to Dr. Rajesh Dave and Dr. Ian Fischer for helping me fill in all the blanks. Also, many thanks to Joey, Dave, Huey, Jerry, Bhaswan, Terry, Andy and Joe for their technical support. Finally, I would like to thank my family for seeing the light at the end of the tunnel.

TABLE OF CONTENTS

LIST OF TABLES

Table **Page**

LIST OF FIGURES

Figure **Page**

Figure **Page**

CHAPTER 1
INTRODUCTION

Particulate matter size segregation imposed by vibration or shaking has been an observed phenomenon that has long plagued the granular materials handling industry. Though much effort has been exhausted to reduce particle segregation, little is known about its nature. Various mechanisms of segregation have been identified, but a consistent theory still remains elusive. In this study, segregation induced by vibration was examined experimentally.

1.1 Literature Survey

To date, research in this field involves the formulation and identification of mechanisms that contribute to particle size segregation. In the context of this work, size segregation is the resulting separation of different size particulates in a granular mixture caused by mechanical processes such as pouring, mixing, vibration, and shearing. The processes listed, though diverse, all rely on one major factor, i.e., particle size difference [Olsen and Rippie, Williams (17,29)]. Although segregation may be desirable in some applications, it is generally problematic where homogeneity of a granular mass is required. The main avenues used to explore this field are through observation, experimentation and computer simulation. This phenomenon was first observed in nature in the form of avalanches [Shreve (25)]. Later, it was studied experimentally in vibrated beds [Brown (4), Olsen & Rippie (17), Williams (29,30), Ahmad & Smalley (2), Jaeger and Nagel (14)]. More recently, computer simulated segregation models have been examined [Meakin (12,13), Rosato (21,22,23), and Haff & Werner (10)].

Segregation occurring from the pouring of materials having size discrepancies is well known [Weidenbaum (28), Brown (4)]. When a material containing different size particles is poured into a heap, the larger particles have a greater tendency to roll down the inclined sides of the heap, while the smaller particles tend to stay in the core of the formed cone-shaped heap. This occurrence has significant implications in the materials handling industry. Frequently, homogeneous mixtures are released onto conveyors in heaps for transport where some degree of segregation occurs regardless of previous preparation (mixing).

Mixing is an anti segregation process used in the granular materials industry to force homogeneity. However, the mixing process may lead to unmixing [Williams (31,32)]. Mixing can produce temporary equilibrium where homogeneity exists; but this situation changes as mixing continues. Williams explains this by considering a granular mixture in which the large spheres lie at the bottom of the bulk. In such a sample, mixing will force the larger spheres to the top. Thus, at some point during their movement towards the top they will reach a near perfect quality mix. Lacey [15] postulated three basic mechanisms of mixing: convective, diffusive and shear mixing. The convective mixer is classified as non-segregating while the shear and diffusive mixer are segregating mixers. The non-segregating mixers rely on the motion of material while segregating mixers rely on surface effects (tumbling). In the material handling process, it is essential to keep mixing as a last step.

In addition to pouring segregation, vibration and percolation also counteract the mixing process during material handling. Percolation is the process by which smaller particles sift through the gaps between large particle in a granular mixture under the influence of gravity. In a study by Bridgewater [24], percolation was observed in binary mixtures where the percolation rate was determined by the aspect ratio. A larger aspect ratio gave more percolation than a smaller aspect ratio with the same

strain. This mechanism is self-evident, however when size discrepancy diminishes in the aspect ratio and sifting cannot occur, vibration can promote size segregation. Indeed, single large particles have been made to rise in a vibrated bed of comparably smaller spheres [Olsen & Rippie (17,19)]. In this study, segregation induced by vibration is studied.

Williams [29] observed the segregation of a large particle by vibrating a bed of comparably smaller spheres. It was found that the large sphere rose even when it was more dense then the bed spheres. Segregation of a larger sphere of a lesser density was explained by buoyancy. However, segregation still occurred when the density of the larger spheres was greater than that of the surrounding bed. Williams hypothesizes a pressure differential as an explanation for this occurrence. The pressure beneath the large sphere must be great enough so that the smaller spheres below it experience no movement. Thus, if the spheres surrounding the large sphere cause an upward movement of the large sphere, the spheres below the large sphere will support the large sphere from falling by flowing beneath the large sphere and holding their position. After obtaining a certain height, the pressure drops and the large sphere can no longer lock the smaller spheres beneath it. A continuous series of such moves can be compared to that of a ratchet. However, this mechanism does not explain why less dense spheres also rise in a vibrated bed. Also, wall effects were not considered by Williams.

Similar experiments, though more extensive, were carried out by Olsen & Rippie [17]. Here segregation of a binary system was examined. The segregation of glass and steel spheres ranging from 3/32" - 1/4" diameter were examined in a 3/4" diameter by 6" high cylinder. It was found that segregation of the systems lead to an equilibrium state described by first-order kinetics. In addition, segregation rate (determined by the method of least squares from the kinetic data) was found to be

influenced strongly by size ratios. Experiments were carried out at a frequency of 17.1 Hz and 0.100 inch amplitude with various binary combinations. However, no correlation between frequency of vibration and segregation rate was made. Moreover, wall effects were completely ignored. The diameter of the cylinder in the experimental set-up was small, at best only eight diameters compared to that of the bed particles, which could quite possibly affect packing and consequently affect segregation.

Later, Ahmad and Smalley [2] studied the segregation rate of a single large particle system. They sought factors which influenced the process. A list of parameters including initial position, frequency, bed acceleration, bed depth and particle size, shape and density were examined in a system similar to that of Williams. Here the aspect ratio between bed particles and the large sphere was large, about 20:1. As in most other investigations, particle size was found the most influential factor. More interesting, acceleration was found to be a critical variable. It was found here that segregation time is inversely proportional to acceleration. That is, for fixed frequencies, segregation time decreased with acceleration increase.

Parsons [18] studied the effects of vibration on the particle size distribution. Experiments performed on granular coarse mixtures, were an attempt to simulate, in a controlled manner, the handling which occurs during material transport. Segregation was present within a wide distribution with fines sifting or percolating. Conversely, narrow particle size distribution led to little difference or segregation.

Jaeger and Nagel [14] conducted experiments similar to those previously mentioned. Here the segregation of a single large glass bead through a bed of smaller beads under vibration was examined. Unlike previous studies, the mechanism of segregation was identified as convection rather than the geometric mechanism of particle rearrangement and piling [12,7,21,22]. It was found that upon vibration, a symmetric convective flow was produced throughout the bed. It is on this flow that

particles larger then the convective zone are pushed upward. When the convection was eliminated from the experiment, no segregation occurred. In addition, variance in the segregation rate was based on bed depth rather then particle size difference.

Simulations have also been put forward to explain the mechanism of segregation. Rosato [19,20] used a modified Monte Carlo simulation in attempt to isolate several parameters which influence segregation, i.e., particle size ratios and shaking amplitude. Results from the simulation showed that size differences among the particles, modeled as disks, created voids beneath the large disk under vibration. The voids created would be filled by the smaller disks which in turn cause the large disk to rise in the bed. In addition, increasing the shaking amplitude increased the segregation rate of the large particle in qualitative agreement with those found in previous experiments [Ahmad and Smalley (2)].

In a simulation done by Jullien, Meakin and Pavlovitch [12], a random packing of two or more different size spheres is generated using the model and algorithm of Visscher and Bolsterli [27]. In a manner analogous to Rosato [21], particles are initially packed and arranged in ascending height of their centers. The mixture is uniformly lifted and then allowed to repack, thereby simulating shaking. Each packing is allowed to come to rest before the next packing or "shake". It was found that segregation rate increases with increase in particle size difference up to a critical size ratio. The monotonic motion found was explained via an analytical model involving the angle of repose as a parameter. This was deduced by assuming that a conical region is formed tangent and below the large sphere during shaking. This void is then filled by smaller spheres during vibration, thus providing the upward motion. The segregation rate is determined by the displacement after a shake. The outcome of the simulation produced a geometric explanation of the segregation in agreement with Rosato [21] while also postulating the existence of a critical size ratio.

Using both experimentation and simulation, Duran et al [7] examined segregation due to vibration. Here a 2-D cell filled with a granular medium, consisting of many small disks and a single large disk, was used. It was found that under induced agitation (step-by-step lifts) the large disk created a void in the medium. The large disk then comes to rest and is either supported by the underlying discs or by a few surrounding disks in a "vault" situation leaving a void beneath the large disk. In turn, the large disk gets lifted when the surrounding supporting disks slip into the void beneath the large disk caused by additional agitation. This is termed the "arching" model from which an algorithm was founded. Contrary to previous simulations [Jullien et al. (12) and Rosato et al. (21)], avalanching was used as the result of the particle ascent rather then the cause. The results of the simulation produced a critical size ratio for segregation which is in agreement with Jullien [12]. In addition, it was found experimentally that a large sphere in a smaller mass will segregate at a constant rate while a smaller sphere will have intermittent motion which is supported by the arching model.

Haff and Werner [10] also used computer simulation to study segregation. Here a 2-d system of inelastic frictional discs was studied. A single large disk was placed on the bottom of a bed of similar smaller discs. Under induced agitation, a harmonic oscillation in both the vertical and horizontal directions, the large particle moved towards the top of the bed. The principal mechanism for segregation was attributed to shear driven rotational motion. The rolling motion of the large particle caused it to move up and over adjacent smaller particles. Since the segregation here was caused by shear induced by the friction between particles, frictionless particles would not have this rotational motion and therefore could not segregate.

In addition to the above mentioned mechanisms, other parameters which affect segregation have been examined, such as static electricity. It has been found that an

increase of static charge in particulate systems eliminates or reduces to some degree the rate of particle interaction [Abouzeid and Fuerstenau (1), Boland and Geldart (3)]. Through experimental means, Bolan and Geldert found that varying the relative humidity of the examined system altered the static electricity discharge. This discharge in turn produced notable changes in segregation rate. In general, lower humidity allowed for greater static build-up which decreased with higher humidity. A median humidity, one which allowed repeatability of results, was found at 60%. Too much humidity, (above 70%), had an inverse effect because of moisture build up. The addition of moisture produced cohesiveness and agglomerates formed which subsequently affect particle movement.

It is clear from the above that this field needs further investigation. The approach in this effort is experimental. The experiments in this study will be mainly concerned with the segregation time and rate, based on a mean velocity, of a large sphere through a bed of vibrated smaller spheres. For four fixed frequencies, a variety of amplitudes and size ratios will be examined. In addition, the influence which convective currents produce during vibration will be examined. Also, wall effects will be investigated to understand their contribution to vibratory segregation.

1.2 Motivation

The driving impetus behind this study is to gain further insight into the phenomenon of particle segregation through experimentation. More specifically, the author sought an understanding of effect and the degree of effect that various parameters have on vibratory segregation. Alternatively, it is hoped to gain knowledge in the field to advance the methods used in industry from trial and error to a science.

1.3 Outline of Chapters

Chapter 2 describes the experimental procedures and the angle of repose results for the material used in the experiments. In addition, the significance and the role of the angle of repose in the study will be discussed. In Chapter 3, the experimental methods used to determine the segregation rate will be described as well as the experimental setup. The experimental data will be presented and analyzed in Chapter 4. Finally, in Chapter 5, conclusions and summaries drawn from the study will be presented, as well as practical considerations for future experiments.

CHAPTER 2
THE ANGLE OF REPOSE

The angle of inclination of a heap of granular material between its surface and the horizontal is known as the angle of repose. The angle of repose is considered to be a measure of the flowability of the granular medium and is thus a property of the material. This angle for the material used in the experiment is obtained since it has been postulated to have a strong effect on particle size segregation. [Meakin (12)]

2.1 Experimental Setup

There are various experimental methods for determining the angle of repose. Six such methods are described by Grey [8]. However, there is controversy as to which angle gives the "correct" measure of the angle of repose. In this experiment, three different methods were employed for comparison purposes. All results presented here were based on a minimum of ten test runs (see Appendix C). The first method involves the pouring of the 1/8" diameter acrylic spheres into a 2-7/8" diameter cylindrical container from which the naturally formed heap is studied (see Fig. 1). Using the Pulnix TM-7CN camera, the image of the heap was captured using AFG (Advanced Frame Grabber) and down-loaded into a PC where the image processing was done using the Visilog (image processing software) library of routines. Here the captured grey-level image was processed and saved to a file as binary edge data. The file was then loaded onto a Sun Sparc 2 workstation where the binary edge data was converted by means of a filter to x-y format. The converted image was then plotted using Templegraph* , a software plotting package. A linear fit was obtained using Templegraph which then gave the slope of the heap and hence the angle of repose (see Appendix C for a

* Templegraph, Mihalisin Associates Inc. 1992.

Figure 1 Cylindrical setup for the determination of the angle of repose by pouring.

complete listing or Figure 2 for an example). An alternate method using a robust fitting technique [6] was utilized to fit the data. The results found here were not significantly different than those obtained from Templegraph (see Table 1). From these experiments, the angle of repose (Θr) of the acrylic spheres via the heap method was 30.04°+/- $.72^\circ$ (see Table 1).

An angle of repose was also determined from a rotating drum experiment. The setup consisted of miniature lathe, Jensen Model 334B400, fitted with a 2-3/4" diameter acrylic cylinder (see Fig. 3a). The face of the cylinder that was chucked to the lathe was opaque while the opposing surface was clear for visual purposes (see Fig. 3b). The lathe was rotated at various rpm's until the 1/8" diameter acrylic spheres reached a state where visual inspection of the formed heap was possible. At this point the dynamic heap angle was captured, processed and analyzed in the same manner as described above. Here the angle of repose was found to be 34.70°+/-1.37° (see Table 1).

Finally, the angle of repose was determined by means of draining a rectangular acrylic box. The box was constructed with three rigid sides and an adjustable fourth side (see Fig. 4). The fourth side placement could be varied in the vertical upward direction, thus allowing for an opening in one side of the box. The box was then filled with the spherical medium and drained through an opening, approximately five times the sizes of the spheres. Once again the angle of the material left after draining was captured, processed and analyzed so that the 2-D slope could be determined. Here the angle of repose was found to be 32.23°+/-1.04° (see Table 1).

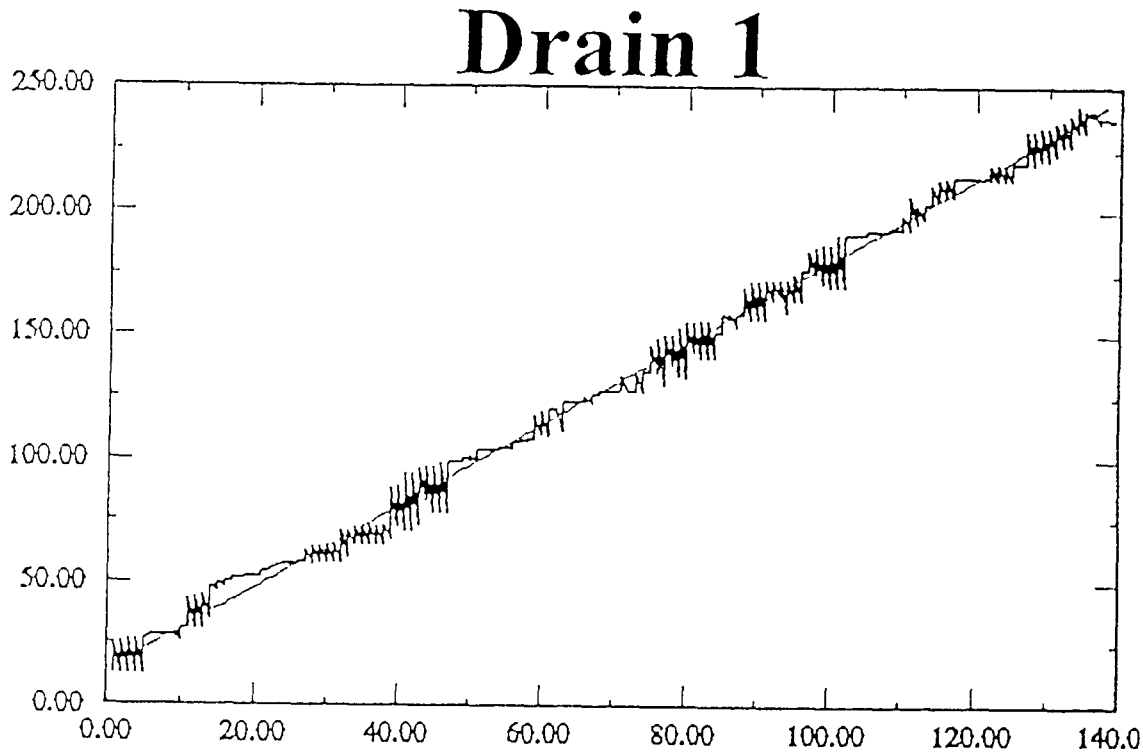

Linear (Y = aX+b) fit of Curve 1 from x = 0 to x = 137.75:
a = 1.65566 +/- 0.00668593 b = 14.6002 +/- 0.522008 Chi-square=15590.7
Linear correlation coefficient: 0.996103; Probability of correlation: 1

Figure 2 Sample of generated plot for angle of repose data.

Run Type	Avg. Θ_R (Templegraph)	Avg. Θ_R (Alt. Technique[6])
Poured Angle of Repose	30.04^{o}+/-$.72^{o}$	29.99^{o}+/-$.76^{o}$
Dynamic Angle of Repose	34.70^{o}+/-1.37^{o}	NA
Drained Angle of Repose	32.23^{o}+/-1.04^{o}	NA

Table 1 Summarized Angle of Repose Data.

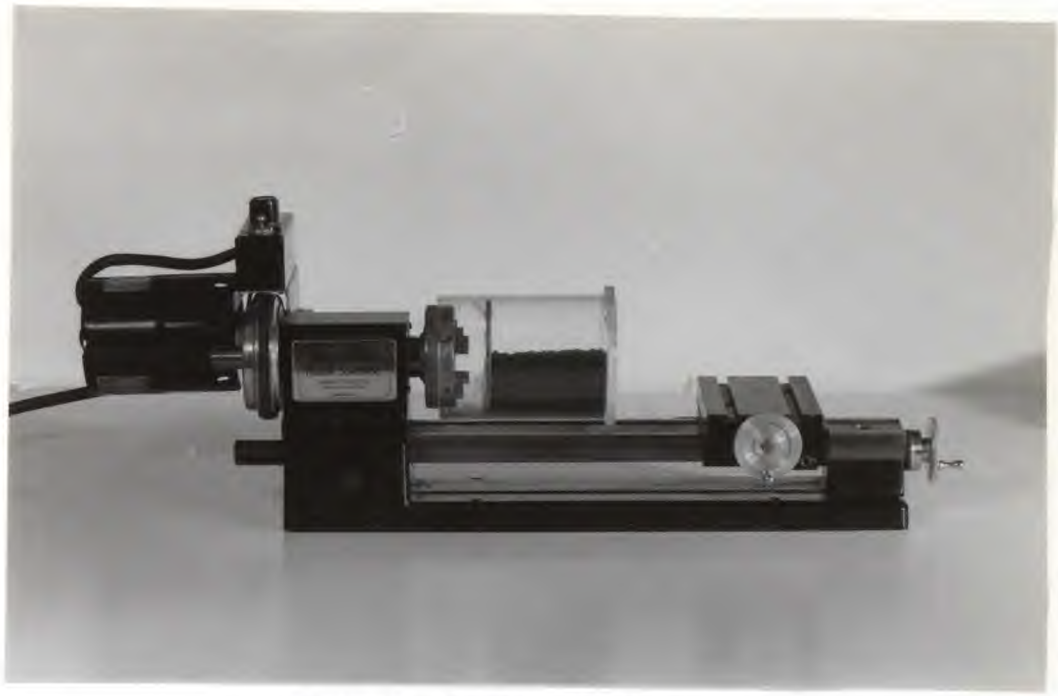

Figure 3a Miniature lathe apparatus.

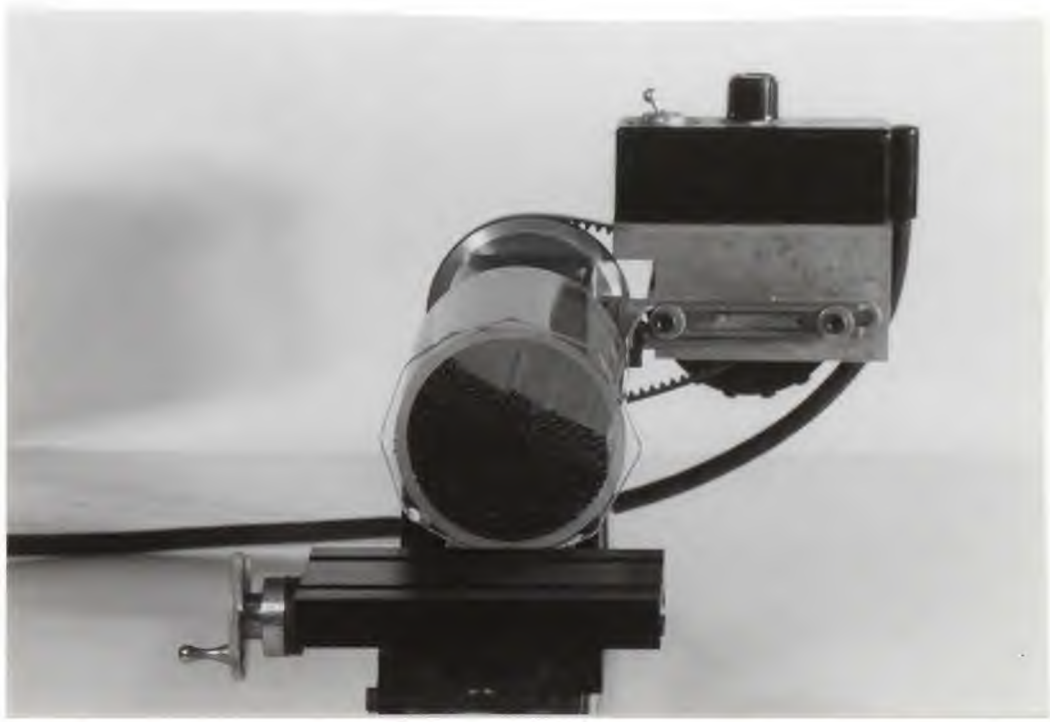

Figure 3b Miniature lathe apparatus for determining the dynamic angle of repose.

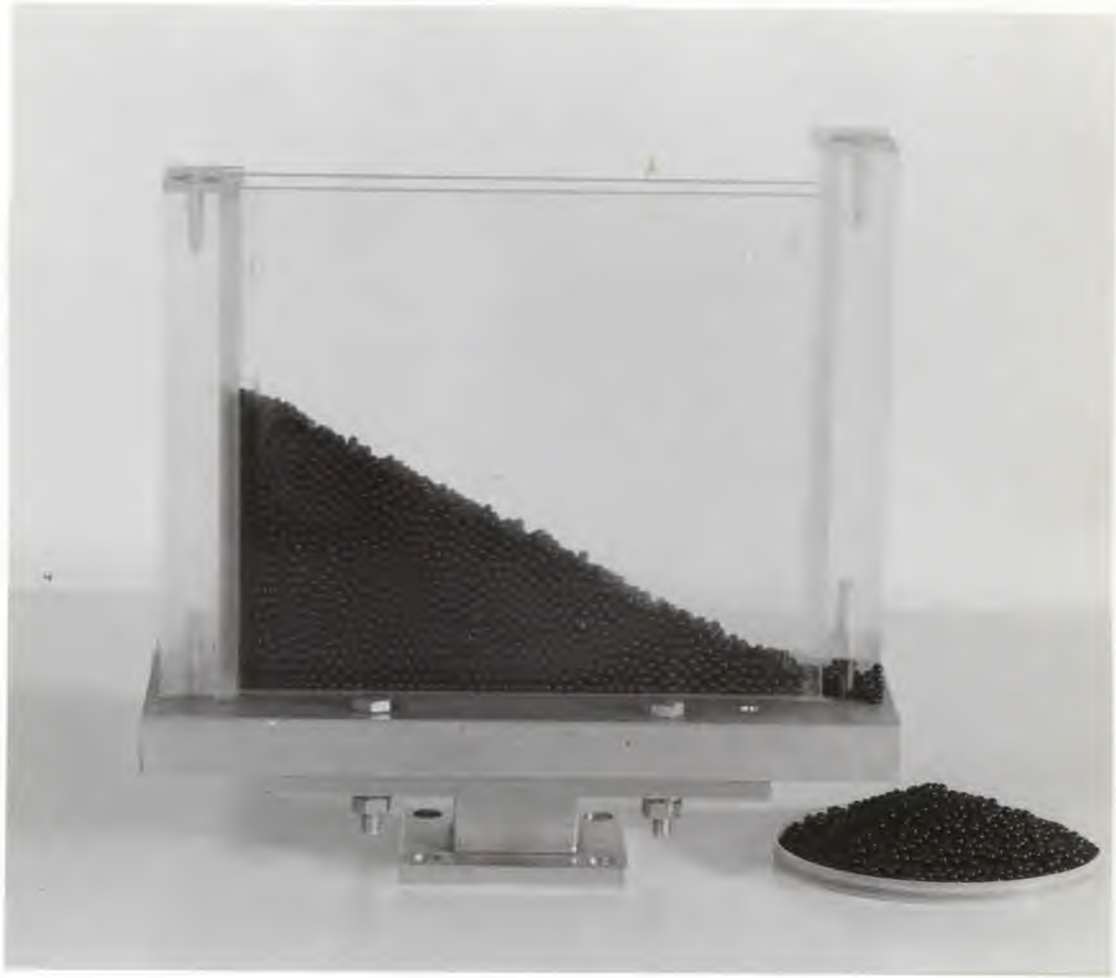

Figure 4 Drainage cell setup for determination of the angle of repose.

2.2 Discussion

Since three different results were found for the same material, a selection criteria was selected, based on that given by Brown and Richards [5], i.e., the steepest angle is chosen as the repose angle. The basis of this selection is that the angle closest to the slippage angle, that angle separating stationary material from flowing material in a formed heap, should be selected.

Having selected an angle of repose, the analytical model of Meakin et al [12] can be examined. They derived an expression for the critical size ratio Qc below which segregation should not occur, i.e.,

$$Qc = (4/\rho)^{1/3}\sin^{2/3}\Theta r/\cos\Theta r$$

In this expression, the angle of repose (Θr) appears as a parameter. For this model, it is assumed that a geometric piling mechanism is responsible for segregation (see Chapter 1). Upon substituting $\Theta r = 34.70^\circ$ (see Table 1) and a density of small sphere packing of $\rho = .58$ [12] we find that $Qc = 1.45$. In this particular study, a $Qc = 1.45$ corresponds to using a large sphere size of 3/16" diameter with 1/8" diameter smaller spheres. Knowing this, the critical size ratio can possibly be experimentally verified provided no convection exists in the system. In this particular study, convection was observed, thus the critical diameter ratio will not be examined.

CHAPTER 3
EXPERIMENTAL INVESTIGATION

Experiments were conducted on the rising of a large sphere through a bed of smaller vibrated spheres for a series of varying parameters. Initially, the large sphere was placed at the bottom of a transparent cylinder filled with a smaller spherical medium. The entire content, being fixed to a vibratory unit, was shaken with a fixed bed height using four different frequencies and a spread of amplitudes. The segregation time of the particle was measured from the base of the cylinder to the top of the bed using the timing feature of a Kodak* high-speed video system. This procedure was repeated for three different large particles in order to examine the effect of size, frequency and amplitude, on segregation. At complete list of parameters used in the experiments is given in Chapter 4.

3.1 Experimental Equipment

For the study, a 2-7/8" inner diameter by 8" high acrylic cylinder, a mass of 1/8" diameter acrylic spheres and a series of larger acrylic spheres (varying from 1/8" to 3/4" in 1/8" increments) was used (see Fig. 5). The vibratory equipment consisted of an electromagnetic shaker and head powered by a power amplifier. The equipment was controlled by an exciter unit which allowed for the variation of frequency. The output of the controller is sinusoidal in a vertical direction and is adjustable by a digital meter to three decimal places. In addition, the displacement/amplitude, velocity and acceleration of the shaking head could be set or read using an accelerometer as a feedback loop. The measurements were again read from a digital meter to three decimal places. All of the vibratory equipment

* Kodak EktaPro 1000 High Speed Digital Imaging System.

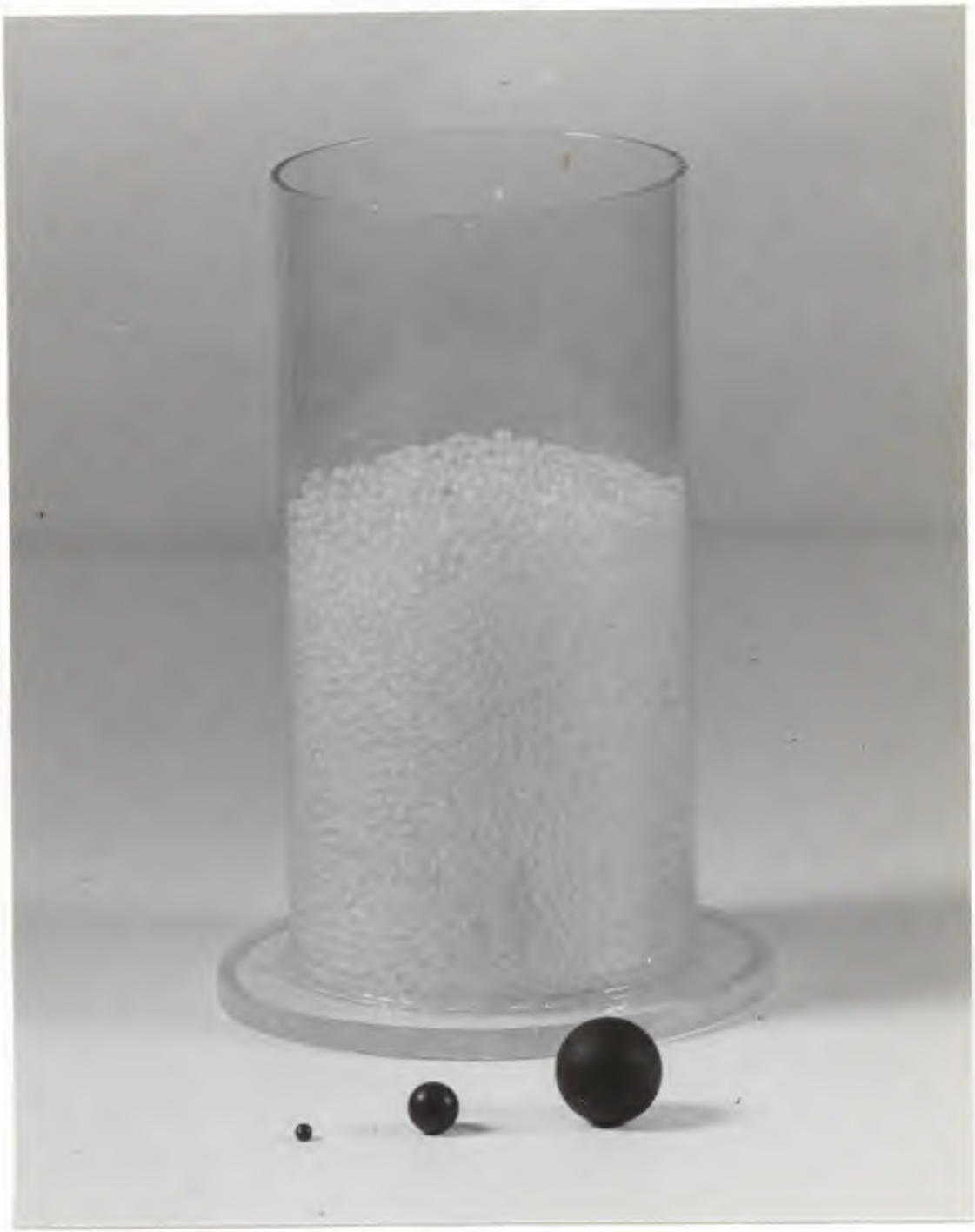

Figure 5 Experimental cell and material used for vibratory experiments.

was manufactured by Bruell and Kjaer (a detailed list of all model numbers are given in Appendix D). Additional equipment consisted of a humidifier with a built in humidstat as well as a hygrometer for reading both the relative humidity and temperature of the surrounding area. Also an Kodak EktaPro 1000 high-speed video image processing system was used to capture the particles movement. All the equipment was arranged in such a manner (described below) such that they were enclosed by a canvas chamber to maintain proper humidity conditions (see Fig. 6a & 6b). A schematic of the setup is given in Figure 6c.

3.2 Experimental Procedure

Initially the frequency was selected using the exciter control unit. In these experiments, frequencies ranging from 10Hz to 25Hz in increments of 5Hz were used. Next, the amplitude was selected by using the feedback provided from the accelerometer. Here the amplitude ranged from .5" (the maximum capability of the equipment) to a lower critical cut-off limit governed by segregation time. Then, the size of the large particle is selected. In this study we chose three particle diameters of 3/4", 3/8", and 1/8" which when compared to the bed spheres corresponded to a 6, 3 and 1:1 diameter ratio, respectively. Following this, the particle is placed in the bottom of the cylinder and filled, by pouring randomly with smaller 1/8" diameter bed spheres to a bed height corresponding to 26 layers of the smaller sphere. The cylinder, completely transparent, is fixed onto a aluminum base which in turn is mounted on the shaking head. The EktaPro 1000 is then mounted by tripod directly above the mounted cylinder so that the top of the bed can be viewed. Auxiliary lighting, which is necessary for proper recording, is then turned on. Next, the humidity is set to about 50% using the

Figure 6a Canvas enclosure for vibratory equipment.

Figure 6b Vibratory equipment and humidifier setup.

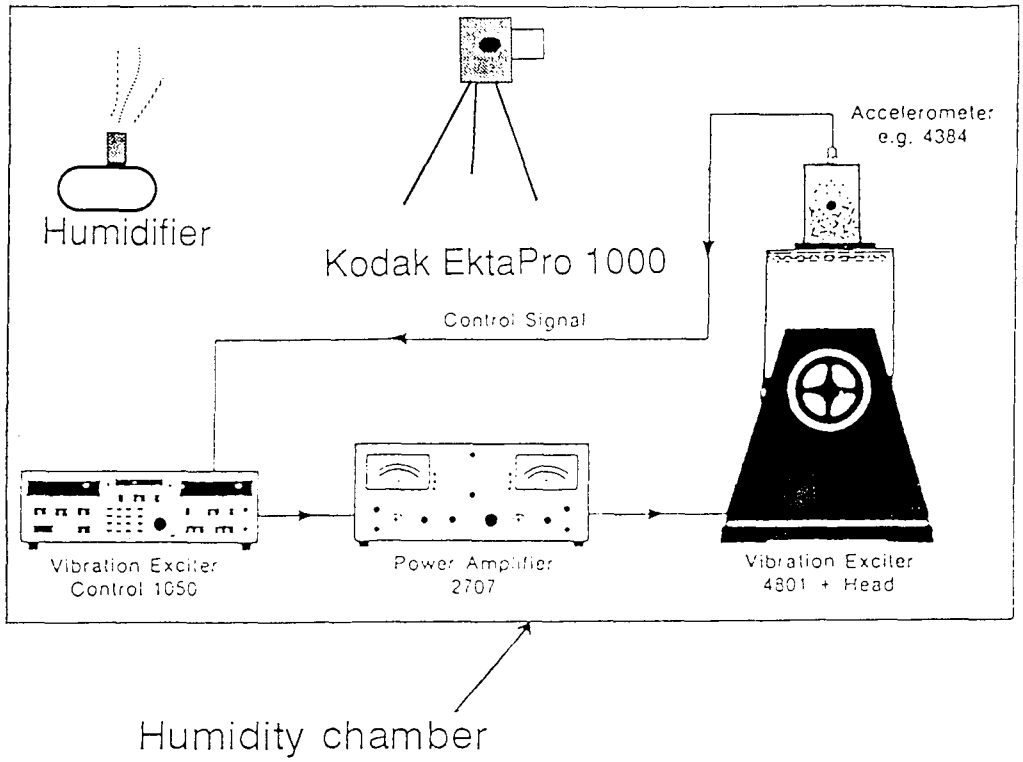

Figure 6c Schematic of experimental apparatus.

humidifier and hygrometer described above. Now complete, the camera and shaker are manually synchronized and powered up. The setup runs until the large sphere rises to the top of the bed. The large sphere is detected optically via a monitor which is contained in the Kodak EktaPro 1000 system. Once a series of runs are complete, the recorded tapes are viewed to obtain the time of travel for the rising of the large sphere in the vibrated bed. The series of runs last for the allotted time on the video tape. This procedure is carried out carefully five times (see Appendix B) for each run for all of the experiments to assure accuracy of results. All the parameters mentioned are controllable and repeatable.

CHAPTER 4
EXPERIMENTAL RESULTS AND ANALYSIS

As detailed in Chapter 3, "segregation" in a vibrated bed was examined. At this point segregation is used to denote the rise of the selected sphere through the bed. The reason for this distinction will be made apparent in the following sections of this chapter.

The experiments were run varying a list of parameters including:

Frequency
Amplitude
Particles Size Difference
Wall Conditions

From the recorded data, plots were generated to analyze and interpret the data. In general, the plots showed results which were in qualitative agreement with two previous studies Jullien [12] and Nagel [14], but which do not support each other. The conflict lies in the degree of influence that particle size difference (diameter ratio between large and bed spheres) makes in a vibrated system. In this study it was found that particle difference influences segregation time and rates quantitatively as in Jullien [12]. On the later side, Nagel [14] found that particle size difference had no qualitative effect on segregation even as the diameter ratio became unity. Since the results found in this study have not been explained by recent theories, a hypothesis is put forward to explain this discrepancy. It is postulated that competition exists among the particles within a convective flow, thus being responsible for particle size discrepancies found in a vibrated bed for this study. In what follows, an attempt will be made to justify the stated hypothesis.

4.1 Results

The results of four typical runs on a system having a diameter ratio of 6:1 are shown in Fig. 7 in Appendix A. These results are for smooth wall conditions which refers to a polished acrylic surface. Frequencies of 10, 15, 20 and 25 Hz were run for a spread of amplitudes ranging from .05" to .5", peak to peak. From the plot it is clear that segregation time decreases with an increase in amplitude for a fixed frequency. Furthermore, segregation time decreases as frequency increases for fixed amplitudes. The trends of the plotted curves appear to be asymptotic, thus suggesting that segregation time becomes very large for a small amplitude. The segregation rate is plotted in Figure 8 (see Appendix A) using the data shown in Figure 7. This curve was generated by dividing the segregation time by the number of layers through which the larger sphere traveled, thus giving the mean velocity or rate. Here we find four curves which appear linear. Figure 8 appears the inverse of Figure 7, but leads to conclusions similar to those of the Figure 7. The results of Figure 7 were scaled by their relative acceleration ratio $\Gamma = a\omega^2/g$ and plotted in Figure 9 (see Appendix A). All of the scaled data falls on one curve indicating that segregation time in these experiments is dependent on acceleration rate only. Identical experimental runs were started, with a diameter ratio of 3, to examine the dependence of segregation time with diameter ratio. However, early on in the experiment, the rise of the large sphere to the bed surface completely stopped. The large sphere could not be made to rise regardless of aspect ratio, frequency and/or amplitude combination. A series of parameters were examined in order to determine the cause of this as discussed below.

Initially, the spheres were removed from the experimental setup and cleaned in a mild soap and water solution. This was done to remove any dirt buildup which could have changed the spheres' surface properties which ultimately could affect segregation. Since this was ineffective, a new cylinder was constructed to regain initial wall

conditions. Repeated attempts to achieve segregation at various vibratory conditions failed. Upon closer inspection, it was observed that the induced vibration caused a sinusoidal shape on the surface of the bed which differed in appearance from earlier experiments. The shape on the surface of the bed during the earlier experiments (those experiments used to generate Figure 7) was in the form of a central heap. Since the bed movement had changed, the output of the shaking head was checked. As described in Chapter 3, the output of the shaking head is sinusoidal in a vertical direction. A deviation in the equipment's output would lead to an altered shaking condition. The vibratory equipment was checked by both the author and a qualified Bruel and Kjaer engineer for defect. The apparatus was operating well within its tolerances, thus it was ruled out as problematic. Next, new identical spheres were purchased. The new spheres, when used with a new cylinder under identical parameters, showed segregation. The results were comparable to that of the previous runs. However, after only one day of experiments, the large sphere would not rise to the top. At this point it was hypothesized that the change in surface properties of the experimental material due to wear could be the source of the problem. Since it was not practical or feasible to purchase and reconstruct a new apparatus for each experiment, other measures were taken.

Since the problem was assumed to be related to surface properties, sand papers of various grits were placed on the cylinder walls. As suspected, the large sphere rose to the bed surface. Although this worked, the bed spheres became significantly damaged. Therefore, spheres equal in diameter to the bed spheres were fixed with adhesive to the walls and base of the cylinder. This was done to achieve a bumpy surface without the abrasive qualities of sandpaper. Experiments, identical to the previous run (see Fig. 7) were performed and showed comparable results to that of

the smooth wall setup. The changes here were quantitative and will be discussed below.

The remainder of the experiments were done with rough wall conditions. The first run taken was a system in which the diameter ratio was 6 (see Fig. 10 in App. A). From Figure 10, it can be seen that segregation time decreases with an increase in amplitude for a fixed frequency. In addition, segregation time decreases as frequency increases for fixed amplitudes. The trends of the plotted curves are again asymptotic. The plots for segregation time versus amplitude for diameter ratios of 3 and 1 are shown in Figures 11 and 12 (see Appendix A), respectively. The results here are in qualitative agreement with both Figure 10 and with the smooth wall results shown in Figure 7. The changes are quantitative, in that segregation time increases, for identical experimental conditions, as the aspect ratio approaches one, indicating that particle size difference does in fact affect segregation. This particle size dependence is seen more clearly in figures 13-16 (see Appendix A). Because of the large range of data, a logarithmic scale was used to plot segregation time as the ordinate. However, this does not facilitate an easy comparison of the results. The magnitude of the difference between the varying runs can be readily seen from the numerical data tabulated in Appendix B. The data taken for this study was based on the mean value taken from five trial runs. Since only five trials were taken, the experimental error of these results can only be estimated by finding the sample deviation from the mean.

The segregation rate for the rough wall experiments was produced in the same manner as for the smooth wall data in Figure 8. This was done to observe whether or not the trends of the segregation rates (based on bed height) compared with those of segregation time. The plots showing the segregation rate, for all the experiments (Figs. 17-19 in App. A), were adjusted to compensate for particle size difference. Although the bed height remained fixed throughout the experiments, the number of layers used to

calculate the segregation rate was based on the bed height minus the radius of the large sphere thus ensuring comparable results. The plots showed curves which appear to be linear. These curves, though adjusted for bed height, yield the same conclusions as drawn from Figures 10-12. All conclusions drawn from the trends of the plots (in Fig. 17-19) were consistent with Figures 10-12 in that their dependency on frequency, amplitude and large particle size difference produced comparable results.

All of the rough wall data was scaled by the relative acceleration rate (Γ) and plotted in Figures 20-22 (see Appendix A). Unlike the smooth wall results of Figure 9, the data did not fall onto one curve, indicating that there is an additional dimensionless group which controls the observed phenomena. An increase in the segregation rate from a diameter ratio of 1:1 to 6:1 can be noticed in Figure 23 (see Appendix A).

The results found here were typical in that they contained characteristics which are in agreement with previous studies [Nagel (7) and Meakin (12)]. However, the underlying cause for our experimental results cannot be solely explained by the theories proposed by either Jullien et al. [12] or Duran et al. [7].

4.2 Interpretation of Results

Initially the effect of particle size on vibratory segregation was to be studied. However, the discontinuity found early on in the smooth wall experiments expanded the study. The focus of the study was expanded to investigate the role of convective velocities in vibrated beds.

The explanation of why a single large particle rises to the top of a vibrated bed has been explored. As explained in Chapter 1, the geometric mechanism of avalanching or piling has been identified as a mechanism for size segregation [Rosato et al. (21)].

This theory readily explains why larger spheres rise faster than do smaller spheres in a vibrated bed. However, based on this hypothesis, a particle equivalent in size to the bed spheres will not rise. In addition, a critical size ratio below which segregation no longer occurs has been hypothesized by Jullien et al [12]. The results found here are in agreement with this in that the larger sphere does in fact rise quicker than the smaller spheres. On the other hand, it was found that spheres, including those equal in size to the bed sphere, also rise. Previous studies would attribute this case of segregation to convection and not avalanching. However, comparing Figures 10-12 one notices that the trends of the plotted data are very similar indicating that one source or mechanism may be responsible for all the results. In addition, as explained earlier, the large particle did not rise to the top when the surface properties of the system changed. By fixing spheres to the walls, convection was increased in the cylinder and consequently segregation, similar to that observed for the smooth wall experiments, was once again present. Recently, Nagel [14] postulated that vibration induced size separation is attributed solely to convective flows rather than avalanching. Nagel [14] found no size segregation in the range he tested. In fact, the segregation rate was found similar regardless of large particle size. If segregation does in fact depend on convection in a vibrated bed, it would imply that all size spheres move upward at the same rate. It is obvious that no particle could rise quicker then the convective current of the bed spheres unless other mechanisms were present. Based on this hypothesis, the mean rate of a rise of a sphere having the same diameter as the bulk spheres should give a value equal to that of the convective velocity of the bed. This was measured (see Appendix B) and plotted in Figure 12. Assuming that the segregation found in this study is based only on convection, the rate for all aspect ratios should be comparable. Nevertheless, the data and plots (see Fig 10-12) clearly do not support this, i.e., segregation time

decreases as the diameter ratio increases. Since neither of the well-known hypotheses encompasses all the results in this study, further investigation was carried out.

While carrying out the experiments using the 1:1 aspect ratio, inconsistencies in the results were observed. Specifically, the time of segregation occasionally became so large that it could not be considered with the otherwise repeatable data. This behavior was not seen for the larger diameter ratios examined. This seemed to indicate that the particle was veering off the convective stream path in its rise to the top of the bed, that is, it was experiencing a significant amount of lateral diffusion. Therefore an experiment that would reduce the possibility of the particle from wandering was devised. Experiments were performed for the diameter ratio of unity in which the quantity of dyed particles was increased. Instead of tracing one dyed particle, ten dyed spheres were used. The dyed spheres were arranged in such a manner that they formed a small pile at the base of the bed of the cylindrical apparatus (see Fig. 24 in App. A). The spheres were placed in a manner that the convective current, if in fact present, would carry them all up. After carrying out the experiment for a fixed amplitude and frequency, a change was noticed (note, due to time constarints not enough data was taken to generate plots). Rise time was reduced in comparison to data which produced the segregation time plots in Figure 12 (see Appendix B). In addition, the results were repeatable in that none of the trials exhibited large deviations from each other. Since the initial vertical locations of the dyed spheres differed no more then one particle diameter, the particle that rose first was timed. This is valid because at worst the initial position of the spheres (that is, its height from the cylinder base) only varied by one diameter as shown in Figure 24. The extra diameter could easily be subtracted out of the bed height in the segregation rate calculation (see Chapter 3). Based on these results, it seems that there is competition for particle levitation in the bed within the convective flow. Statistically, one of ten dyed particles has a much greater chance of

rising to the top of the bed then does one out of one dyed particles. The possibility of the dyed particle getting off path is reduced as was found above. The idea of this competition between rising particles in a vibrated bed is discussed below.

The existence of competition in the convective flow can explain size "segregation" produced by convection. As the diameter of the large sphere approaches the size of the bed spheres, its ability to resist velocity change imposed by the interaction of the surrounding bed spheres becomes less. When the aspect ratio reaches unity, any sphere may effectively move another sphere. Thus a small sphere is more likely to veer off the path during its movement to the top than is a large sphere. The larger the sphere the greater the mass and inertia which gives it a greater ability to resist velocity change. In a rectangular cell this competition was observed. A rectangular cell was mounted on the shaker in a manner similar to that of the cylinder. The cell was filled with bed spheres identical to that of the cylindrical setup. A convective flow was produced with mass of spheres containing one tracer sphere. The tracer after a brief transient period, developed up a convective motion. However, during inspection it was noticed that the sphere spuriously moved out of the convective zone. In addition, the tracer particle also oscillated within the convective zone sometimes causing it to become stuck in a small volume. If the behavior is similar in the cylinder, it could explain the inconsistencies found in the 1:1 diameter ratio experiments. Assuming that the previous assumptions are true, it is believed that the motion of the largest particle examined in this study is closer to the actual convective velocity than that of the smaller sphere (1:1 aspect ratio).

Since segregation was regenerated by inducing convection, the mechanism for the large sphere rising to the top of the bed is attributed to the convective flow. However, as outlined above, the author believes that interactive particle dynamics also plays a significant role in this behavior. The term segregation means a sorting of

particles by some property, which, in this case is size. Since convection does not differentiate between sizes, then convection is not strictly a segregation mechanism. Rather, it may be regarded as a mixing mechanism. The experimental results for the different size ratios clearly indicate a competition between the induced vibratory convection stream and the local particle level influence.

CHAPTER 5
SUMMARY

As of present, several mechanisms of size segregation have been identified but are yet to be fully explained. The objective of this study was to examine the effects of particle size on vibratory segregation through experimental means in hope of gaining insight into this phenomenon. The term size segregation is used to describe the sorting of particles by size. In the context of this study, segregation was used to describe the rise of an examined sphere through a vibrated bed. The author found that convection in conjunction with local particle interactions are responsible for the observed "segregation" and its characteristics. For the range of parameters studied the following conclusions were drawn:

[1] An increase in amplitude was always accompanied by a decrease in segregation time for fixed frequencies regardless of aspect ratio.

[2] An increase in frequency decreased segregation time for fixed amplitudes.

[3] Segregation time shortened as diameter ratios became greater.

[4] Spheres with a diameter ratio of unity also rose to the top of the vibrated bed. This along with the rising of the larger diameter ratios is attributed to the convection stream in the center of the cell.

[5] Early in the experiments the rising of the larger sphere in the bed ceased. Because of this, a rough-wall experimental setup was introduced. The roughened wall produced convection within the examined cell which in turn levitated the examined sphere through the vibrated bed and allowed for the experiments to be continued.

[6] There exists a competition in the convection stream which could be responsible for the change in rise time for the different diameter ratios examined.

The experiments performed gave results necessary for a fundamental analysis. Much more investigation needs to be done in this area if the phenomenon of segregation is to be fully characterized. The following are some considerations for future work:

[1] The convection velocity of the bed needs to be measured more carefully for comparison with the particles of interest in the bed. Once accomplished, the convective velocity may be combined, possibly subtracted out, with the rate found for the examined particle.

[2] An experimental setup where the bed is vibrated independently from the walls need be constructed. Such a setup could give insight to what roll wall effects have in segregation. The setup could consist of a fixed cylinder in which a piston moves vertically thus moving only the payload.

[3] Experiments where the ratio between the bed spheres diameter and cylinder diameter should be varied. A series of experiments identical in all parameters except for this ratio could also aid in explaining wall effects.

[4] Different wall roughnesses could be used for all of the setups mentioned above to further examine wall effects. This can be achieved by varying the diameter of the spheres which are adhered to walls.

[5] Tracing the examined particle by a non-intrusive tracking system would aid in understanding particle dynamics and possibly give insight to the segregation phenomenon.

[6] A setup where a granular medium was lifted slowly, dropped and repeated need be constructed. A setup of this sort would simulate shaking and at the same time eliminate convective flows. If no convection is present, other mechanisms, if present, could be examined.

APPENDIX A

Chapter 4 Figures

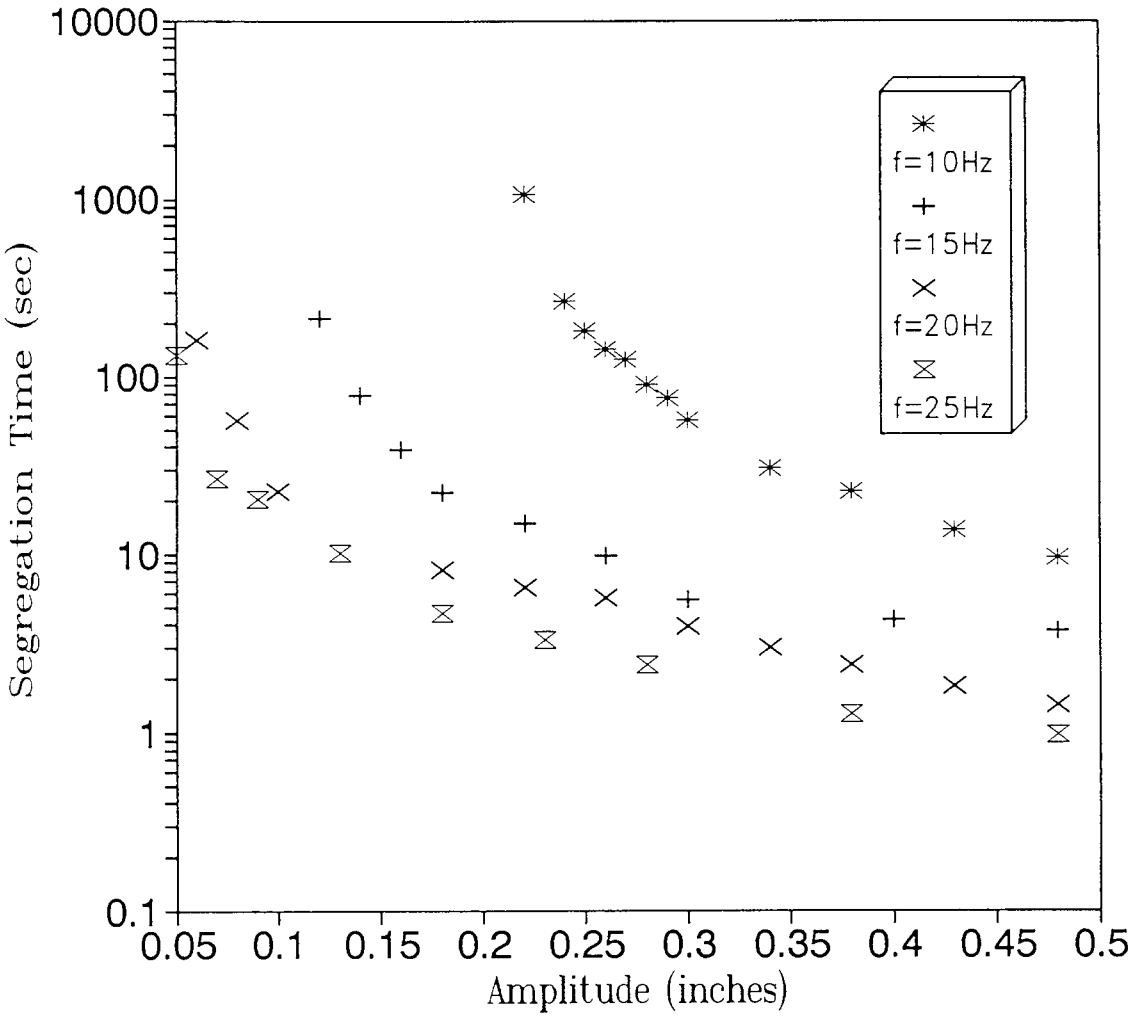

Figure 7 Segregation time vs. amplitude for an aspect ratio of 6:1 with a bed height of 26 layers for smooth wall conditions.

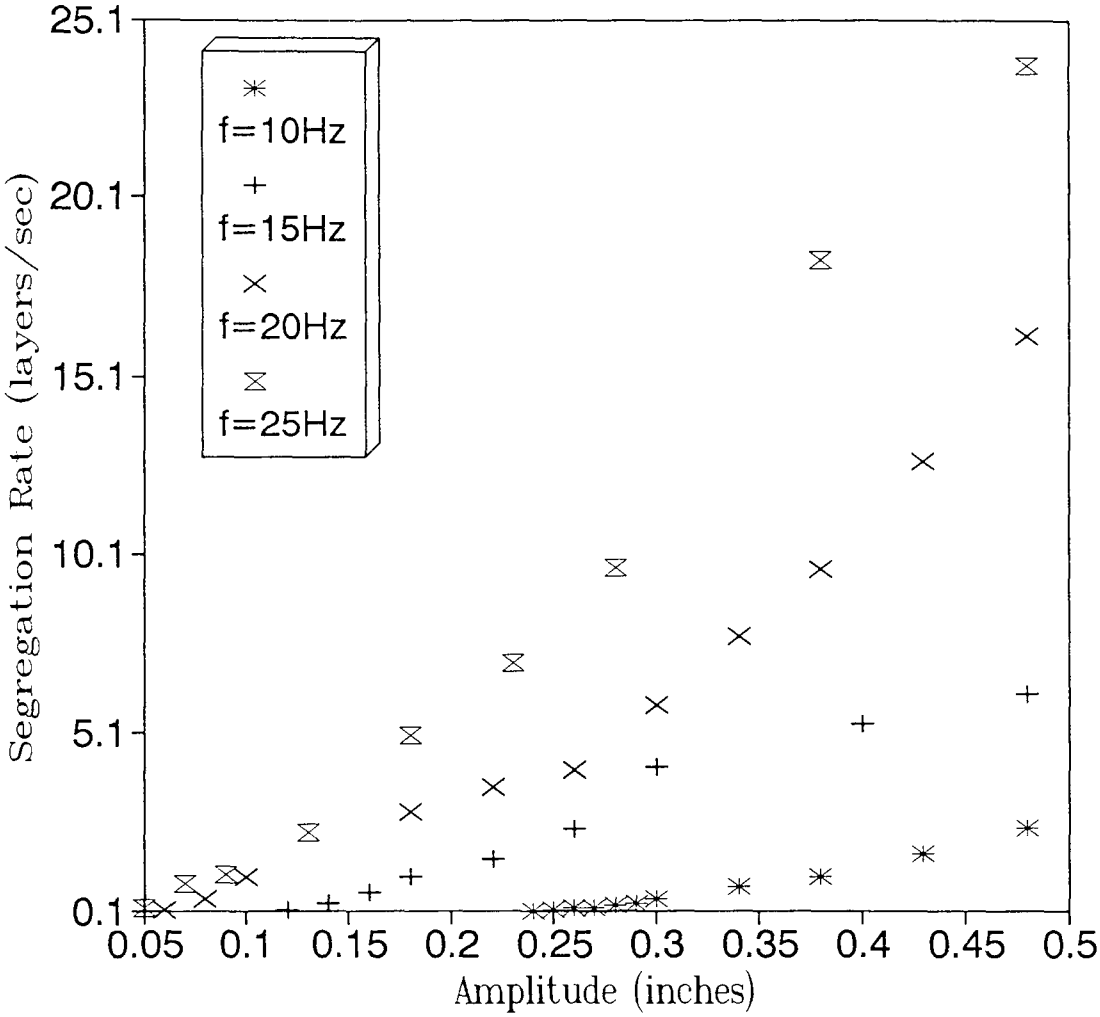

Figure 8 Segregation rate vs. amplitude for an aspect ratio of 6:1 with a bed height of 26 layers for smooth wall conditions.

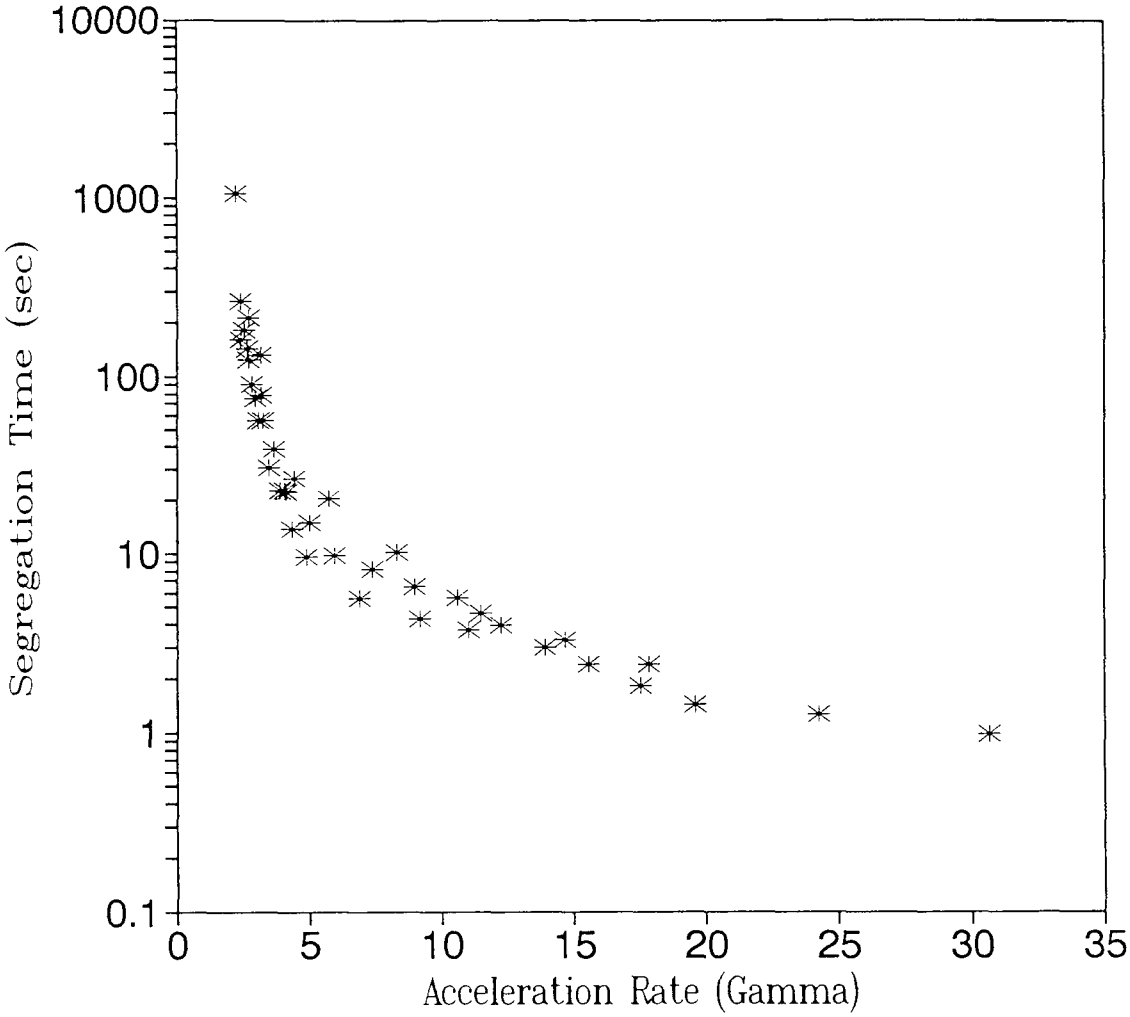

Figure 9 Segregation time vs. acceleration rate for an aspect ratio of 6:1 with a bed height of 26 layers for smooth wall conditions. The asterisks represent the 4 frequencies tested.

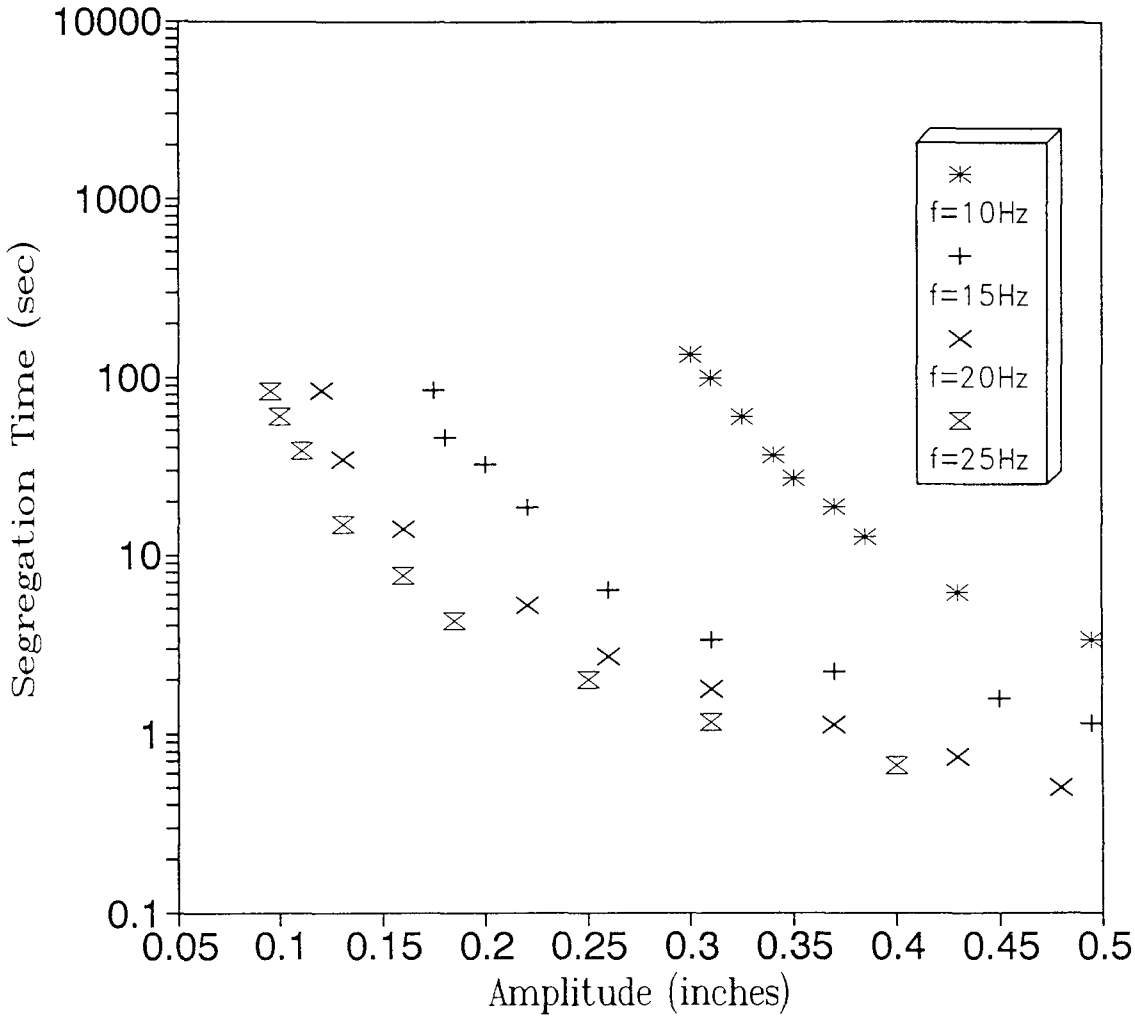

Figure 10 Segregation time vs. amplitude for an aspect ratio of 6:1 with a bed height of 26 layers for rough wall conditions.

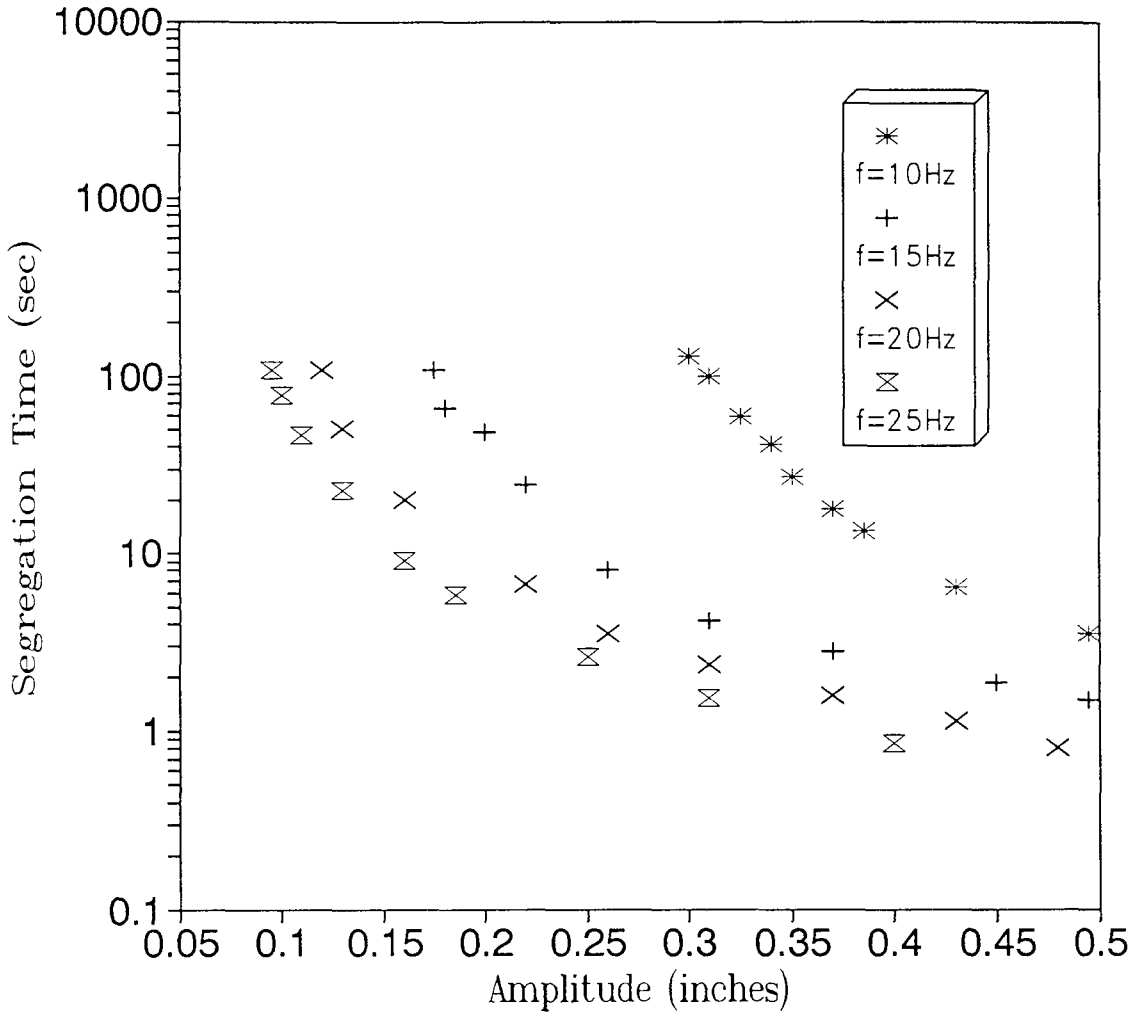

Figure 11 Segregation time vs. amplitude for an aspect ratio of 3:1 with a bed height of 26 layers for rough wall conditions.

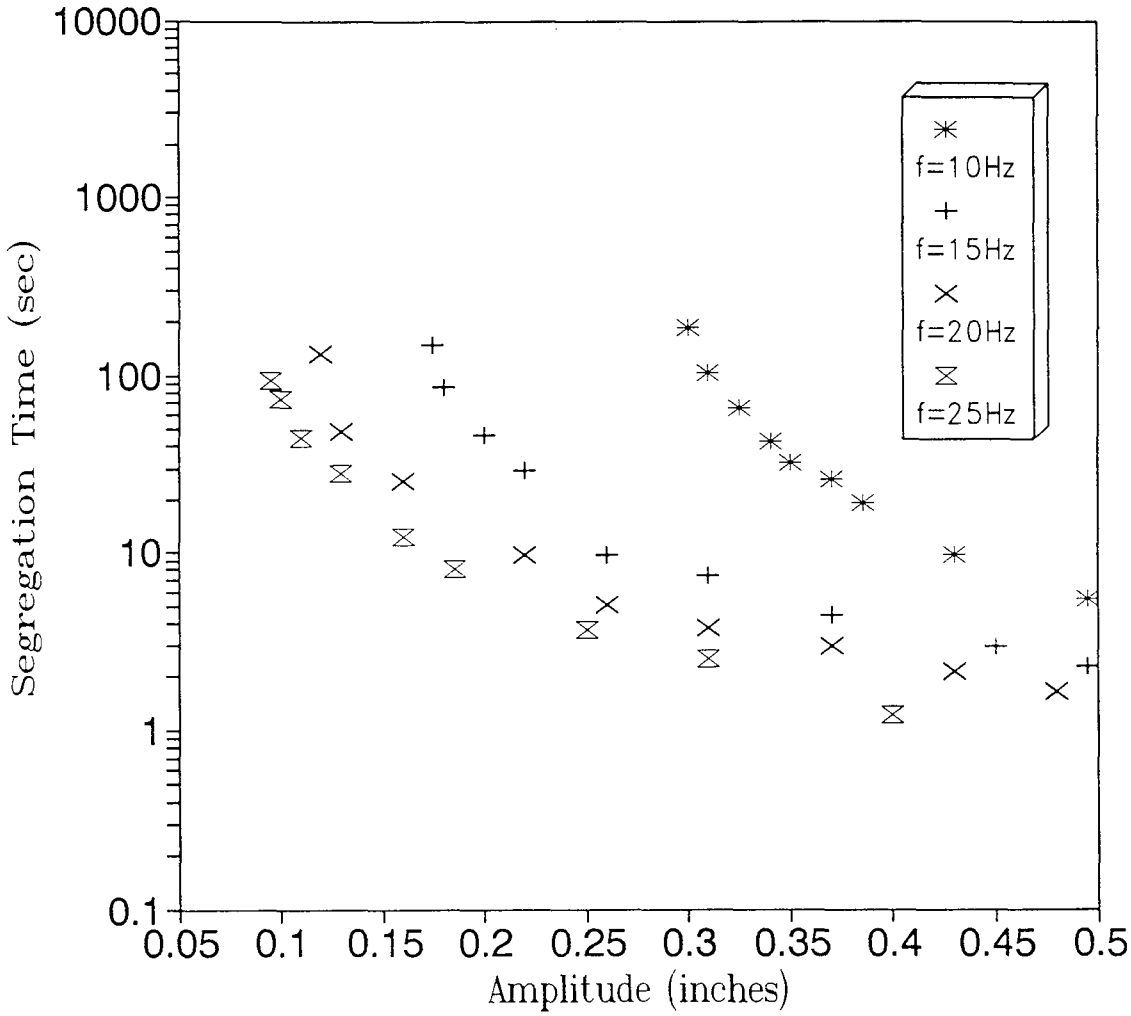

Figure 12 Segregation time vs. amplitude for an aspect ratio of 1:1 with a bed height of 26 layers for rough wall conditions

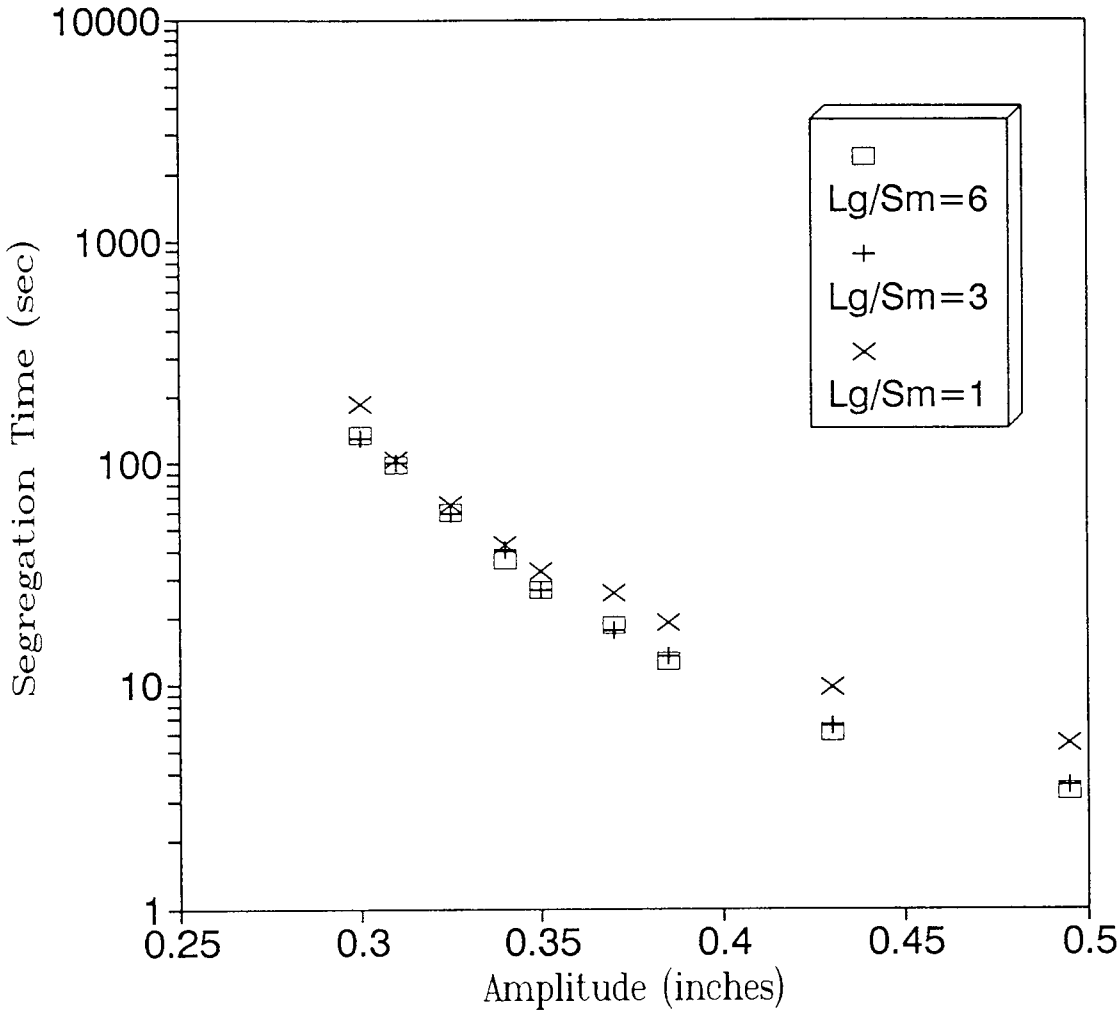

Figure 13 Segregation time vs. amplitude for f=10Hz with a bed height of 26 layers for rough wall conditions.

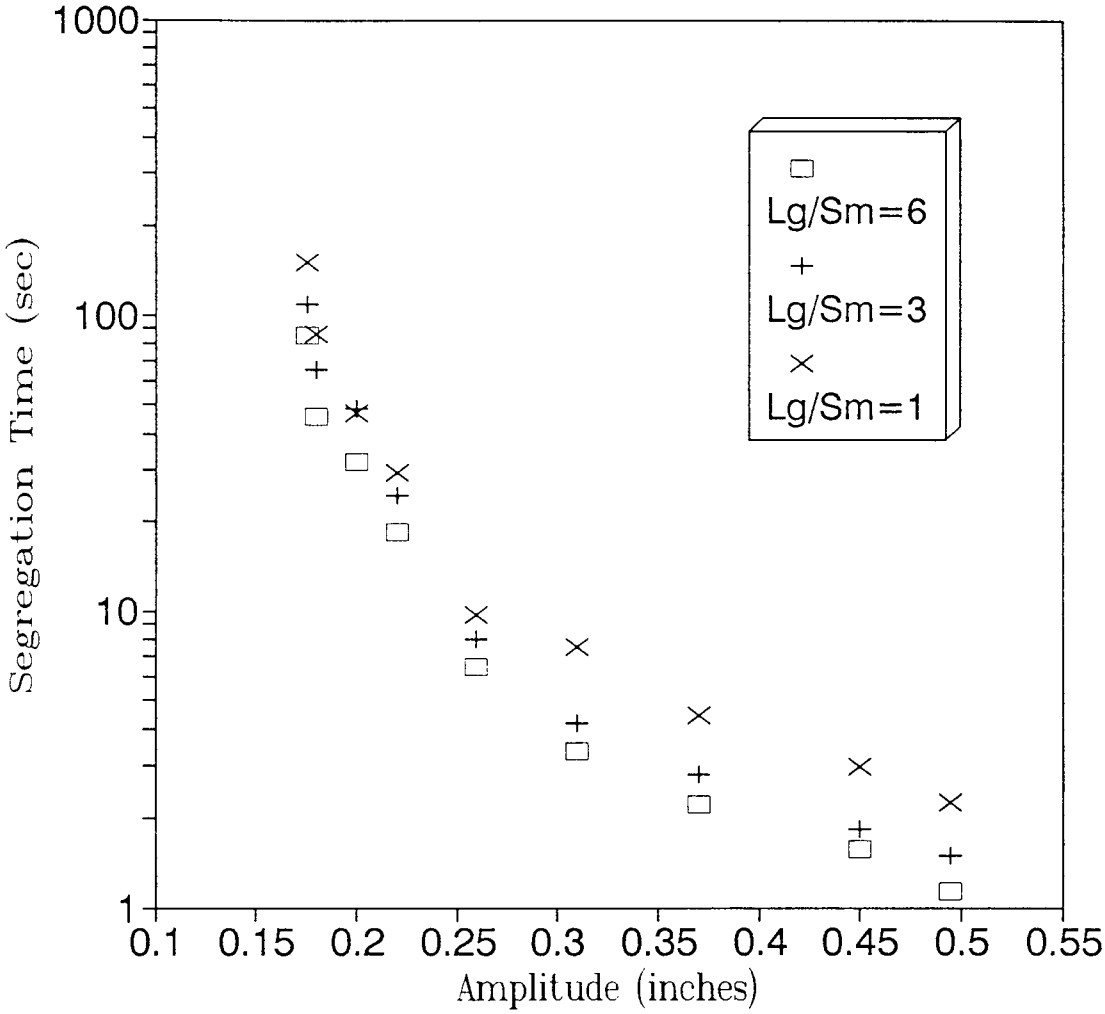

Figure 14 Segregation time vs. amplitude for f=15Hz with a bed height of 26 layers for rough wall conditions

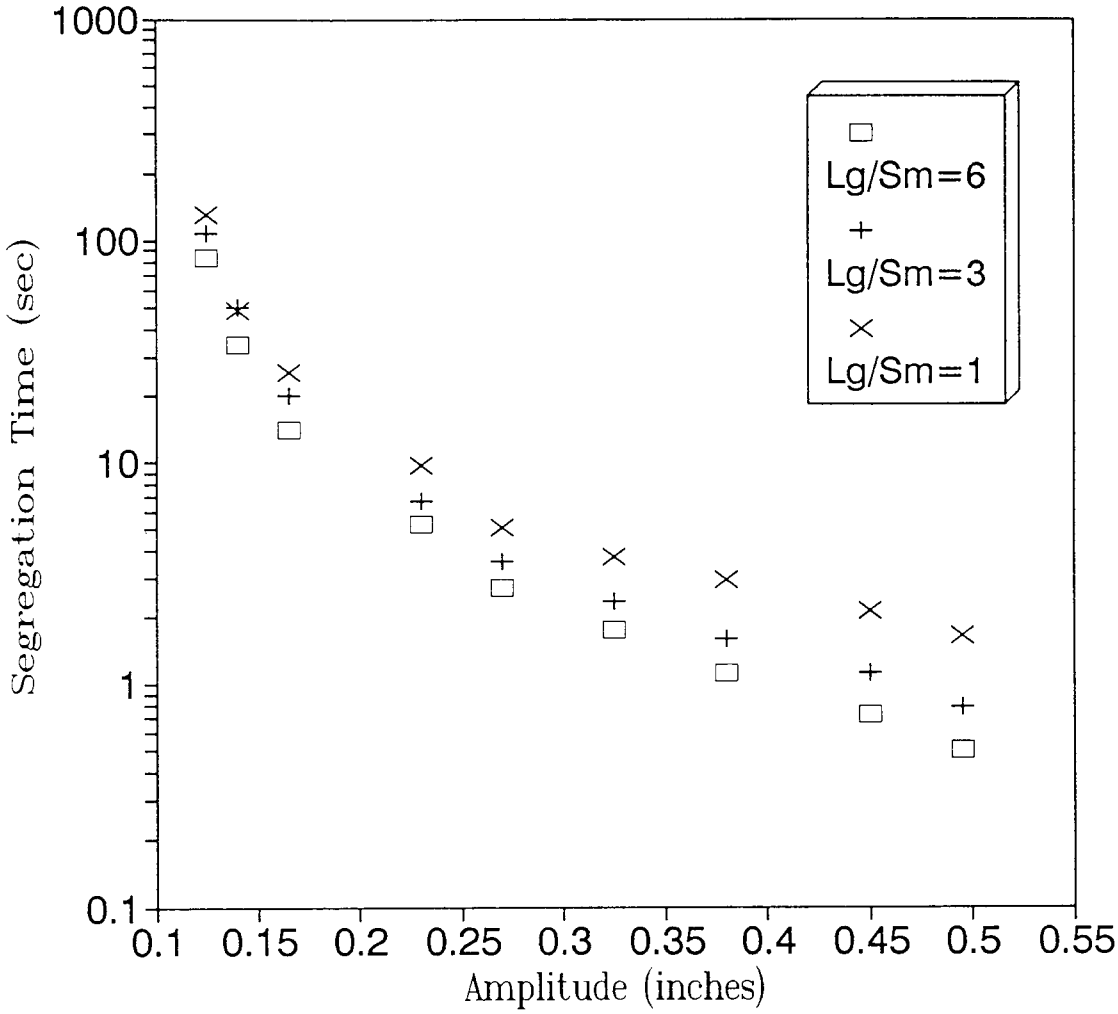

Figure 15 Segregation time vs. amplitude for f=20Hz with a bed height of 26 layers for rough wall conditions.

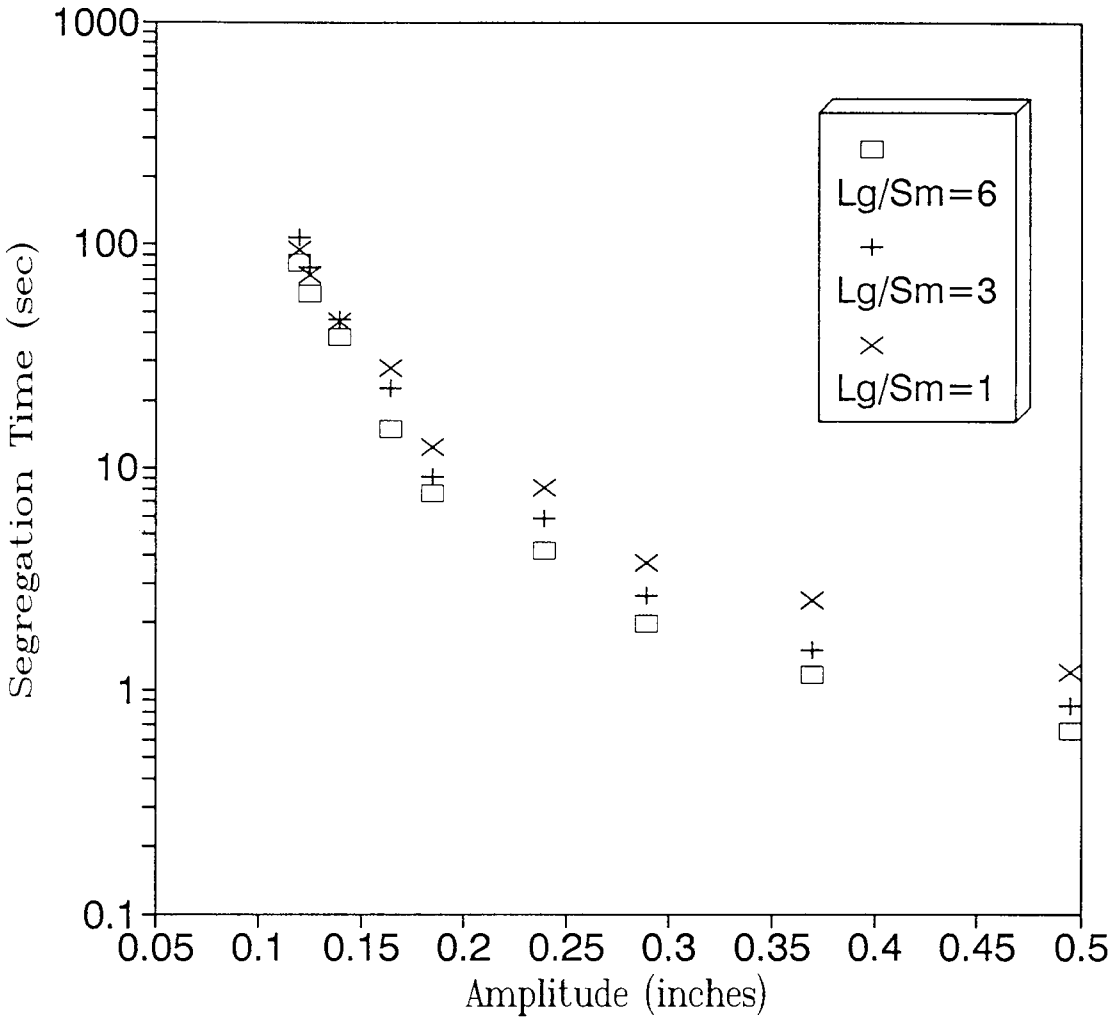

Figure 16 Segregation time vs. amplitude for f=25Hz with a bed height of 26 layers for rough wall conditions..

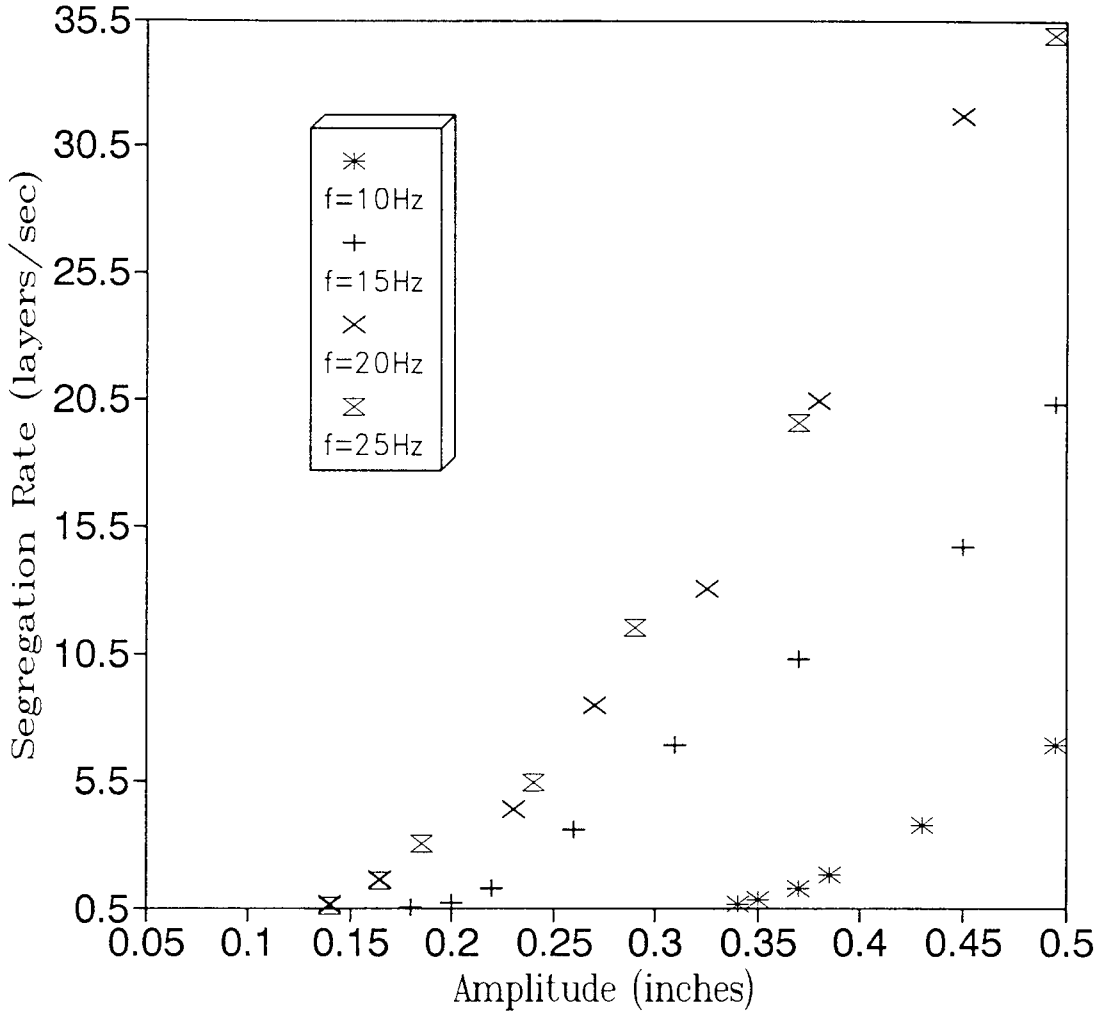

Figure 17 Segregation rate vs. amplitude for an aspect ratio of 6:1 with a bed height of 26 layers for rough wall conditions

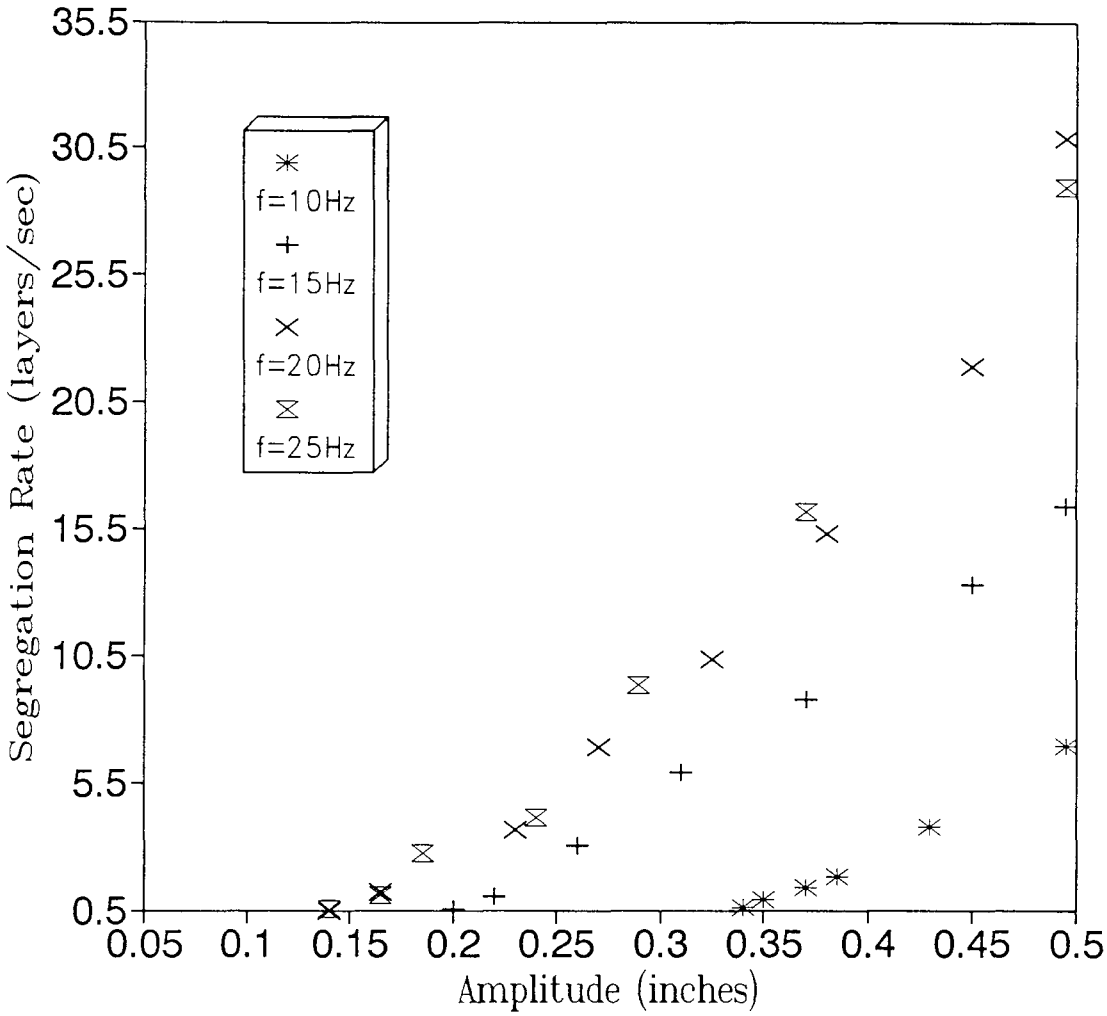

Figure 18 Segregation rate vs. amplitude for an aspect ratio of 3:1 with a bed height of 26 layers for rough wall conditions.

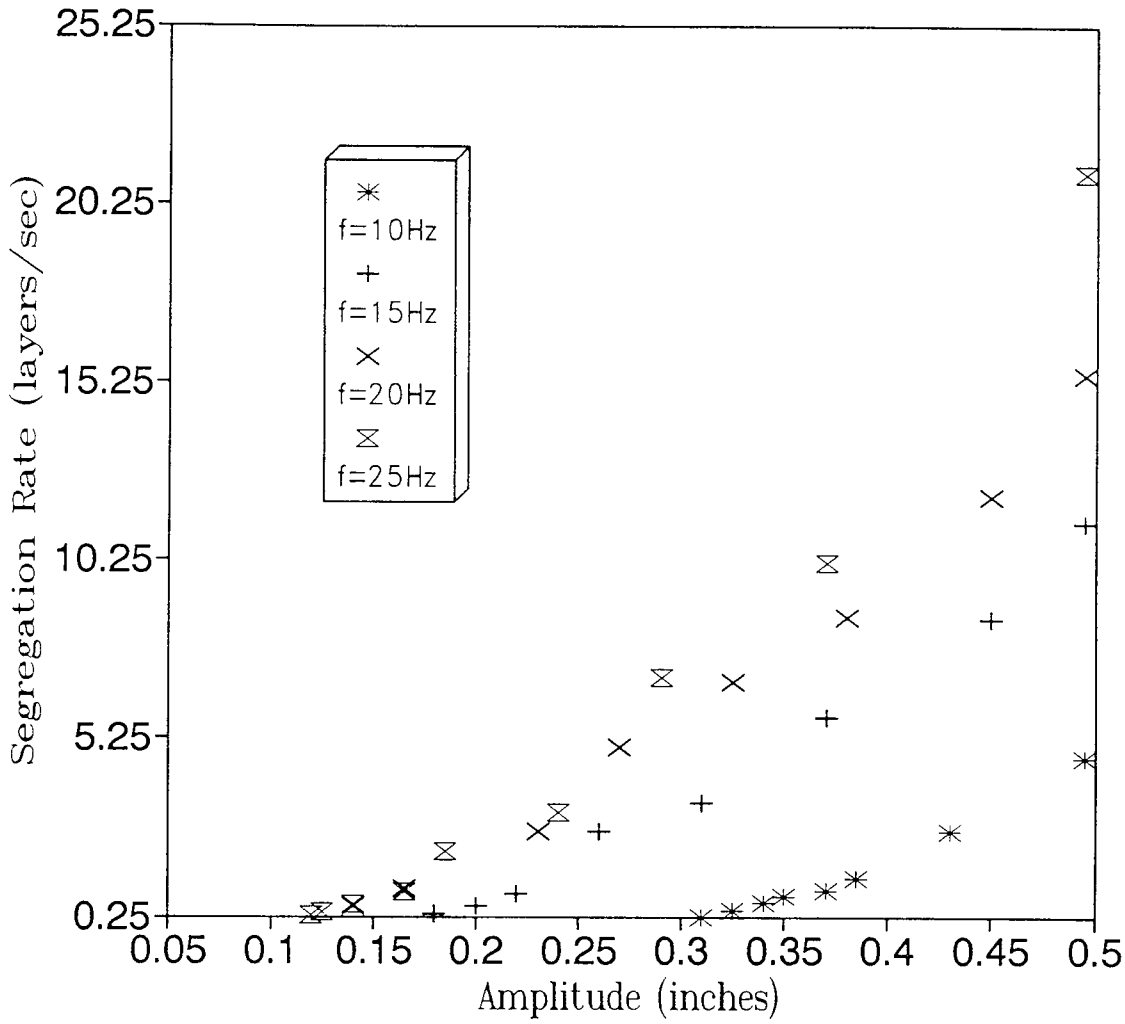

Figure 19 Segregation rate vs. amplitude for an aspect ratio of 1:1 with a bed height of 26 layers for rough wall conditions.

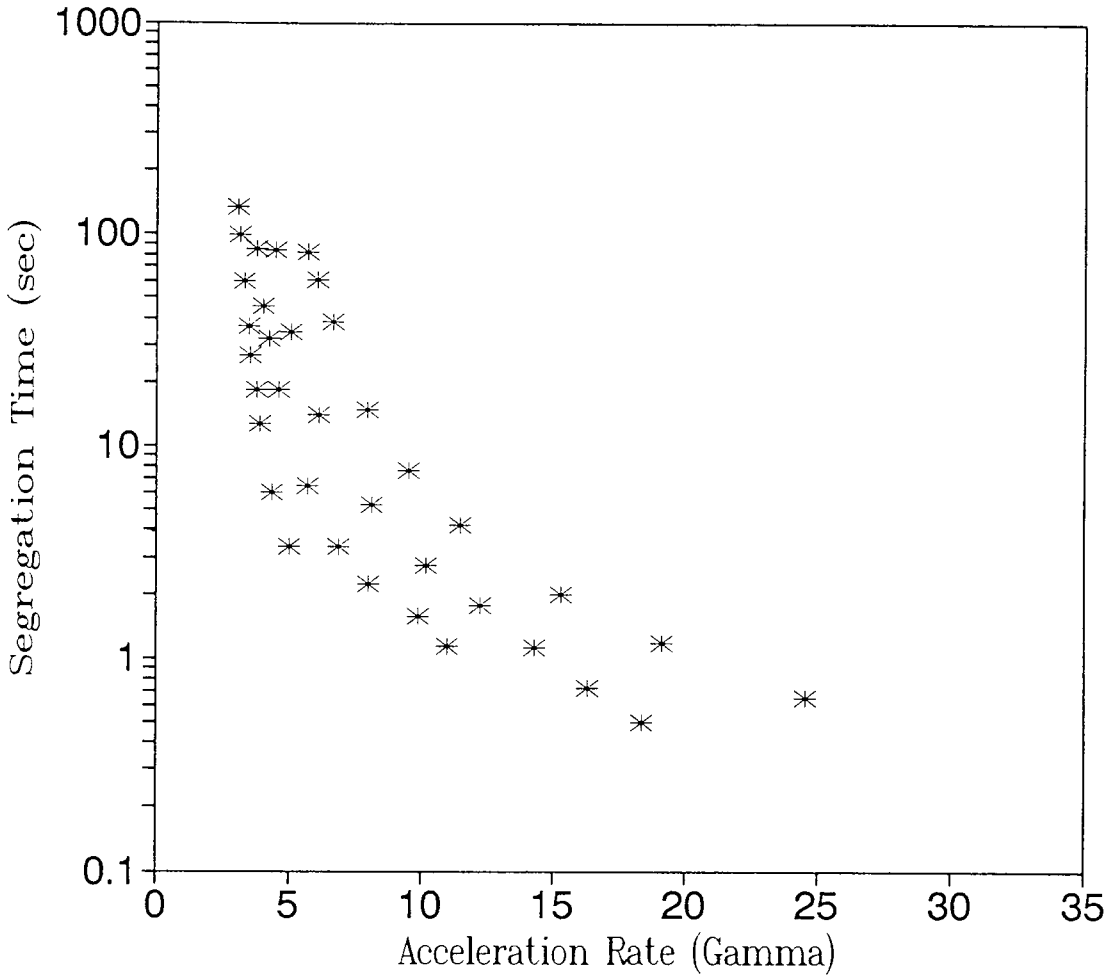

Figure 20 Segregation time vs. acceleration rate for an aspect ratio of 6:1 with a bed height of 26 layers for rough wall conditions. The asterisks represent the 4 frequencies tested.

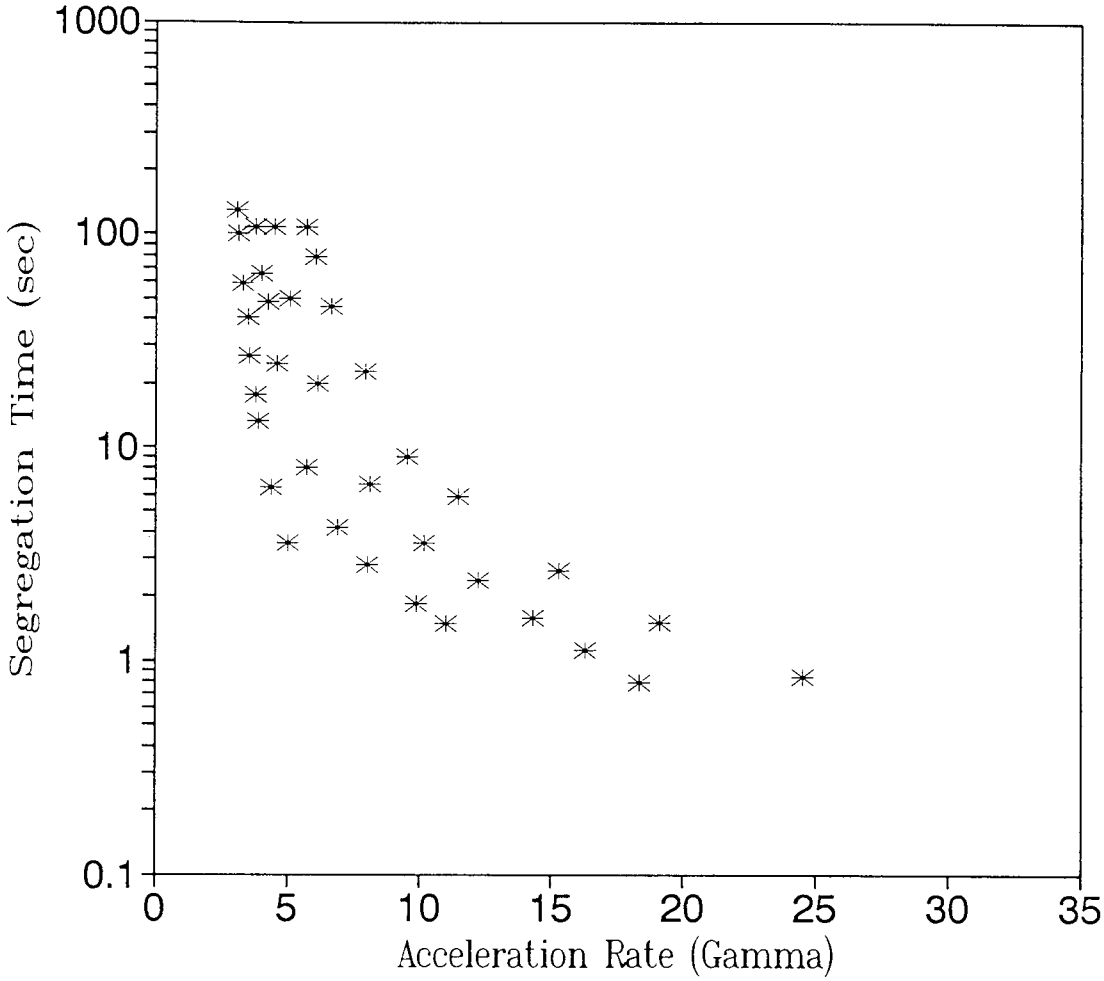

Figure 21 Segregation time vs acceleration rate for an aspect ratio of 3:1 with a bed height of 26 layers for rough wall conditions. The asterisks represent the 4 frequencies tested.

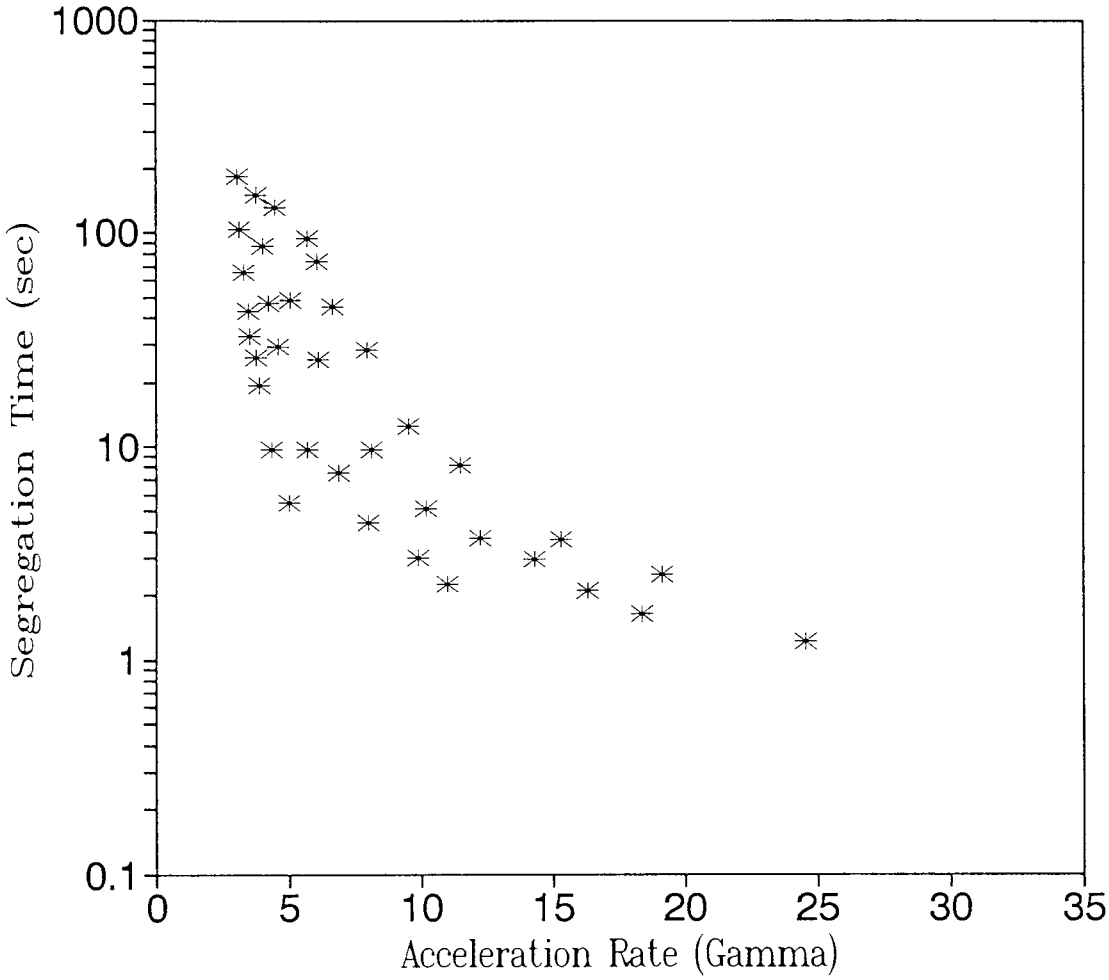

Figure 22 Segregation time vs. acceleration rate for an aspect ratio of 1:1 with a bed height of 26 layers for rough wall conditions. The asterisks represent the 4 frequencies tested.

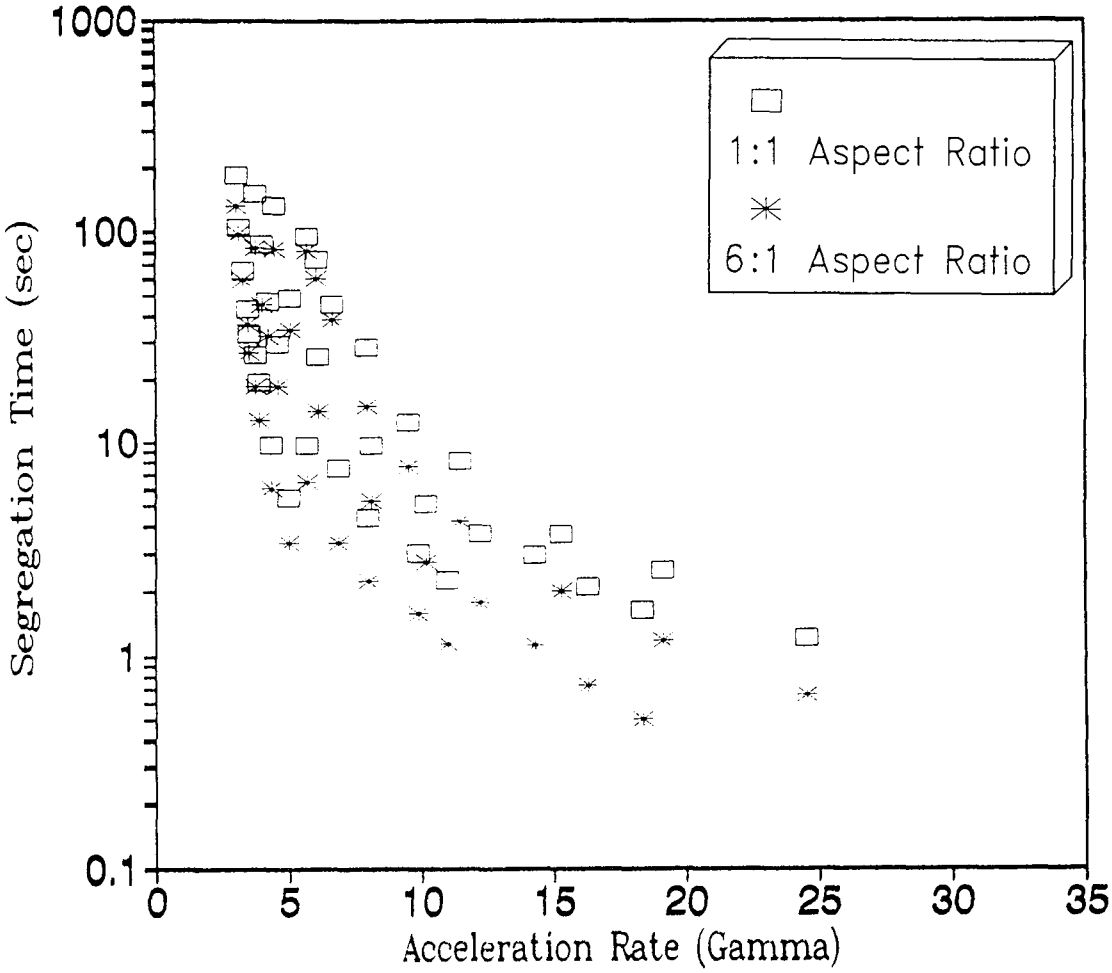

Figure 23 Segregation time vs acceleration rate for aspect ratios of 1:1 and 6:1 with a bed height of 26 layers for rough wall conditions The plot is representative of the 4 frequencies tested

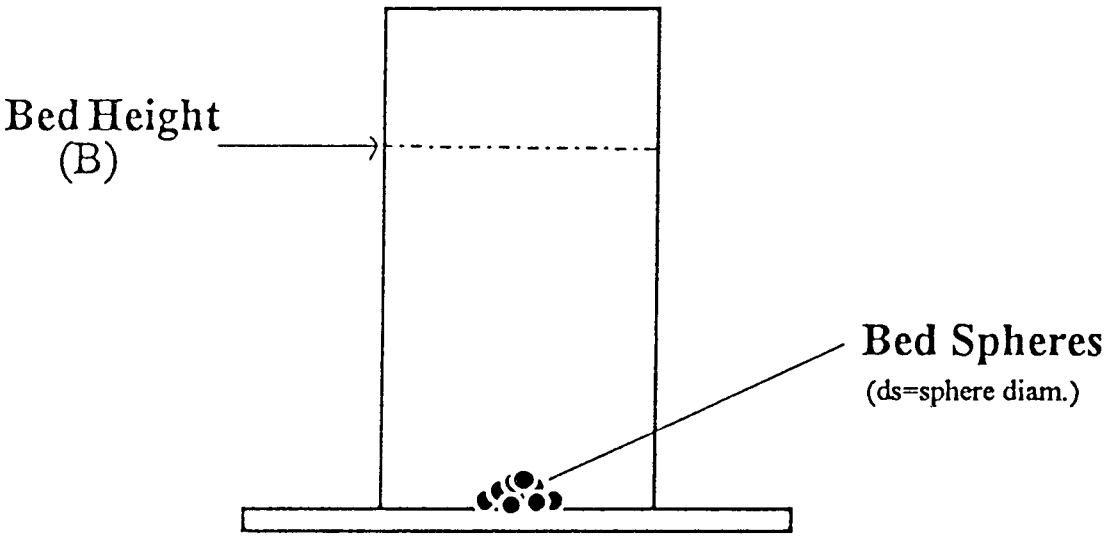

Figure 24 Experimental setup with adjusted bed height for ten dyed spheres.

APPENDIX B

The following is the data taken for the experimental setup having a smooth cylindrical wall. There are four data sets.

Data Set 1

f=10Hz Weight=305g #layers=26 Lg/sm=6

Amp. [in]	Gain [volts]	Humidity [%]	Time [sec]	Avg. Time [sec]
0.469	4.35	50	9.983	
"	"	50	9.202	
"	"	51	9.433	9.45
"	"	50	9.199	
"	"	51	9.433	
0.433	4	50	14.001	
"	"	51	13.781	
"	"	50	13.566	13.666
"	"	53	13.633	
"	"	50	13.299	
0.385	3.6	51	25.001	
"	"	50	22.733	
"	"	49	21.599	22.613
"	"	50	21.766	
"	"	51	21.966	
0.351	3.2	50	32.399	
"	"	51	32.799	
"	"	50	29.299	30.492
"	"	50	30.299	
"	"	51	27.666	
0.3	2.8	50	58.001	
"	"	49	58.499	
"	"	52	55.299	56.713
"	"	51	56.599	
"	"	52	55.166	
0.289	2.7	50	71.166	
"	"	52	71.133	
"	"	53	77.399	74.067
"	"	52	74.202	
"	"	50	75.833	
0.28	2.6	52	96.433	
"	"	53	84.433	
"	"	52	89.333	88.88
"	"	52	87.466	
"	"	52	86.933	
0.268	2.5	53	128.399	
"	"	51	120.433	
"	"	51	128.631	124.406
"	"	52	123.933	
"	"	50	120.633	
0.259	2.4	50	135.299	
"	"	51	140.499	
"	"	51	158.633	142.773
"	"	50	138.966	
"	"	51	140.466	
0.254	2.35	52	184.699	
"	"	51	178.499	
"	"	49	184.001	181.106
"	"	51	177.833	
"	"	52	180.499	

Data Set 2

f=15HZ Weight=305g #layers=26 Lg/sm=6

Amp. [in]	Gain [volts]	Humidity [%]	Time [sec]	Avg. Time [sec]
0.472	6.3	48	3.899	
"	"	49	3.899	
"	"	49	3.566	3.719
"	"	50	3.666	
"	"	50	3.566	
0.391	5.2	50	4.433	
"	"	49	4.199	
"	"	48	4.099	4.299
"	"	49	4.366	
"	"	48	4.399	
0.287	3.8	48	5.766	
"	"	48	5.333	
"	"	48	5.599	5.553
"	"	49	5.966	
"	"	49	5.099	
0.235	3.1	50	10.001	
"	"	50	9.666	
"	"	50	9.833	9.766
"	"	51	9.599	
"	"	51	9.433	
0.19	2.6	50	14.733	
"	"	51	14.199	
"	"	50	14.766	14.646
"	"	50	14.666	
"	"	51	14.866	
0.174	2.35	50	21.799	
"	"	50	21.966	
"	"	50	22.001	22.039
"	"	50	22.399	
"	"	50	22.033	
0.153	2.06	50	38.001	
"	"	50	38.666	
"	"	52	39.333	39.006
"	"	53	38.099	
"	"	51	40.933	
0.136	1.83	48	64.299	
"	"	48	72.933	
"	"	48	72.566	78.559
"	"	48	89.033	
"	"	48	93.966	
0.116	1.55	52	200.233	
"	"	51	212.333	
"	"	54	219.066	213.266
"	"	51	210.666	
"	"	52	224.033	

Data Set 3

f=20HZ Weight=305g #layers=26 Lg/Sm=6

Amp. [in]	Gain [volts]	Humidity [%]	Time [sec]	Avg. Time [sec]
0.457	7.9	50	1.233	
"	"	48	1.533	
"	"	48	1.299	1.419
"	"	48	1.599	
"	"	51	1.433	
0.409	7.1	50	1.733	
"	"	53	1.699	
"	"	53	1.833	1.813
"	"	53	1.833	
"	"	50	1.966	
0.35	6	49	2.399	
"	"	49	2.033	
"	"	50	2.233	2.966
"	"	48	2.733	
"	"	50	2.533	
0.321	5.55	51	3.033	
"	"	50	3.199	
"	"	52	2.966	2.966
"	"	49	2.766	
"	"	49	2.866	
0.287	4.9	49	3.766	
"	"	49	3.933	
"	"	50	3.501	3.913
"	"	49	4.099	
"	"	51	4.199	
0.235	4.15	50	5.366	
"	"	50	5.433	
"	"	52	5.566	5.686
"	"	54	6.199	
"	"	51	5.866	
0.21	3.65	55	5.933	
"	"	51	6.933	
"	"	51	6.466	6.453
"	"	50	6.633	
"	"	51	6.299	
0.179	3.1	49	7.003	
"	"	49	10.003	
"	"	50	7.499	8.026
"	"	51	7.066	
"	"	51	8.499	
0.103	1.83	52	22.899	
"	"	51	22.633	
"	"	53	22.133	22.386
"	"	51	22.233	
"	"	51	22.033	
0.08	1.43	49	58.133	
"	"	49	55.433	
"	"	52	53.533	56.733
"	"	50	59.599	
"	"	48	56.966	
0.067	1.175	54	146.166	
"	"	49	189.399	
"	"	55	157.199	160.833
"	"	52	169.533	
"	"	51	147.866	

Data Set 4

f=25HZ Weight=305g #layers=26 Lg/Sm=6

Amp. [in]	Gain [volts]	Humidity [%]	Time [sec]	Avg. Time [sec]
0.45	9.7	53	0.996	
"	"	50	1.001	
"	"	50	0.899	0.966
"	"	49	1.001	
"	"	51	0.933	
0.358	7.95	48	1.266	
"	"	51	1.233	
"	"	50	1.266	1.255
"	"	52	1.236	
"	"	48	1.274	
0.254	5.6	48	2.333	
"	"	48	2.433	
"	"	49	2.366	2.377
"	"	50	2.466	
"	"	48	2.288	
0.216	4.8	45	3.166	
"	"	46	3.333	
"	"	48	3.233	3.279
"	"	47	3.433	
"	"	49	3.233	
0.18	4	48	4.466	
"	"	49	4.266	
"	"	48	4.866	4.626
"	"	46	4.833	
"	"	47	4.799	
0.117	2.7	46	10.099	
"	"	46	10.199	
"	"	47	10.166	10.026
"	"	48	9.766	
"	"	50	9.899	
0.089	2.06	46	21.399	
"	"	47	18.933	
"	"	47	19.266	20.339
"	"	46	22.033	
"	"	47	26.066	
0.07	1.625	48	25.499	
"	"	48	26.233	
"	"	47	26.499	26.153
"	"	48	26.633	
"	"	49	25.849	
0.048	1.1	47	146.733	
"	"	47	120.001	
"	"	46	121.833	130.14
"	"	48	134.633	
"	"	47	127.499	

The following is the data taken for the experimental setup having a rough cylindrical wall. There are twelve data sets.

Data Set 1

f=10Hz Weight=305g #layers=26 Lg/sm=6

Amp. [in]	Gain [volts]	Humidity [%]	Time [sec]	Avg. Time [sec]
0.495	4.9	54	3.466	
"	"	54	3.499	
"	"	55	3.166	3.333
"	"	54	3.333	
"	"	52	3.199	
0.43	4.18	52	6.299	
"	"	52	6.466	
"	"	51	6.033	6.073
"	"	51	6.066	
"	"	51	5.533	
0.385	3.7	49	11.866	
"	"	50	12.199	
"	"	53	14.366	12.699
"	"	54	13.133	
"	"	54	11.933	
0.37	3.5	53	19.199	
"	"	54	16.733	
"	"	53	19.499	18.359
"	"	53	17.733	
"	"	52	18.633	
0.35	3.3	51	25.766	
"	"	51	27.199	
"	"	55	26.899	26.679
"	"	56	25.366	
"	"	56	28.166	
0.34	3.18	53	36.399	
"	"	50	35.866	
"	"	50	36.633	36.353
"	"	55	35.866	
"	"	51	37.033	
0.325	3.05	52	56.399	
"	"	52	68.733	
"	"	51	59.066	60.073
"	"	55	60.033	
"	"	55	56.133	
0.31	2.9	52	91.833	
"	"	53	101.833	
"	"	53	104.633	98.5
"	"	53	102.133	
"	"	55	92.066	
0.3	2.8	50	120.733	
"	"	51	114.599	
"	"	50	133.066	133.933
"	"	50	156.866	
"	"	50	144.399	

Data Set 2

f=15HZ Weight=305g #layers=26 Lg/sm=6

Amp. [in]	Gain [volts]	Humidity [%]	Time [sec]	Avg. Time [sec]
0.48	6.4	64	1.266	
"	"	64	1.166	
"	"	63	1.066	1.133
"	"	62	1.133	
"	"	61	1.033	
0.425	5.65	57	1.399	
"	"	57	1.433	
"	"	57	1.566	1.566
"	"	56	1.966	
"	"	56	1.466	
0.35	4.7	56	2.233	
"	"	57	2.233	
"	"	54	2.166	2.226
"	"	53	2.333	
"	"	52	2.166	
0.3	4.05	54	3.433	
"	"	54	3.266	
"	"	52	3.233	3.346
"	"	52	3.333	
"	"	52	3.466	
0.25	3.38	55	6.366	
"	"	52	6.733	
"	"	52	6.433	6.433
"	"	52	6.399	
"	"	52	6.233	
0.2	2.65	51	18.033	
"	"	51	18.366	
"	"	51	18.166	18.379
"	"	52	18.899	
"	"	51	18.433	
0.185	2.42	50	34.466	
"	"	50	32.533	
"	"	52	32.666	32.073
"	"	53	30.733	
"	"	51	29.966	
0.175	2.38	51	45.399	
"	"	51	45.566	
"	"	51	45.866	45.353
"	"	50	47.866	
"	"	52	42.066	
0.165	2.2	52	84.766	
"	"	51	89.933	
"	"	54	82.299	84.946
"	"	51	80.966	
"	"	52	86.766	

Data Set 3

f=20HZ Weight=305g #layers=26 Lg/Sm=6

Amp. [in]	Gain [volts]	Humidity [%]	Time [sec]	Avg. Time [sec]
0.45	8.1	52	0.499	
"	"	54	0.466	
"	"	57	0.533	0.499
"	"	56	0.533	
"	"	55	0.466	
0.4	7.02	51	0.733	
"	"	55	0.733	
"	"	56	0.733	0.726
"	"	57	0.699	
"	"	53	0.699	
0.35	6.1	54	1.066	
"	"	53	1.099	
"	"	53	1.099	1.126
"	"	52	1.266	
"	"	52	1.099	
0.3	5.2	51	1.633	
"	"	51	1.799	
"	"	51	1.766	1.759
"	"	51	1.866	
"	"	53	1.733	
0.25	4.35	54	2.699	
"	"	52	2.699	
"	"	51	2.733	2.719
"	"	50	2.799	
"	"	50	2.666	
0.2	3.45	51	5.266	
"	"	53	5.233	
"	"	53	5.199	5.259
"	"	53	5.366	
"	"	50	5.233	
0.15	2.62	50	14.399	
"	"	50	13.866	
"	"	51	13.533	13.959
"	"	51	14.199	
"	"	50	13.799	
0.125	2.19	51	34.766	
"	"	51	34.833	
"	"	50	32.566	34.059
"	"	51	33.833	
"	"	50	34.299	
0.11	1.9	50	85.599	
"	"	52	79.733	
"	"	51	87.633	82.886
"	"	52	84.566	
"	"	53	76.899	

Data Set 4

f=25HZ Weight=305g #layers=26 Lg/Sm=6

Amp. [in]	Gain [volts]	Humidity [%]	Time [sec]	Avg. Time [sec]
0.385	8.4	55	0.633	
"	"	53	0.699	
"	"	54	0.699	0.659
"	"	55	0.599	
"	"	55	0.666	
0.3	6.59	52	1.166	
"	"	51	1.166	
"	"	52	1.133	1.173
"	"	49	1.133	
"	"	50	1.266	
0.24	5.4	52	2.033	
"	"	52	1.899	
"	"	53	1.966	1.999
"	"	53	2.099	
"	"	54	2.001	
0.18	4	53	4.266	
"	"	53	4.166	
"	"	53	4.266	4.239
"	"	53	4.199	
"	"	53	4.299	
0.15	3.38	53	7.833	
"	"	52	7.599	
"	"	49	7.666	7.586
"	"	53	7.499	
"	"	53	7.333	
0.125	2.8	54	15.599	
"	"	54	15.133	
"	"	54	14.533	14.856
"	"	54	14.399	
"	"	54	14.566	
0.105	2.38	54	36.599	
"	"	54	37.066	
"	"	54	40.133	38.366
"	"	53	38.133	
"	"	54	39.333	
0.095	2.1	54	60.166	
"	"	51	60.166	
"	"	52	59.299	60.126
"	"	53	61.233	
"	"	52	59.766	
0.0898	2	52	82.766	
"	"	53	84.799	
"	"	52	80.433	82.539
"	"	53	79.533	
"	"	54	85.166	

Data Set 5

f=10Hz Weight=305g #layers=26 Lg/Sm=3

Amp. [in]	Gain [volts]	Humidity [%]	Time [sec]	Avg. Time [sec]
0.495	4.9	57	3.699	
"	"	57	3.466	
"	"	56	3.533	3.526
"	"	55	3.599	
"	"	55	3.333	
0.43	4.18	57	7.033	
"	"	54	6.433	
"	"	52	6.499	6.493
"	"	51	5.999	
"	"	54	6.499	
0.385	3.7	57	12.799	
"	"	57	13.466	
"	"	57	14.399	13.333
"	"	58	13.066	
"	"	53	12.933	
0.37	3.5	55	17.399	
"	"	51	17.033	
"	"	52	17.866	17.753
"	"	52	17.399	
"	"	52	19.099	
0.35	3.3	53	27.299	
"	"	53	28.566	
"	"	52	25.033	26.926
"	"	52	26.299	
"	"	52	27.466	
0.34	3.18	52	38.299	
"	"	52	41.933	
"	"	51	44.499	40.726
"	"	51	40.733	
"	"	51	38.166	
0.325	3.05	51	56.733	
"	"	51	52.899	
"	"	51	63.266	58.366
"	"	50	56.566	
"	"	50	62.366	
0.31	2.9	53	90.766	
"	"	53	97.866	
"	"	52	106.333	99.593
"	"	52	100.599	
"	"	50	102.599	
0.3	2.8	50	131.299	
"	"	51	129.766	
"	"	50	128.366	128.519
"	"	50	125.899	
"	"	50	127.266	

Data Set 6

f=15HZ Weight=305g #layers=26 Lg/Sm=3

Amp. [in]	Gain [volts]	Humidity [%]	Time [sec]	Avg. Time [sec]
0.48	6.4	51	1.499	
"	"	54	1.466	
"	"	55	1.533	1.493
"	"	54	1.466	
"	"	54	1.499	
0.425	5.65	54	1.866	
"	"	53	1.833	
"	"	53	1.933	1.846
"	"	54	1.733	
"	"	53	1.866	
0.35	4.7	52	2.606	
"	"	50	2.733	
"	"	52	2.933	2.801
"	"	53	2.899	
"	"	54	2.833	
0.3	4.05	54	4.233	
"	"	54	4.166	
"	"	54	4.166	4.166
"	"	54	3.966	
"	"	54	4.299	
0.25	3.38	54	8.533	
"	"	54	7.366	
"	"	53	8.199	8.039
"	"	52	8.099	
"	"	52	8.001	
0.2	2.65	52	21.933	
"	"	51	25.833	
"	"	51	24.533	24.573
"	"	50	25.333	
"	"	50	25.233	
0.185	2.42	50	48.899	
"	"	51	45.066	
"	"	51	51.433	48.086
"	"	51	49.399	
"	"	50	45.633	
0.175	2.38	51	62.433	
"	"	51	63.499	
"	"	50	65.533	64.953
"	"	50	64.466	
"	"	50	68.866	
0.165	2.2	55	111.032	
"	"	50	110.599	
"	"	52	108.499	108.16
"	"	50	106.333	
"	"	52	104.333	

Data Set 7

f=20HZ Weight=305g #layers=26 Lg/Sm=3

Amp. [in]	Gain [volts]	Humidity [%]	Time [sec]	Avg. Time [sec]
0.45	8.1	55	0.933	
"	"	56	0.733	
"	"	56	0.799	0.793
"	"	56	0.766	
"	"	57	0.733	
0.4	7.02	56	1.133	
"	"	51	1.133	
"	"	51	1.199	1.119
"	"	51	1.099	
"	"	51	1.033	
0.35	6.1	51	1.666	
"	"	51	1.599	
"	"	51	1.599	1.599
"	"	50	1.566	
"	"	50	1.566	
0.3	5.2	50	2.433	
"	"	50	2.366	
"	"	52	2.366	2.366
"	"	50	2.399	
"	"	51	2.266	
0.25	4.35	52	3.799	
"	"	53	3.433	
"	"	53	3.666	3.573
"	"	52	3.599	
"	"	52	3.366	
0.2	3.45	50	6.866	
"	"	50	6.399	
"	"	51	6.699	6.686
"	"	51	6.866	
"	"	51	6.599	
0.15	2.62	53	18.566	
"	"	53	19.033	
"	"	51	21.466	19.966
"	"	51	21.866	
"	"	53	18.899	
0.125	2.19	51	53.899	
"	"	54	47.366	
"	"	53	48.566	49.899
"	"	52	49.333	
"	"	51	50.333	
0.11	1.9	50	107.833	
"	"	51	109.199	
"	"	49	117.366	108.259
"	"	50	100.966	
"	"	51	105.933	

Data Set 8

f=25HZ Weight=305g #layers=26 Lg/Sm=3

Amp. [in]	Gain [volts]	Humidity [%]	Time [sec]	Avg. Time [sec]
0.385	8.4	56	0.833	
"	"	55	0.833	
"	"	55	0.833	0.846
"	"	54	0.833	
"	"	57	0.899	
0.3	6.59	58	1.399	
"	"	57	1.566	
"	"	56	1.466	1.513
"	"	56	1.599	
"	"	54	1.533	
0.24	5.4	50	2.599	
"	"	55	2.699	
"	"	54	2.799	2.632
"	"	55	2.366	
"	"	54	2.699	
0.18	4	54	5.566	
"	"	54	6.033	
"	"	54	5.799	5.899
"	"	54	5.866	
"	"	53	6.233	
0.15	3.38	53	8.566	
"	"	53	8.899	
"	"	53	9.001	9.019
"	"	52	9.433	
"	"	52	9.199	
0.125	2.8	51	20.433	
"	"	53	23.133	
"	"	51	21.766	22.54
"	"	51	25.633	
"	"	51	21.733	
0.105	2.38	50	44.699	
"	"	54	44.733	
"	"	54	48.199	45.906
"	"	53	46.766	
"	"	53	45.133	
0.095	2.1	54	77.733	
"	"	53	80.766	
"	"	53	76.699	78.626
"	"	52	78.499	
"	"	53	79.433	
0.0898	2	53	102.499	
"	"	54	108.799	
"	"	53	104.566	107.686
"	"	52	115.133	
"	"	53	107.433	

Data Set 9

f=10Hz Weight=305g #layers=26 Lg/Sm=1

Amp. [in]	Gain [volts]	Humidity [%]	Time [sec]	Avg. Time [sec]
0.495	4.9	51	5.233	
"	"	54	5.566	5.477
"	"	55	5.633	
0.43	4.18	51	9.566	
"	"	52	9.699	9.71
"	"	53	9.866	
0.385	3.7	57	19.399	
"	"	57	20.033	19.133
"	"	57	18.066	
0.37	3.5	51	25.899	
"	"	53	25.933	25.966
"	"	53	26.066	
0.35	3.3	53	34.333	
"	"	53	30.466	32.498
"	"	52	32.699	
0.34	3.18	52	44.001	
"	"	52	42.499	42.477
"	"	51	40.931	
0.325	3.05	51	60.099	
"	"	51	69.766	65.055
"	"	51	65.299	
0.31	2.9	53	102.766	
"	"	53	110.766	103.844
"	"	52	98.001	
0.3	2.8	50	169.499	
"	"	51	205.766	183.505
"	"	50	175.251	

Data Set 10

f=15HZ Weight=305g #layers=26 Lg/Sm=1

Amp. [in]	Gain [volts]	Humidity [%]	Time [sec]	Avg. Time [sec]
0.48	6.4	56	2.133	
"	"	54	2.133	2.266
"	"	53	2.533	
0.425	5.65	50	2.766	
"	"	53	3.001	2.977
"	"	54	3.166	
0.35	4.7	54	4.133	
"	"	54	4.766	4.411
"	"	55	4.333	
0.3	4.05	50	7.533	
"	"	50	7.001	7.511
"	"	50	8.001	
0.25	3.38	50	9.899	
"	"	51	10.333	9.744
"	"	49	9.001	
0.2	2.65	51	26.001	
"	"	50	29.899	29.266
"	"	50	31.899	
0.185	2.42	50	46.899	
"	"	49	45.766	46.266
"	"	50	46.133	
0.175	2.38	50	83.501	
"	"	50	88.133	86.133
"	"	50	86.766	
0.165	2.2	52	150.133	
"	"	53	141.766	149.144
"	"	50	155.533	

Data Set 11

f=20Hz Weight=305g #layers=26 Lg/Sm=1

Amp. [in]	Gain [volts]	Humidity [%]	Time [sec]	Avg. Time [sec]
0.45	8.1	58	1.899	
"	"	55	1.266	1.655
"	"	55	1.799	
0.4	7.02	55	2.233	
"	"	56	2.133	2.122
"	"	56	2.001	
0.35	6.1	56	2.899	
"	"	53	2.966	2.955
"	"	52	3.001	
0.3	5.2	56	3.766	
"	"	55	4.001	3.755
"	"	55	3.501	
0.25	4.35	55	4.766	
"	"	55	5.233	5.122
"	"	54	5.366	
0.2	3.45	54	10.233	
"	"	53	9.166	9.722
"	"	53	9.766	
0.15	2.62	53	26.001	
"	"	52	28.133	25.455
"	"	53	22.233	
0.125	2.19	52	51.166	
"	"	52	47.233	48.466
"	"	51	46.999	
0.11	1.9	52	132.133	
"	"	53	132.799	130.488
"	"	52	126.533	

Data Set 12

f=25HZ Weight=305g #layers=26 Lg/Sm=1

Amp. [in]	Gain [volts]	Humidity [%]	Time [sec]	Avg. Time [sec]
0.385	8.4	54	1.233	
"	"	53	1.133	1.211
"	"	53	1.266	
0.3	6.59	51	2.799	
"	"	53	2.266	2.51
"	"	52	2.466	
0.24	5.4	54	3.199	
"	"	50	3.899	3.688
"	"	52	3.966	
0.18	4	49	8.266	
"	"	50	8.001	8.133
"	"	50	8.133	
0.15	3.38	52	12.566	
"	"	53	12.133	12.344
"	"	52	12.333	
0.125	2.8	51	33.499	
"	"	51	22.899	27.966
"	"	51	27.499	
0.105	2.38	54	45.233	
"	"	52	43.366	44.911
"	"	53	46.133	
0.095	2.1	53	67.733	
"	"	51	74.566	73.222
"	"	55	77.366	
0.0898	2	50	96.766	
"	"	52	90.233	93.711
"	"	52	94.133	

APPENDIX C

Angle of Repose Plots

The following are the plots generated from the Angle of Repose experiments.

The plots shown here were generated using Templegraph software.

Pour 1

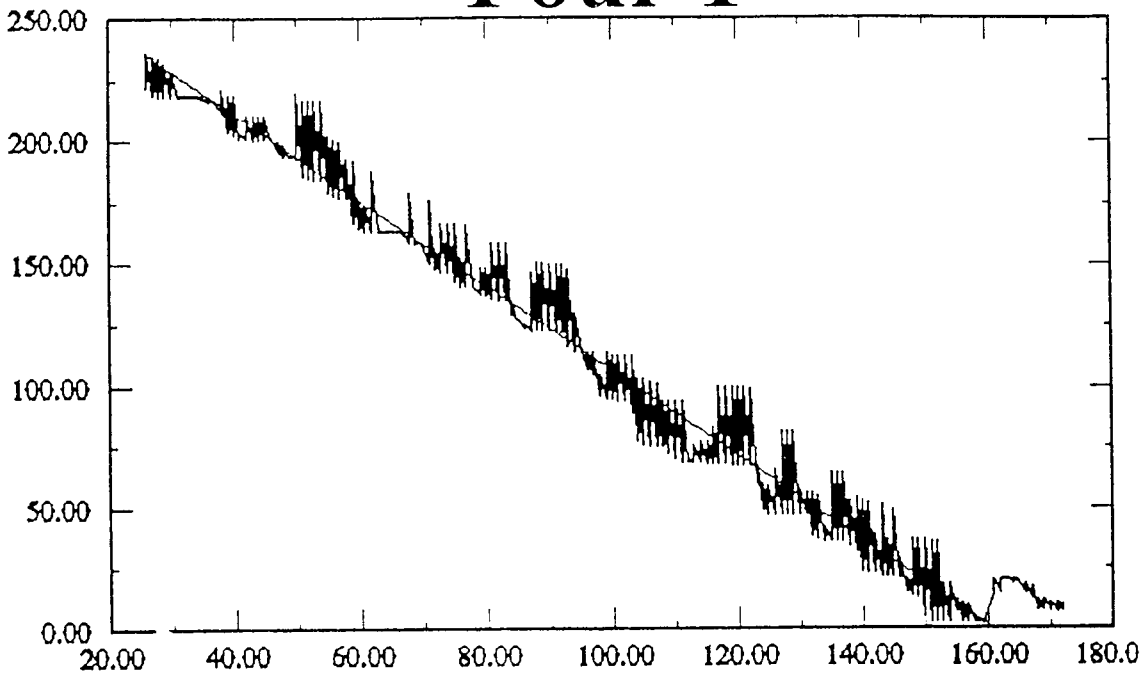

Linear (Y = aX+b) fit of Curve 1 from x = 25.7143 to x = 160.857:
a = -1.74422 +/- 0.0105233 b = 280.556 +/- 1.11124 Chi-square=67182.5
Linear correlation coefficient: -0.988042; Probability of correlation: 1

Pour 2

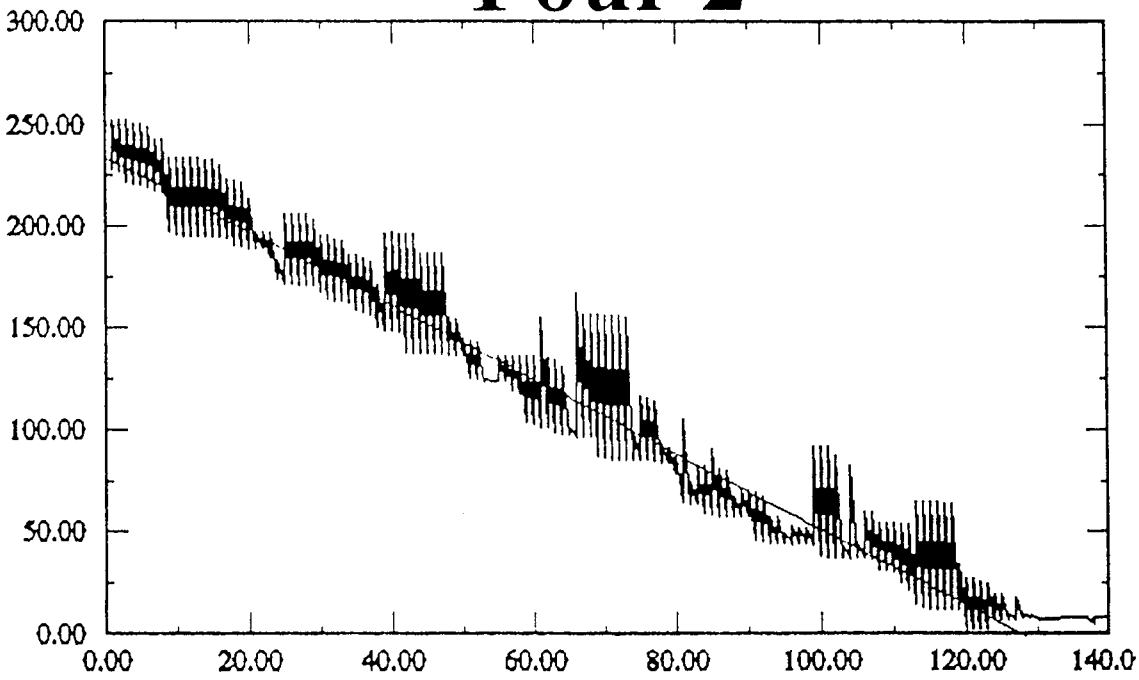

Linear (Y = aX+b) fit of Curve 1 from x = 0 to x = 128.25:
a = -1.82987 +/- 0.0141308 b = 233.637 +/- 1.02133 Chi-square=170194
Linear correlation coefficient: -0.976912; Probability of correlation: 1

Pour 3

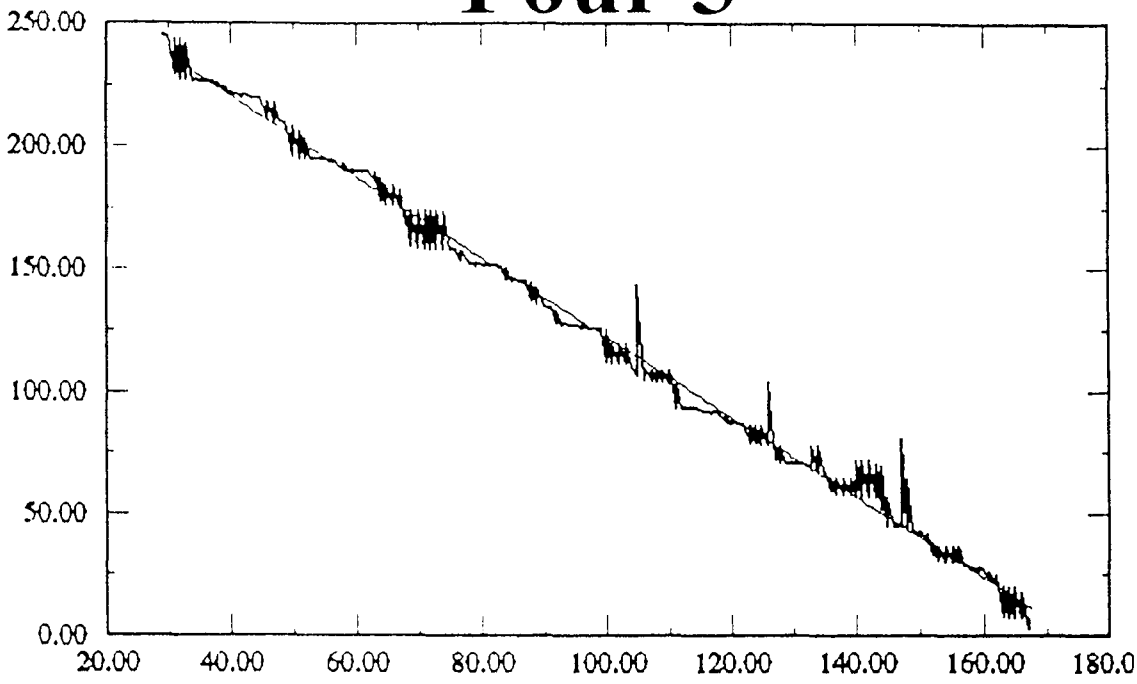

Linear (Y = aX+b) fit of Curve 1 from x = 28.5714 to x = 167.429:
a = -1.63837 +/- 0.00639347 b = 285.959 +/- 0.760119 Chi-square=16442.6
Linear correlation coefficient: -0.996009; Probability of correlation: 1

Pour 4

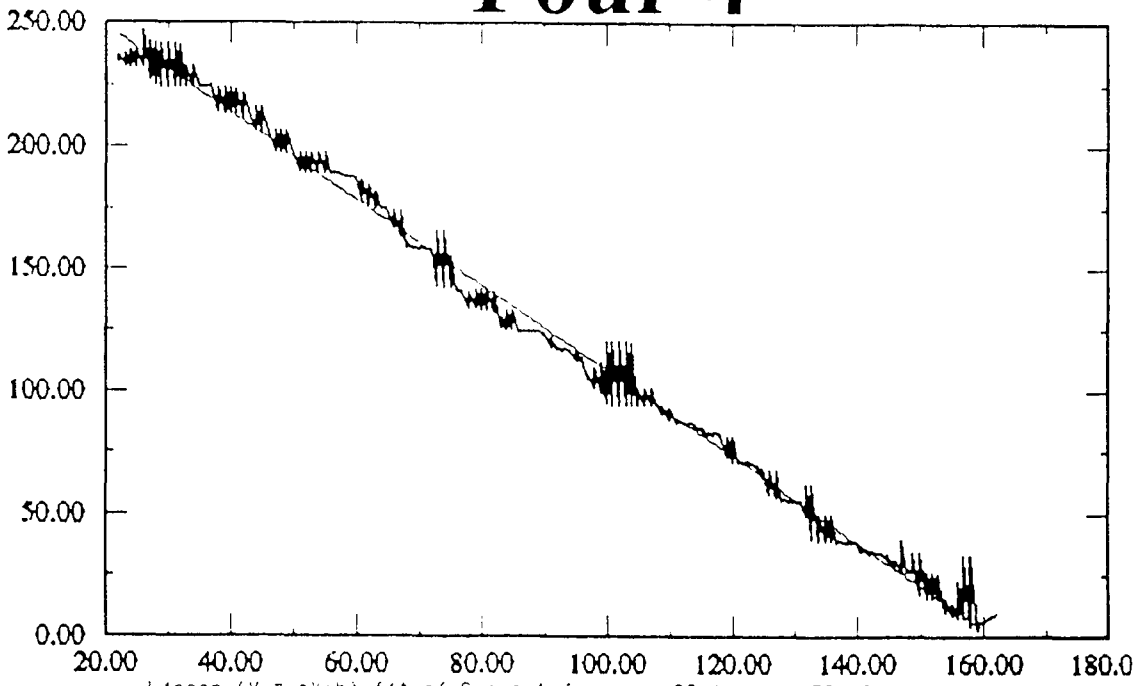

Linear (Y = aX+b) fit of Curve 1 from x = 22 to x = 159.429:
a = -1.75278 +/- 0.00742277 b = 283.598 +/- 0.718556 Chi-square=18877.7
Linear correlation coefficient: -0.995983; Probability of correlation: 1

Pour 5

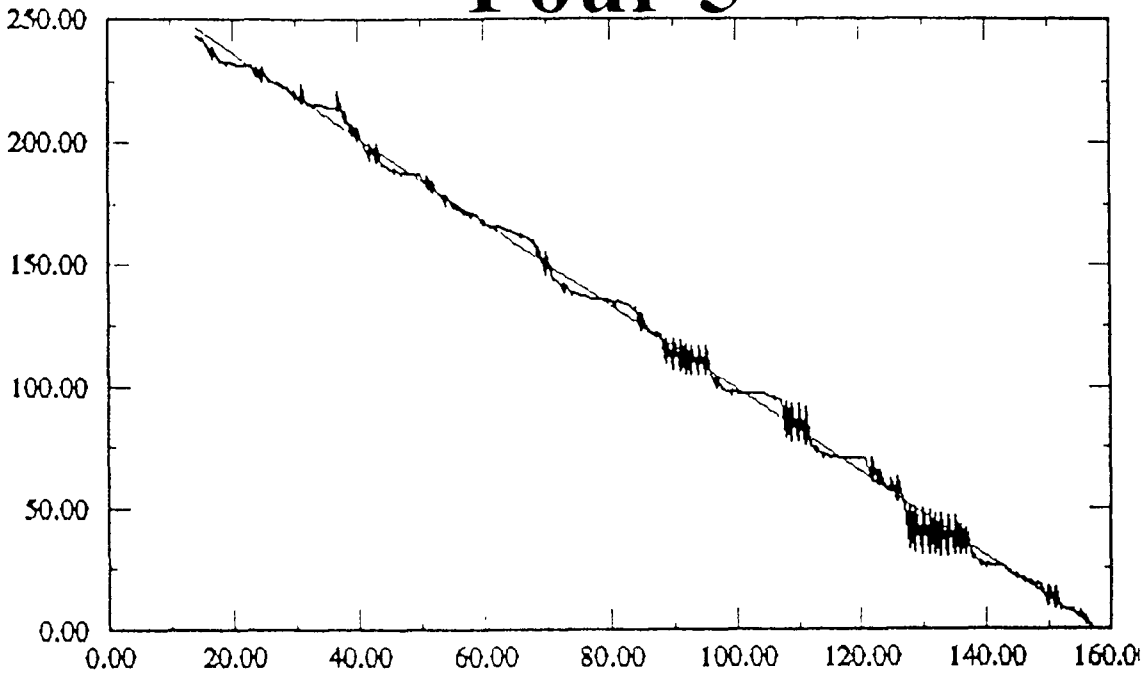

Linear (Y = aX+b) fit of Curve 1 from x = 14 to x = 156.857:
a = -1.71639 +/- 0.00607552 b = 270.711 +/- 0.589718 Chi-square=9936.34
Linear correlation coefficient: -0.997491; Probability of correlation: 1

Pour 6

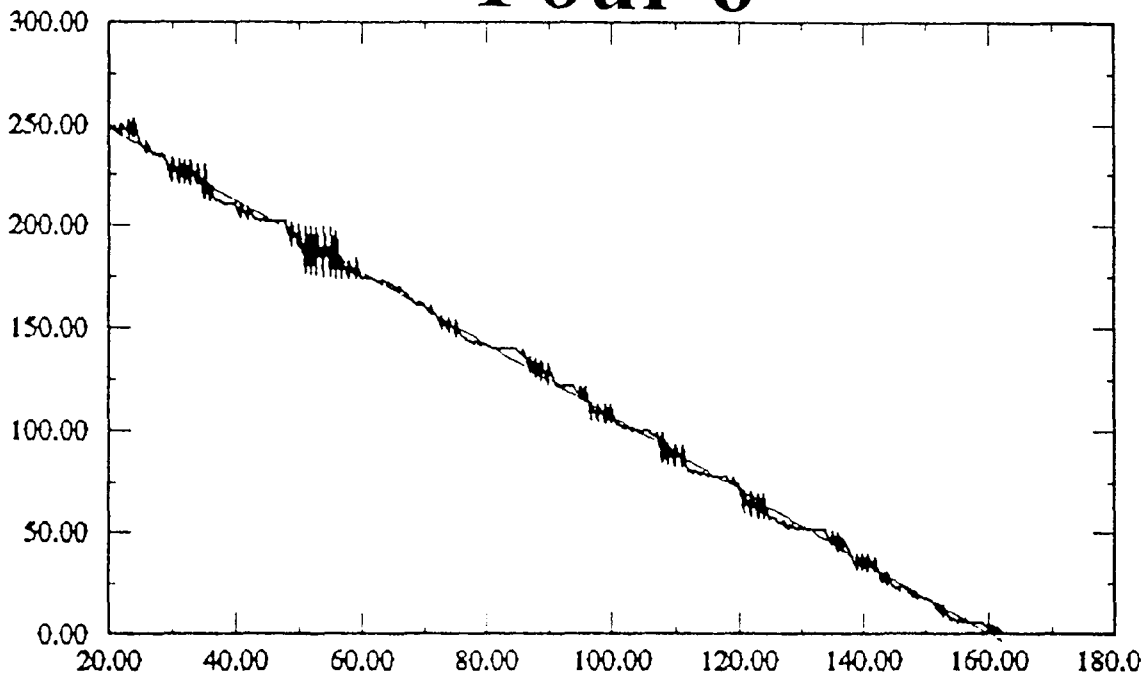

Linear (Y = aX+b) fit of Curve 1 from x = 20 to x = 162:
a = -1.76685 +/- 0.00566237 b = 283.013 +/- 0.543898 Chi-square=10409.6
Linear correlation coefficient: -0.997743; Probability of correlation: 1

Pour 7

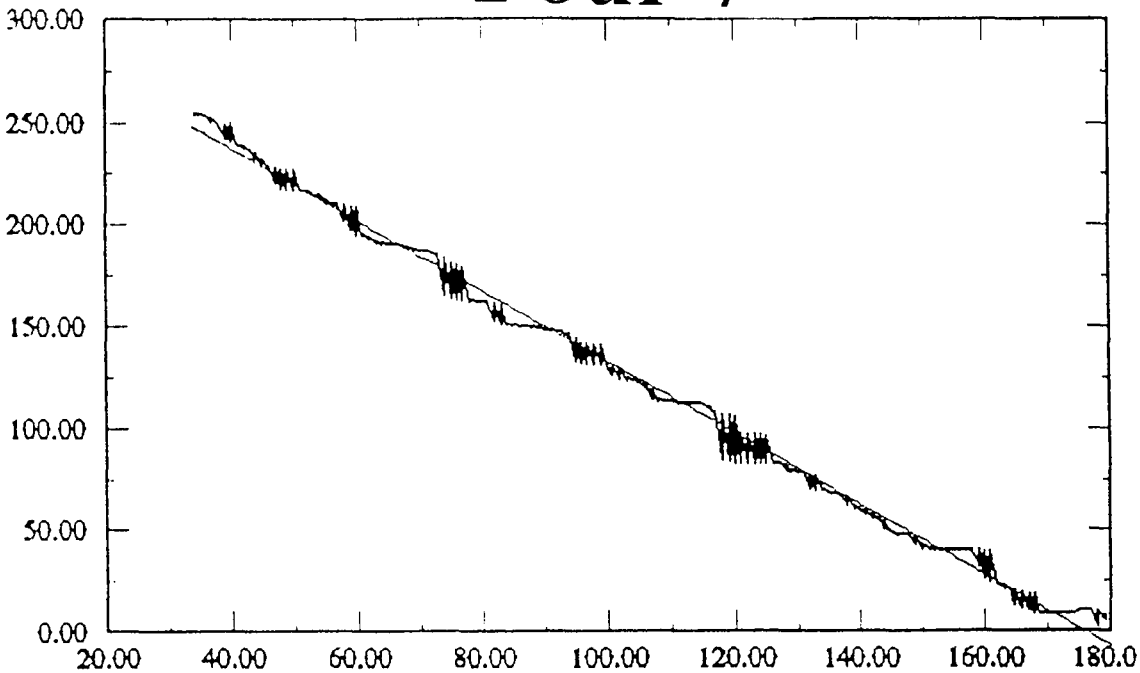

Linear (Y = aX+b) fit of Curve 1 from x = 33.7143 to x = 180:
a = -1.74533 +/- 0.00683579 b = 306.959 +/- 0.773265 Chi-square=14787.4
Linear correlation coefficient: -0.996771; Probability of correlation: 1

Pour 8

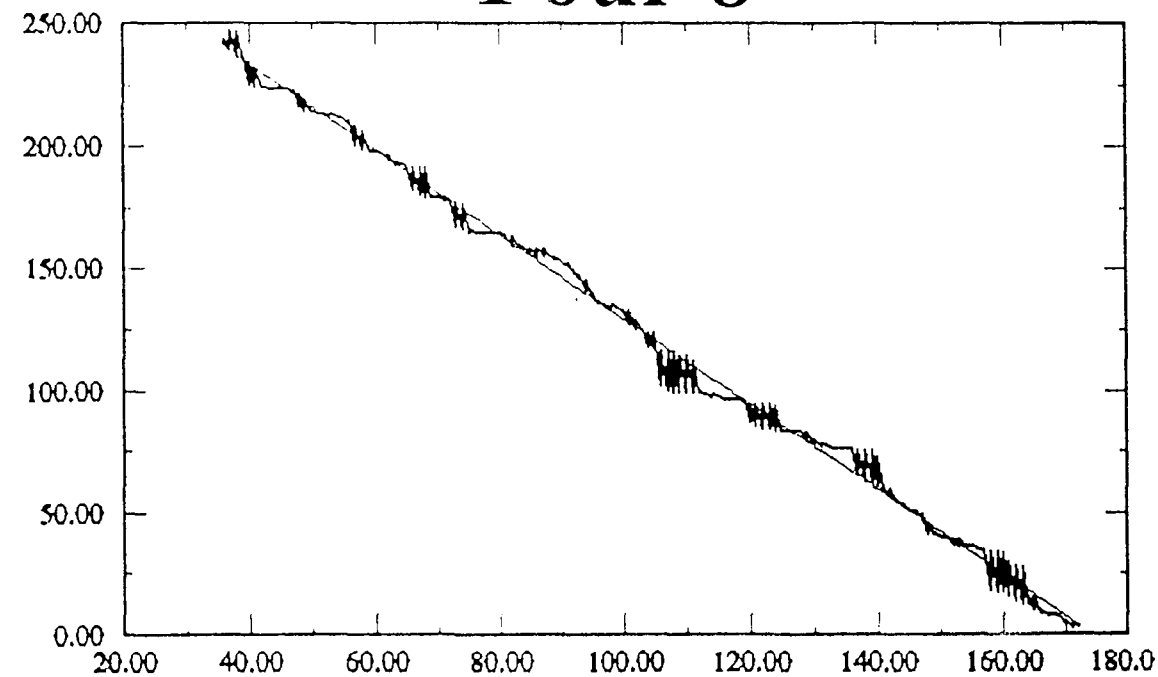

Linear (Y = aX+b) fit of Curve 1 from x = 35.4286 to x = 172.286:
a = -1.7382 +/- 0.00666658 b = 302.86 +/- 0.738033 Chi-square=10879
Linear correlation coefficient: -0.997129; Probability of correlation: 1

Pour 9

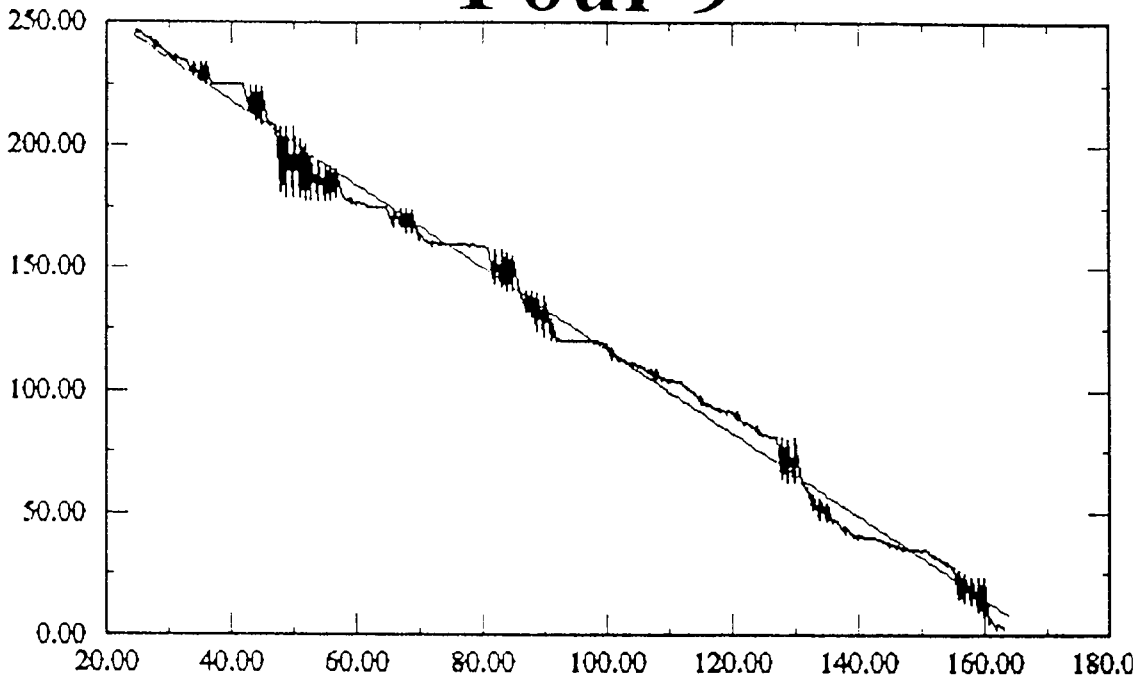

Linear (Y = aX+b) fit of Curve 1 from x = 24.2857 to x = 163.714:
a = -1.69415 +/- 0.00882727 b = 285.871 +/- 0.88819 Chi-square=20375.5
Linear correlation coefficient: -0.994601; Probability of correlation: 1

Pour 10

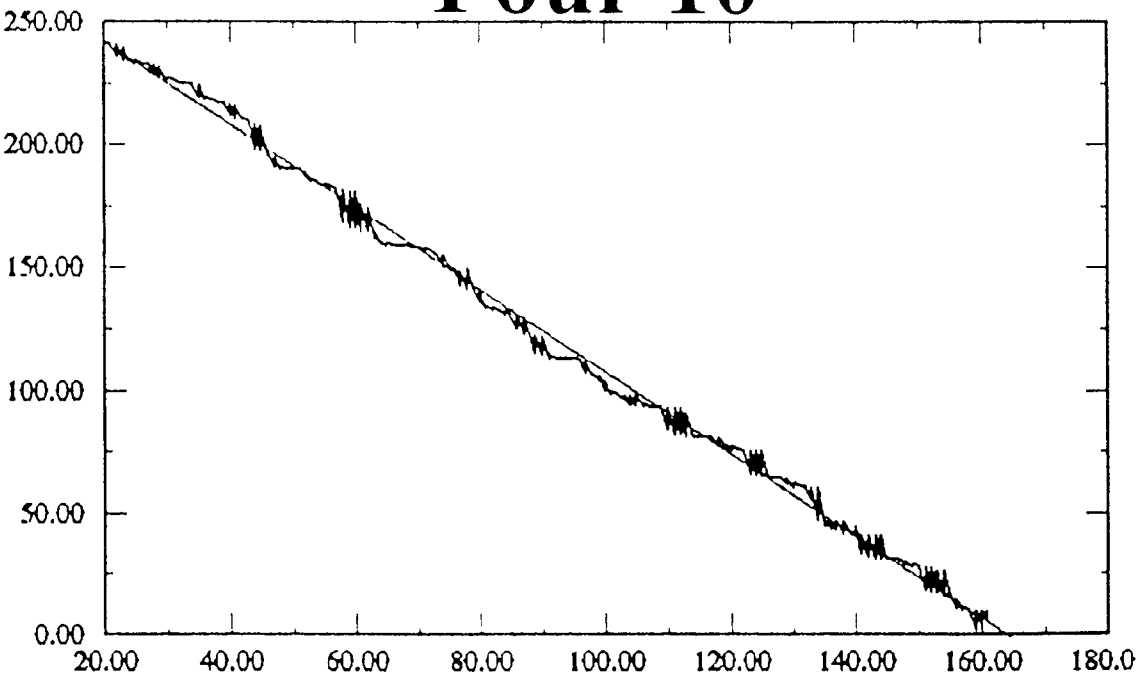

Linear (Y = aX+b) fit of Curve 1 from x = 20 to x = 180:
a = -1.67715 +/- 0.00541424 b = 275.12 +/- 0.548235 Chi-square=7708.3
Linear correlation coefficient: -0.997964; Probability of correlation: 1

Tumble 1

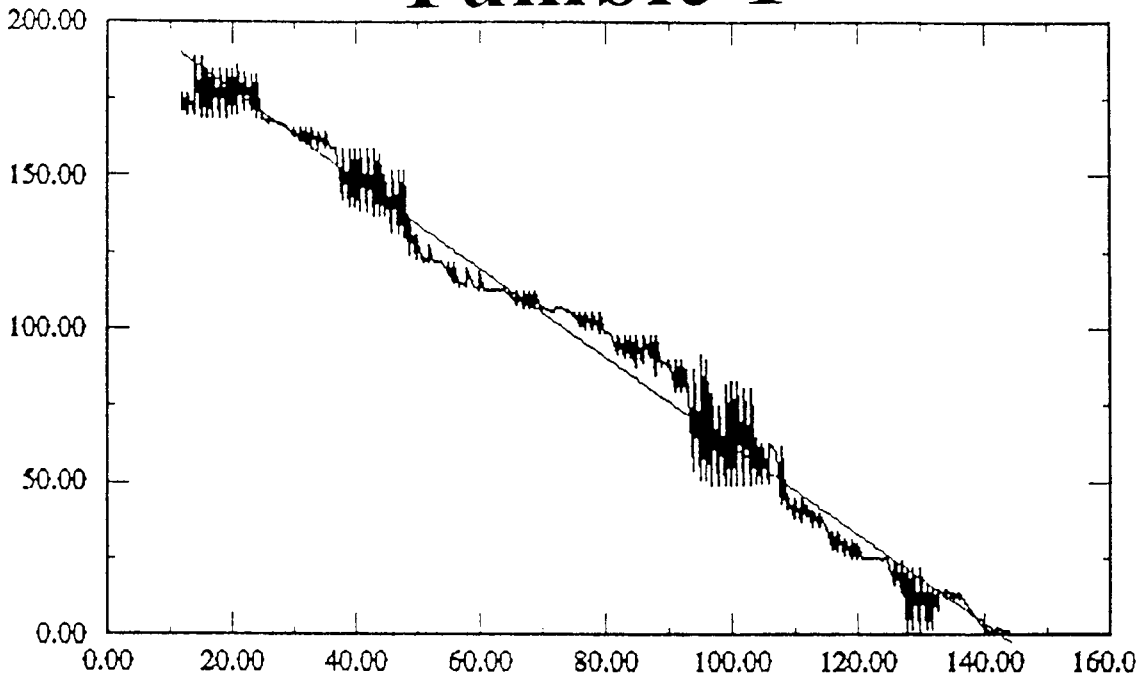

Linear (Y = aX+b) fit of Curve 1 from x = 11.7143 to x = 144.286:
a = -1.45134 +/- 0.0105208 b = 206.968 +/- 0.895223 Chi-square=39288.3
Linear correlation coefficient: -0.987015; Probability of correlation: 1

Tumble 2

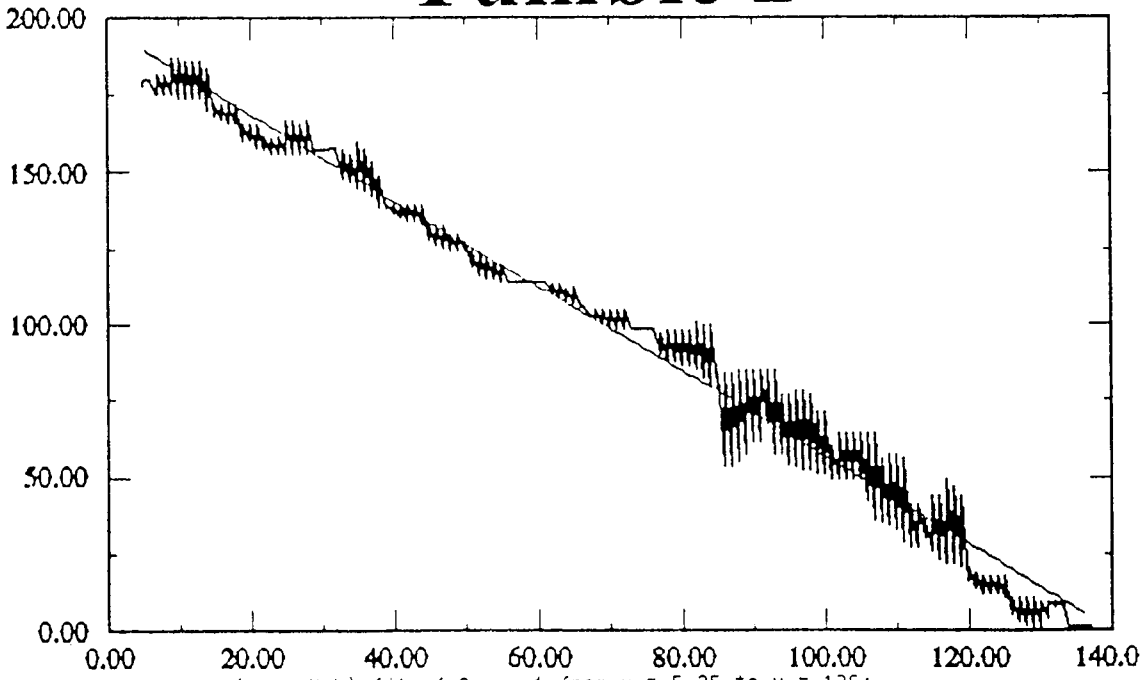

Linear (Y = aX+b) fit of Curve 1 from x = 5.25 to x = 136:
a = -1.40449 +/- 0.00853491 b = 196.746 +/- 0.722187 Chi-square=37097.1
Linear correlation coefficient: -0.988942; Probability of correlation: 1

Tumble3

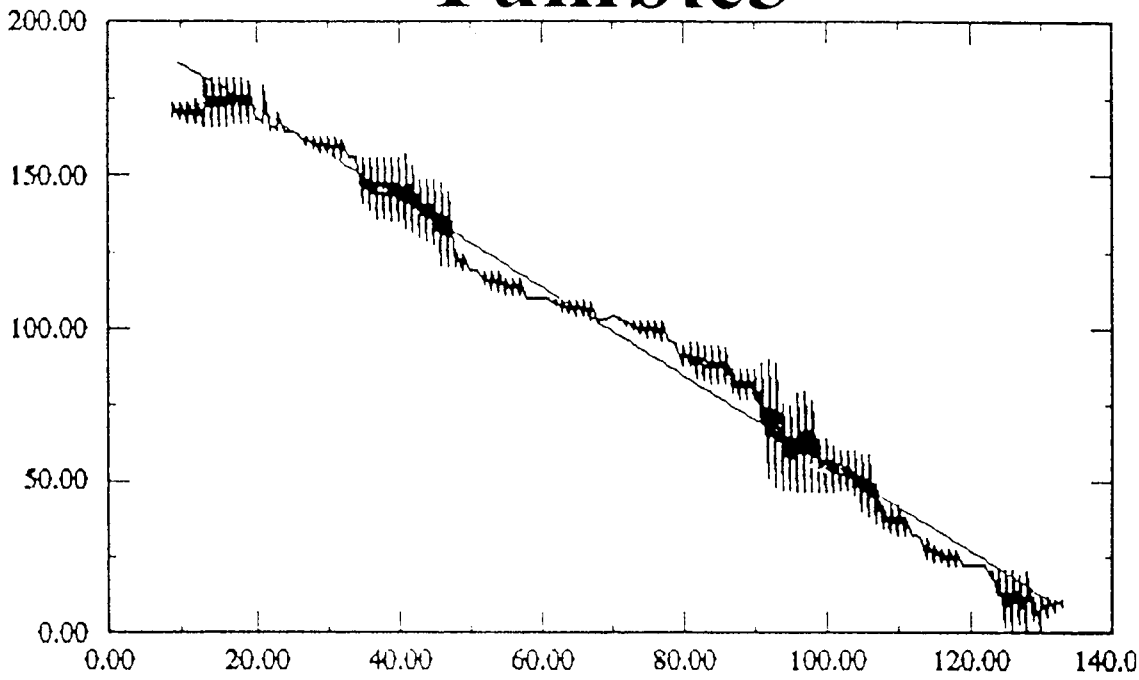

Linear (Y = aX+b) fit of Curve 1 from x = 9.5 to x = 132:
a = -1.4487 +/- 0.0105502 b = 200.623 +/- 0.880527 Chi-square=39587.7
Linear correlation coefficient: -0.985854; Probability of correlation: 1

Tumble 4

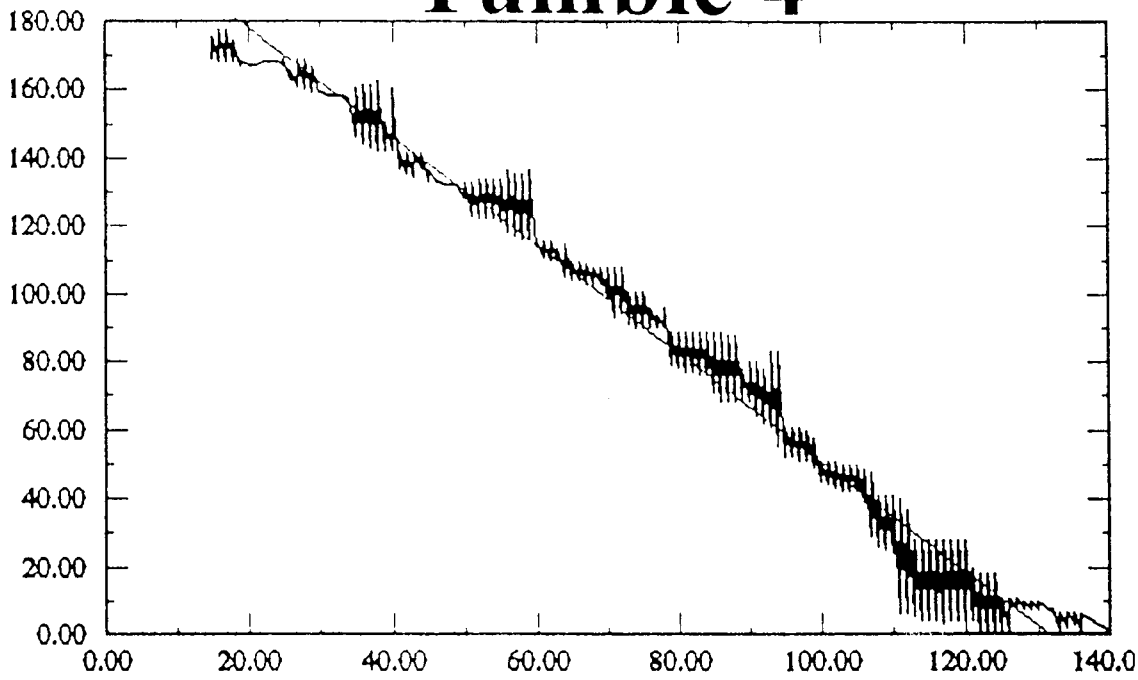

Linear (Y = aX+b) fit of Curve 1 from x = 14.5 to x = 140:
a = -1.59796 +/- 0.0102732 b = 210.162 +/- 0.891311 Chi-square=40494.2
Linear correlation coefficient: -0.987847; Probability of correlation: 1

Tumble 5

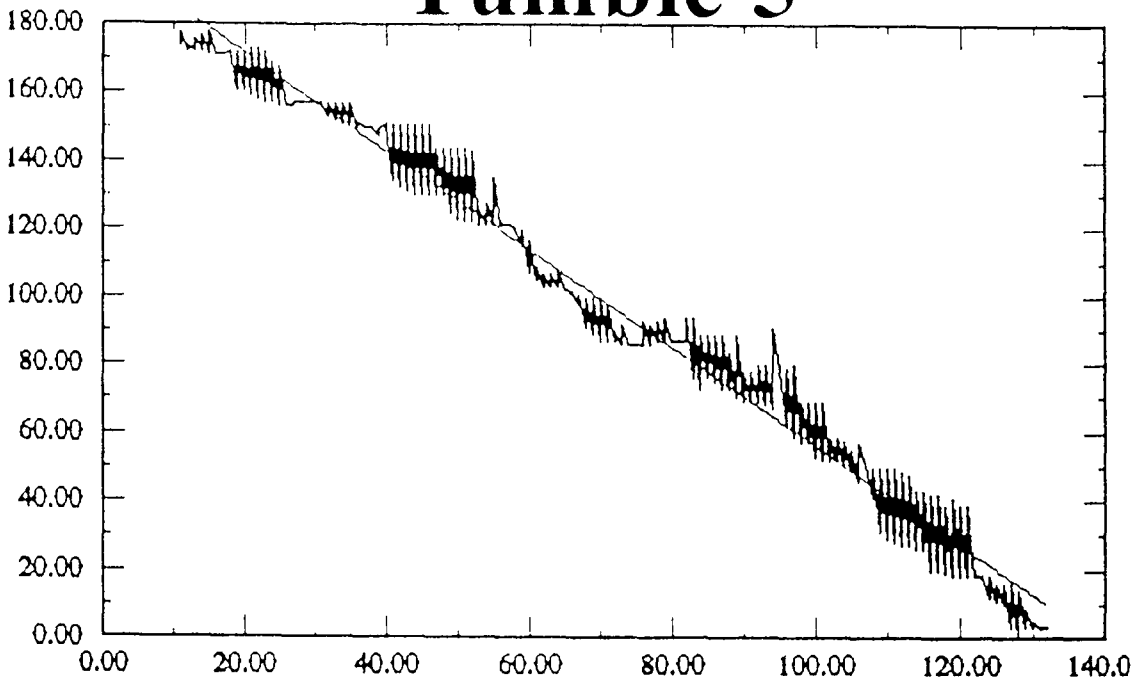

Linear (Y = aX+b) fit of Curve 1 from x = 11 to x = 131.5:
a = -1.44613 +/- 0.0097788 b = 200.665 +/- 0.805072 Chi-square=26663.3
Linear correlation coefficient: -0.993071; Probability of correlation: 1

Tumble 6

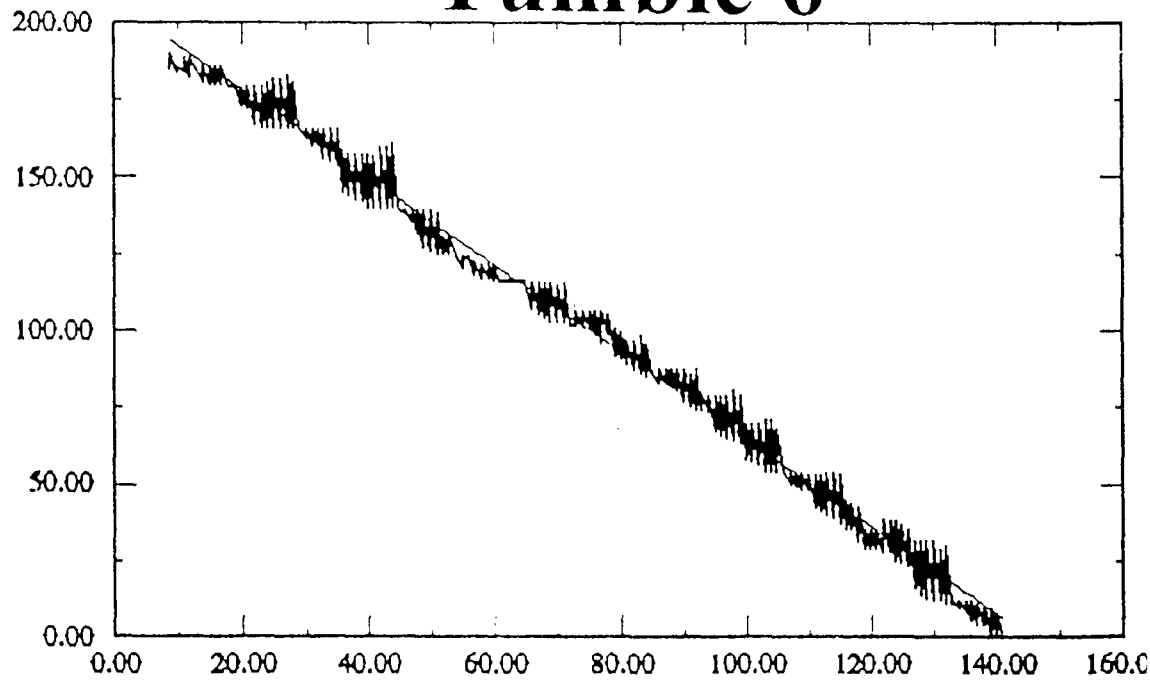

Linear (Y = aX+b) fit of Curve 1 from x = 8.85714 to x = 140.857:
a = -1.42303 +/- 0.00581424 b = 206.829 +/- 0.497098 Chi-square=18736.2
Linear correlation coefficient: -0.994848; Probability of correlation: 1

Tumble 7

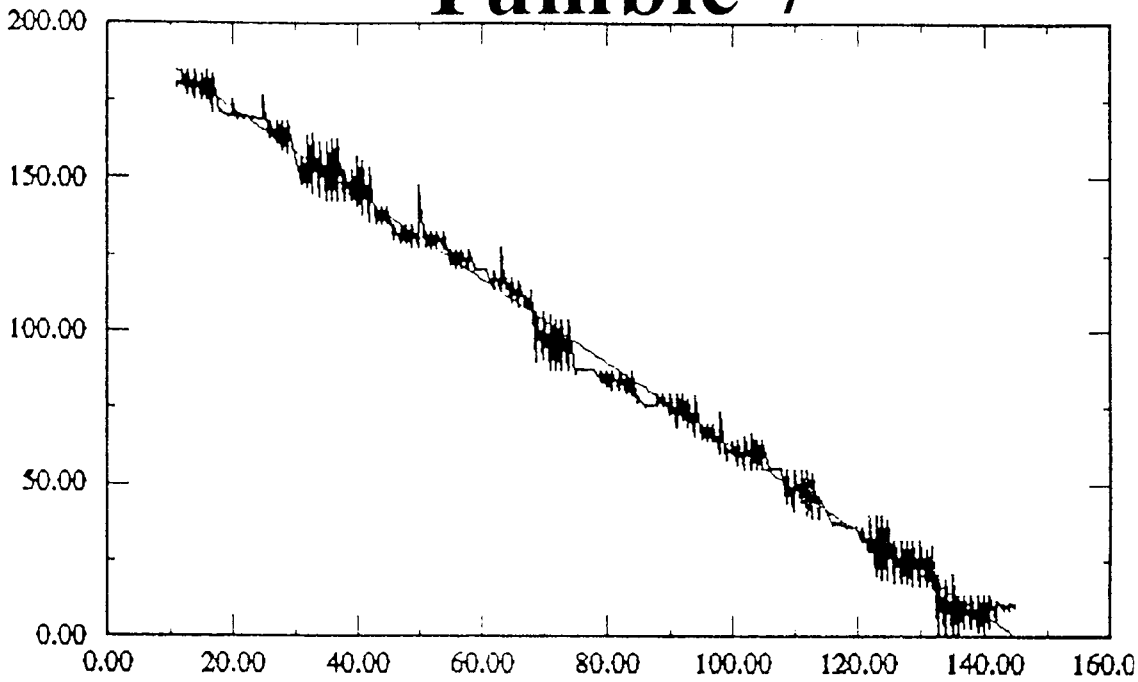

Linear (Y = aX+b) fit of Curve 1 from x = 10.8571 to x = 145.143:
a = -1.37805 +/- 0.00591195 b = 200.011 +/- 0.516615 Chi-square=16808.8
Linear correlation coefficient: -0.994913; Probability of correlation: 1

Tumble 8

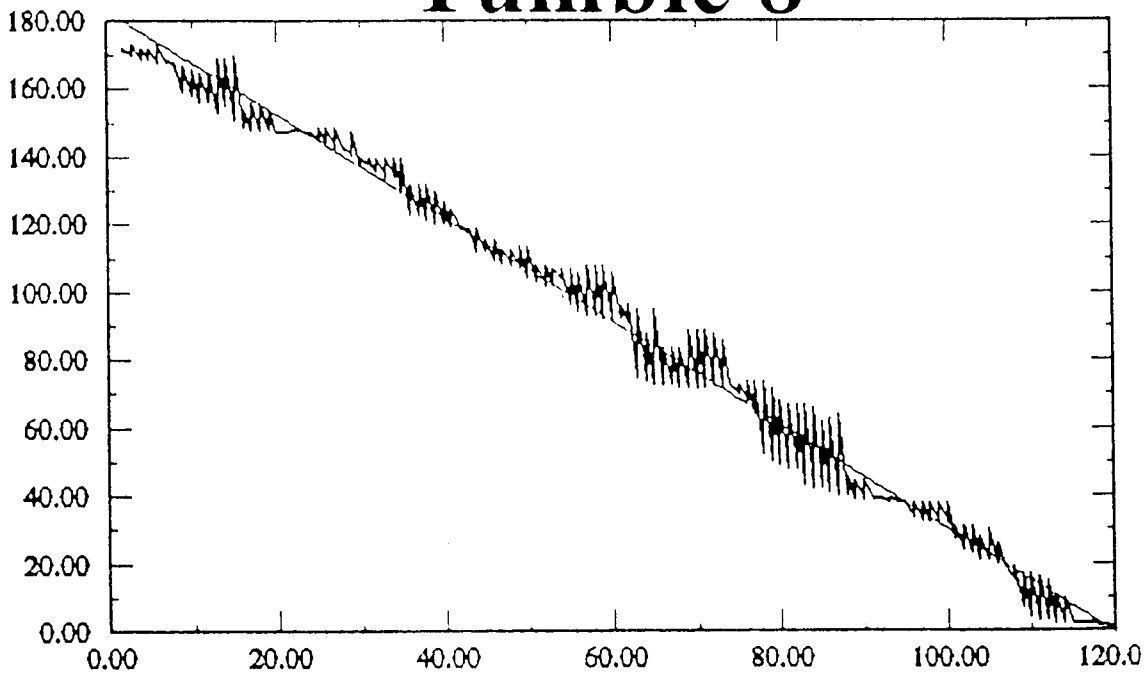

Linear (Y = aX+b) fit of Curve 1 from x = 1.92857 to x = 120:
a = -1.52764 +/- 0.00817277 b = 182.891 +/- 0.565771 Chi-square=17249
Linear correlation coefficient: -0.992808; Probability of correlation: 1

Tumble 9

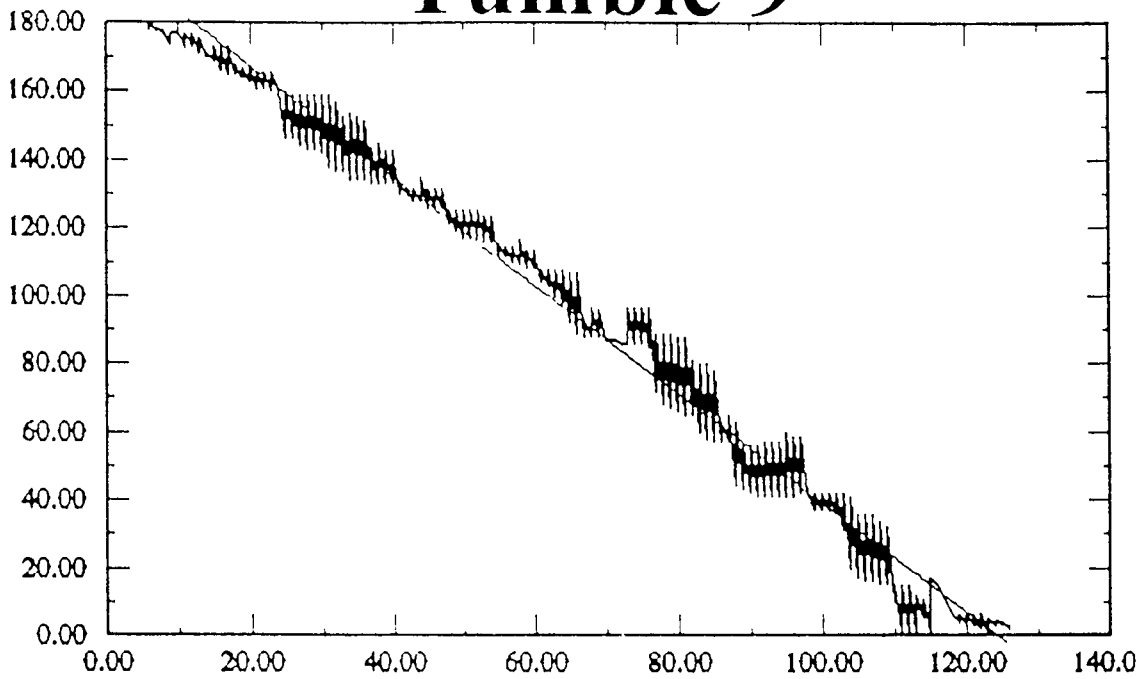

Linear (Y = aX+b) fit of Curve 1 from x = 6.75 to x = 125.5:
a = -1.60532 +/- 0.00930962 b = 199.46 +/- 0.710254 Chi-square=28498.2
Linear correlation coefficient: -0.990616; Probability of correlation: 1

Tumble 10

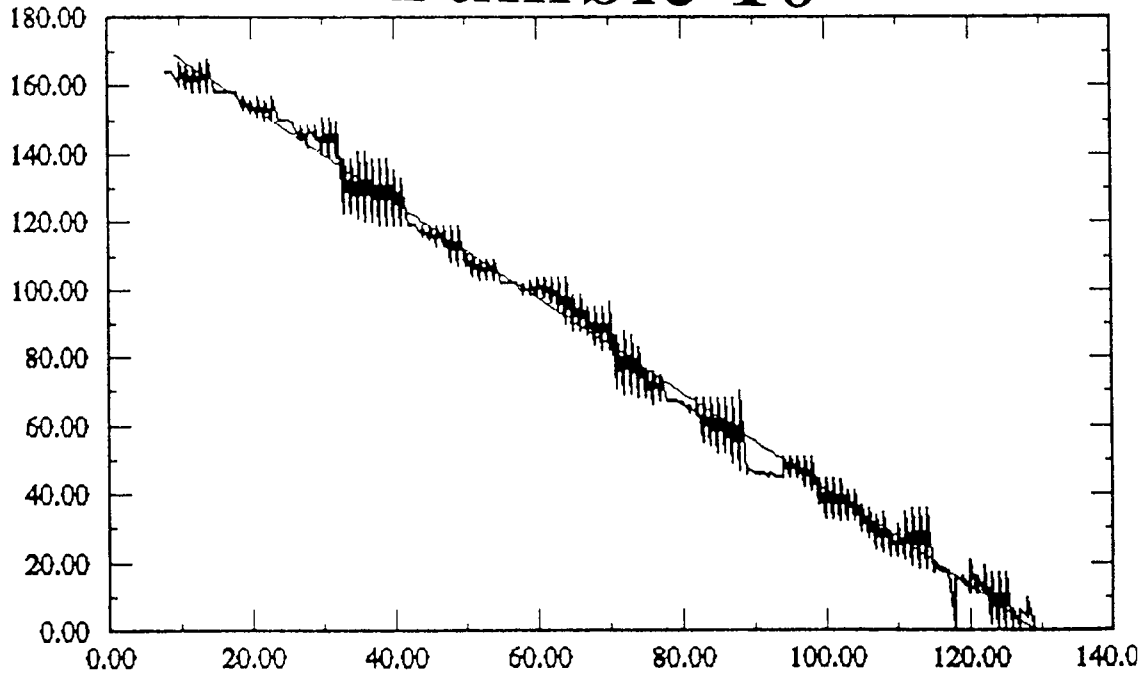

Linear (Y = aX+b) fit of Curve 1 from x = 9.25 to x = 128.5:
a = -1.41097 +/- 0.00724935 b = 182.271 +/- 0.568612 Chi-square=16344.5
Linear correlation coefficient: -0.992986; Probability of correlation: 1

Tumble 11

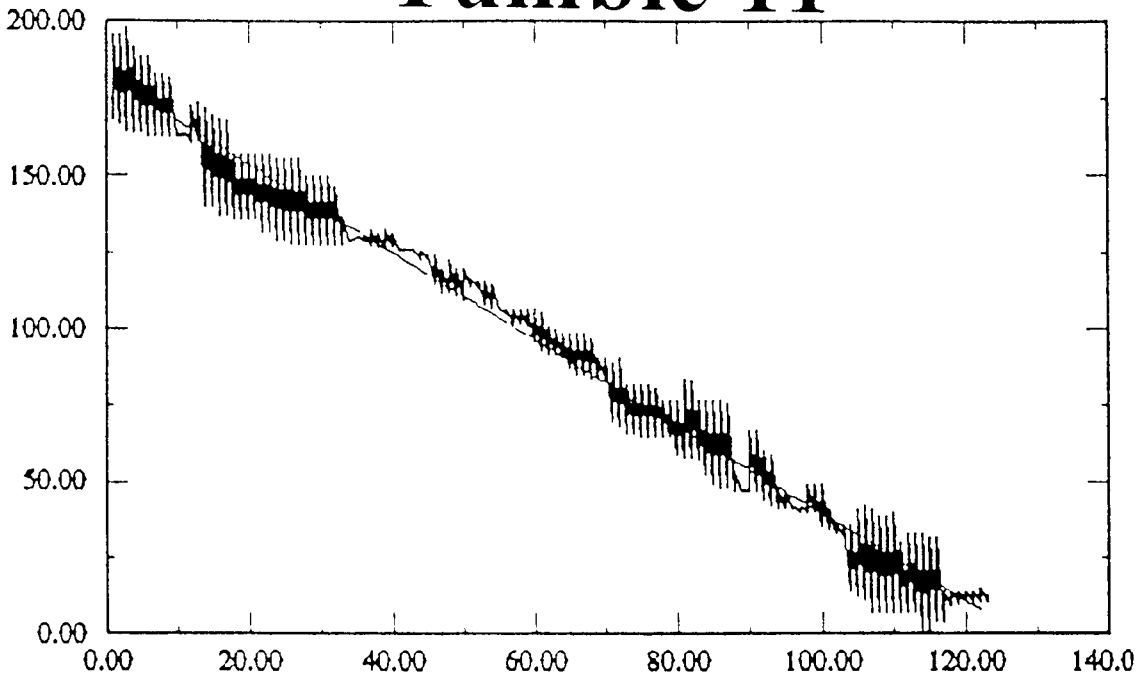

Linear (Y = aX+b) fit of Curve 1 from x = 0.75 to x = 122:
a = -1.4288 +/- 0.00921337 b = 182.18 +/- 0.654444 Chi-square=52711.2
Linear correlation coefficient: -0.986574; Probability of correlation: 1

Tumble 12

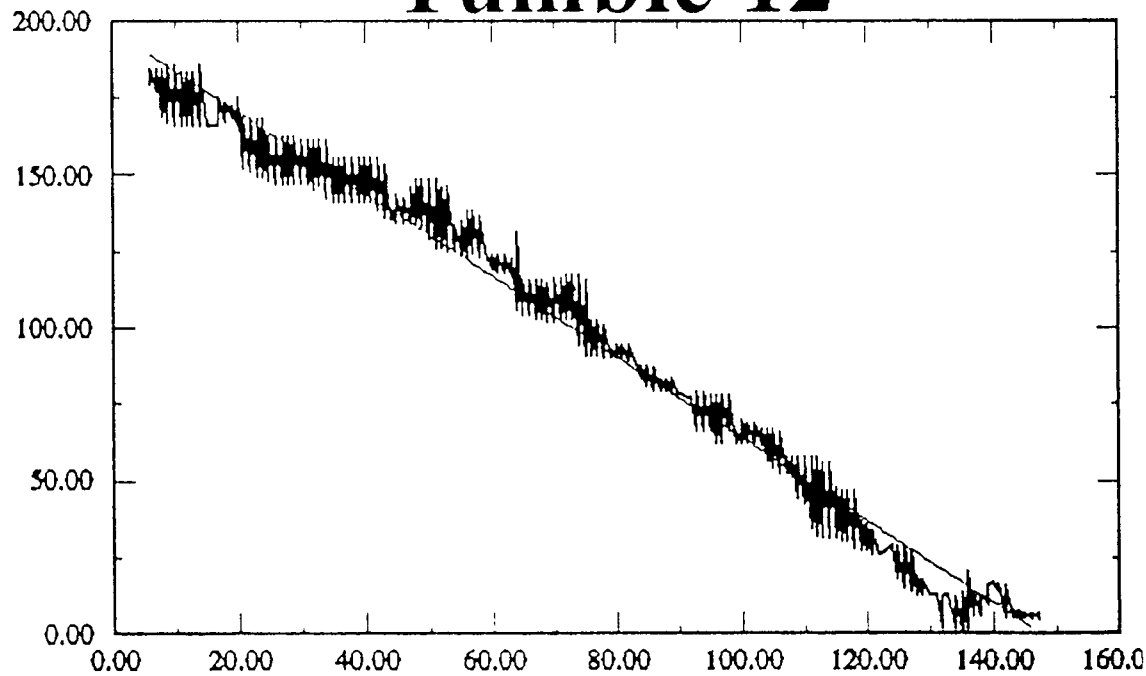

Linear (Y = aX+b) fit of Curve 1 from x = 6 to x = 145.714:
a = -1.33527 +/- 0.00802655 b = 196.995 +/- 0.652433 Chi-square=39649.5
Linear correlation coefficient: -0.988966; Probability of correlation: 1

Tumble 13

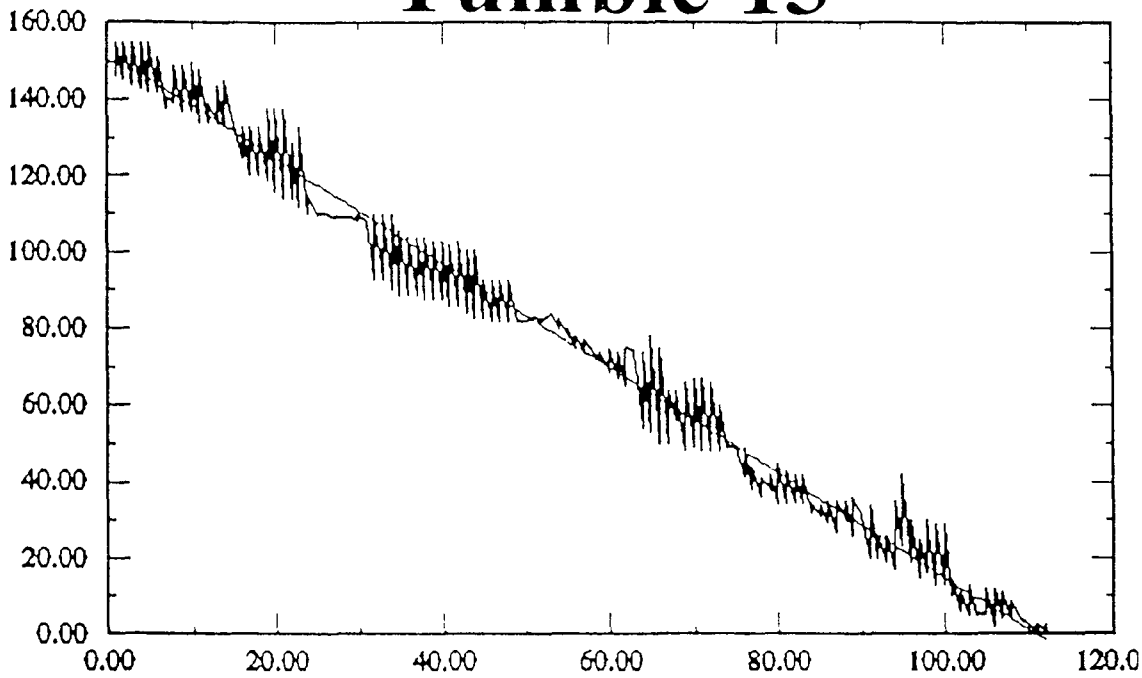

Linear (Y = aX+b) fit of Curve 1 from x = 1.07143 to x = 111.857:
a = -1.37418 +/- 0.0085548 b = 152.149 +/- 0.534137 Chi-square=18894.4
Linear correlation coefficient: -0.990469; Probability of correlation: 1

Tumble 14

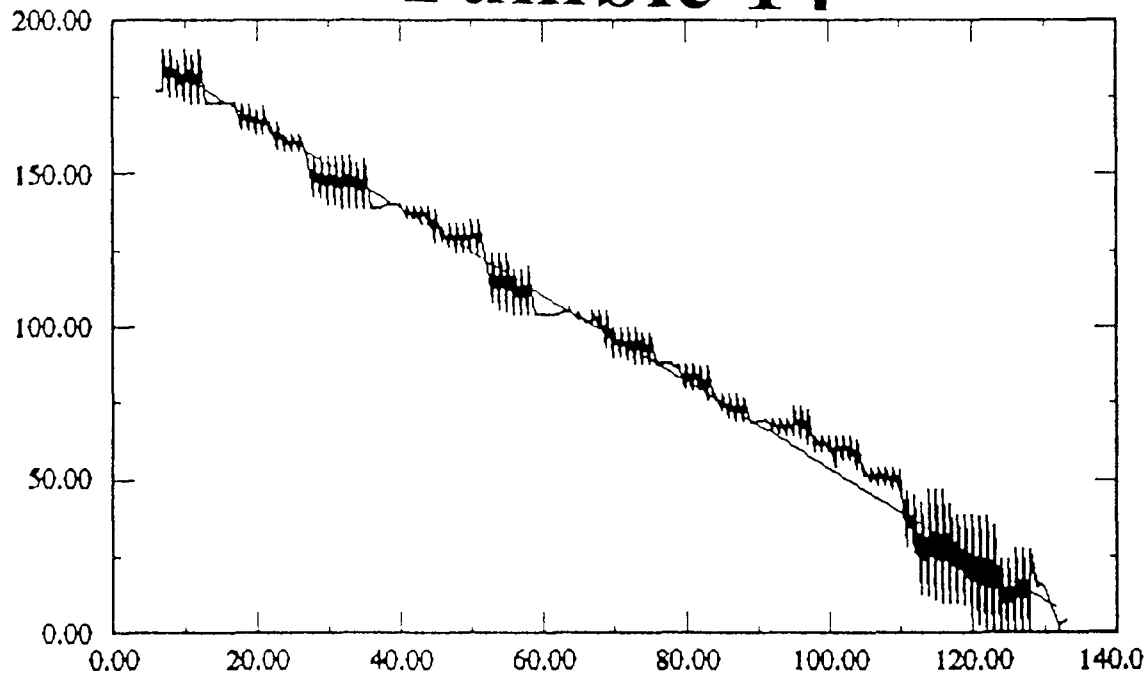

Linear (Y = aX+b) fit of Curve 1 from x = 6.25 to x = 131.5:
a = -1.42239 +/- 0.00849124 b = 195.627 +/- 0.710535 Chi-square=35963.1
Linear correlation coefficient: -0.989823; Probability of correlation: 1

Drain 1

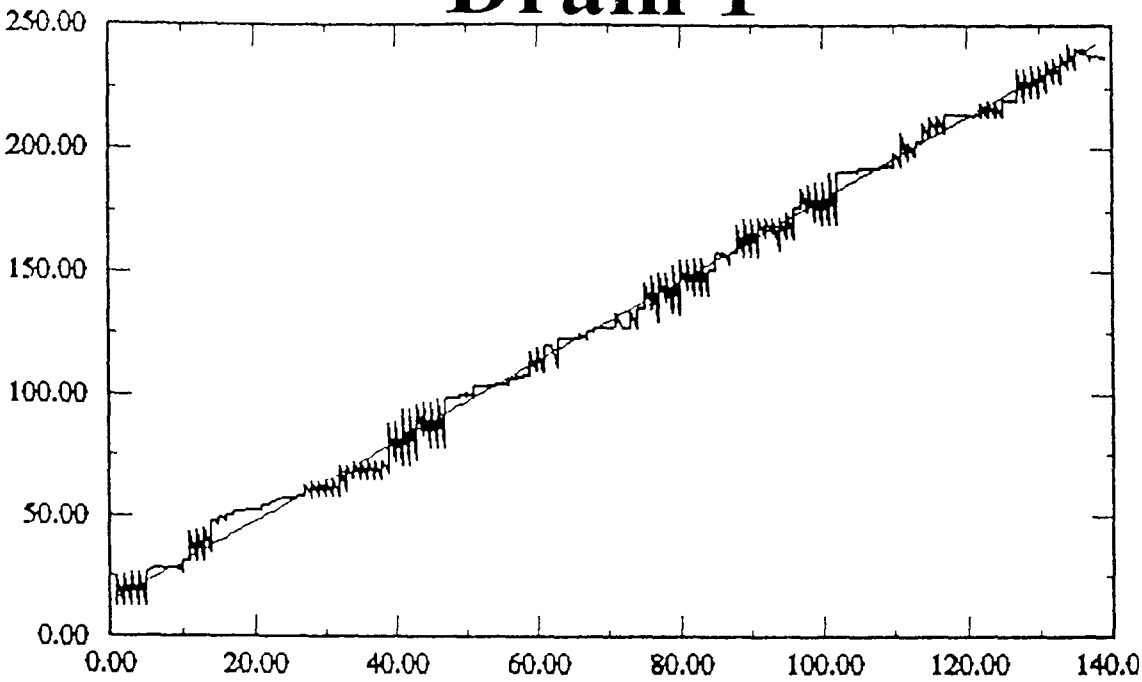

Linear (Y = aX+b) fit of Curve 1 from x = 0 to x = 137.75:
a = 1.65566 +/- 0.00668599 b = 14.6002 +/- 0.522008 Chi-square=15590.7
Linear correlation coefficient: 0.996109; Probability of correlation: 1

Drain 2

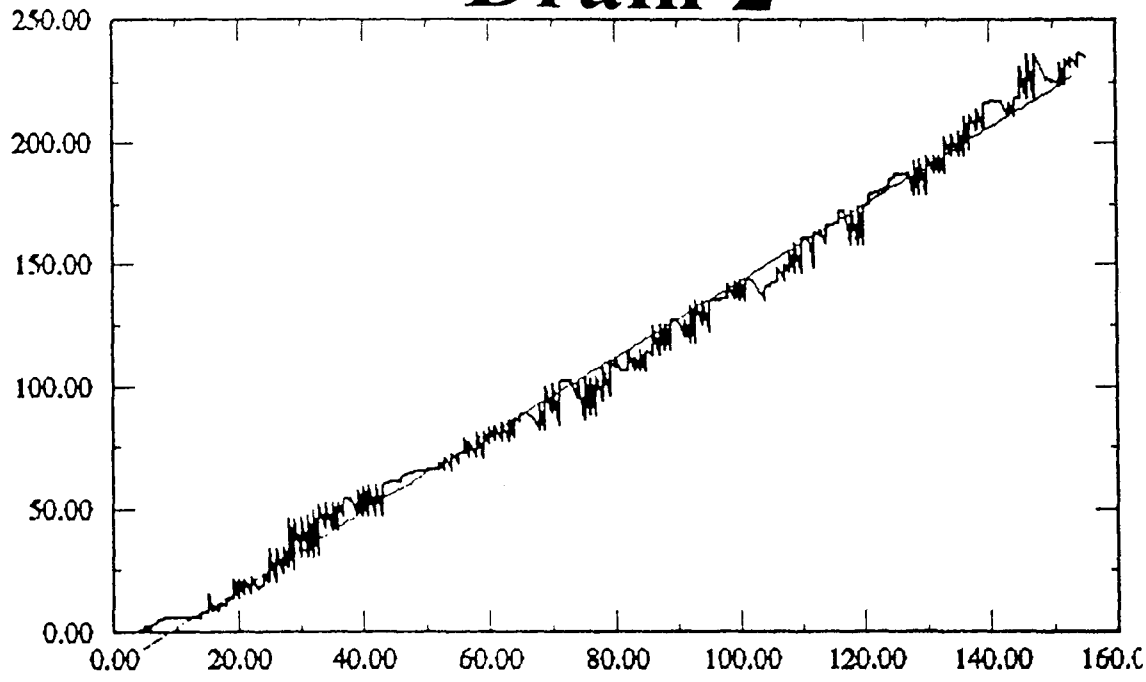

Linear (Y = aX+b) fit of Curve 1 from x = 4.57143 to x = 152.857:
a = 1.57396 +/- 0.00712203 b = -13.8793 +/- 0.654115 Chi-square=24947.3
Linear correlation coefficient: 0.994648; Probability of correlation: 1

Drain 3

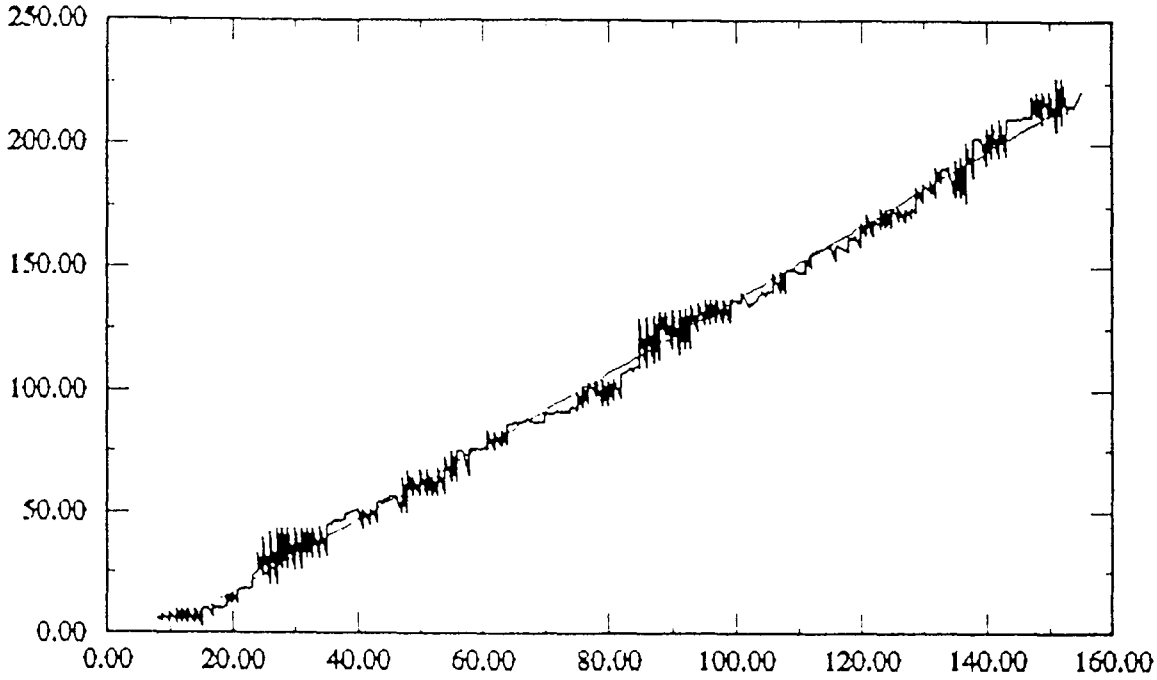

Linear (Y = aX+b) fit of Curve 1 from x = 13.7143 to x = 151.429:
a = 1.50231 +/- 0.00646068 b = -12.9281 +/- 0.593135 Chi-square=17655.8
Linear correlation coefficient: 0.995408; Probability of correlation: 1

Drain 4

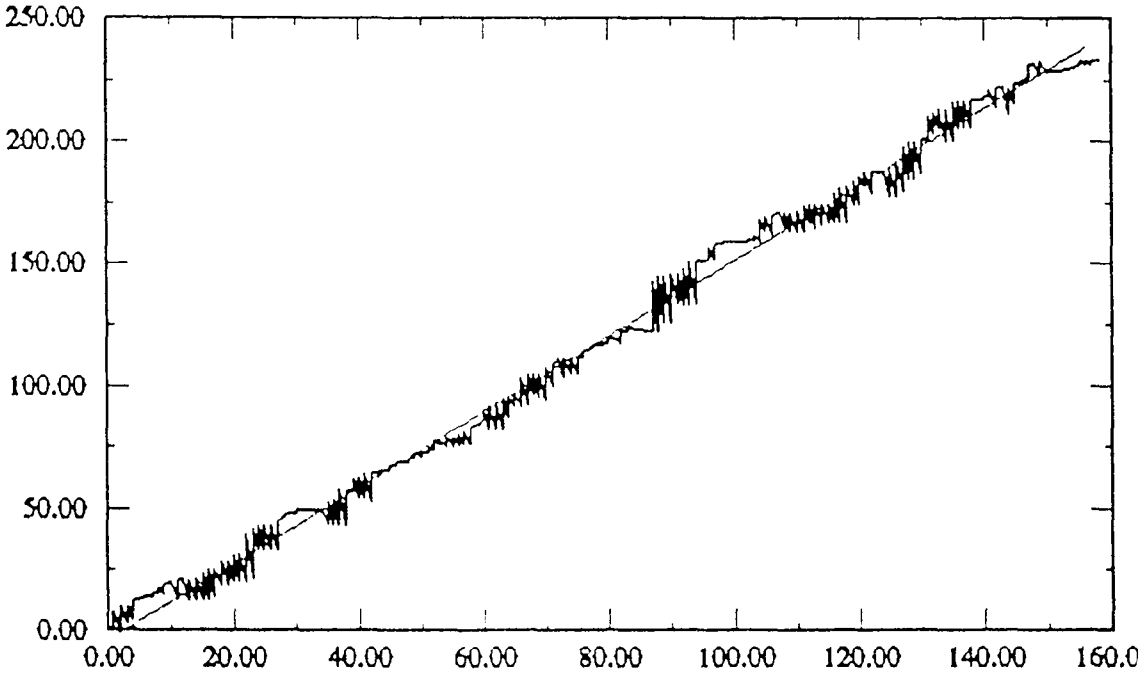

Linear (Y = aX+b) fit of Curve 1 from x = 0 to x = 155.714:
a = 1.55146 +/- 0.00567284 b = -3.4945 +/- 0.502204 Chi-square=17986.2
Linear correlation coefficient: 0.996443; Probability of correlation: 1

Drain 5

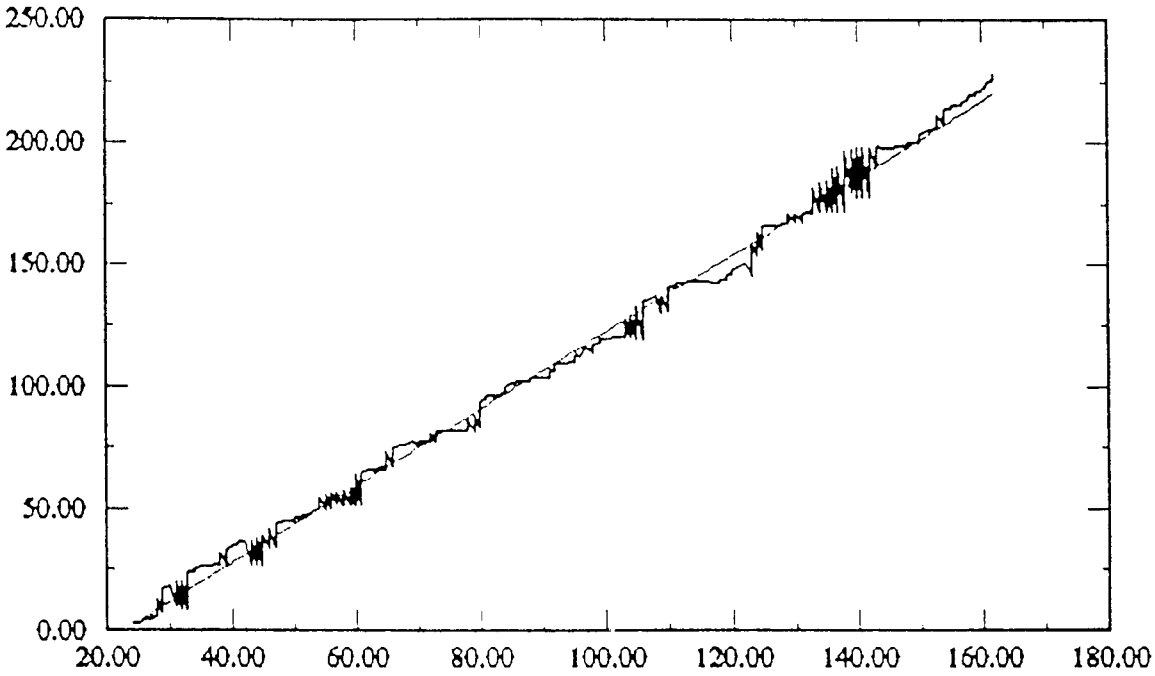

Linear (Y = aX+b) fit of Curve 1 from x = 25.4286 to x = 161.714:
a = 1.57902 +/- 0.00622301 b = -35.2136 +/- 0.639777 Chi-square=9337.2
Linear correlation coefficient: 0.997031; Probability of correlation: 1

Drain 6

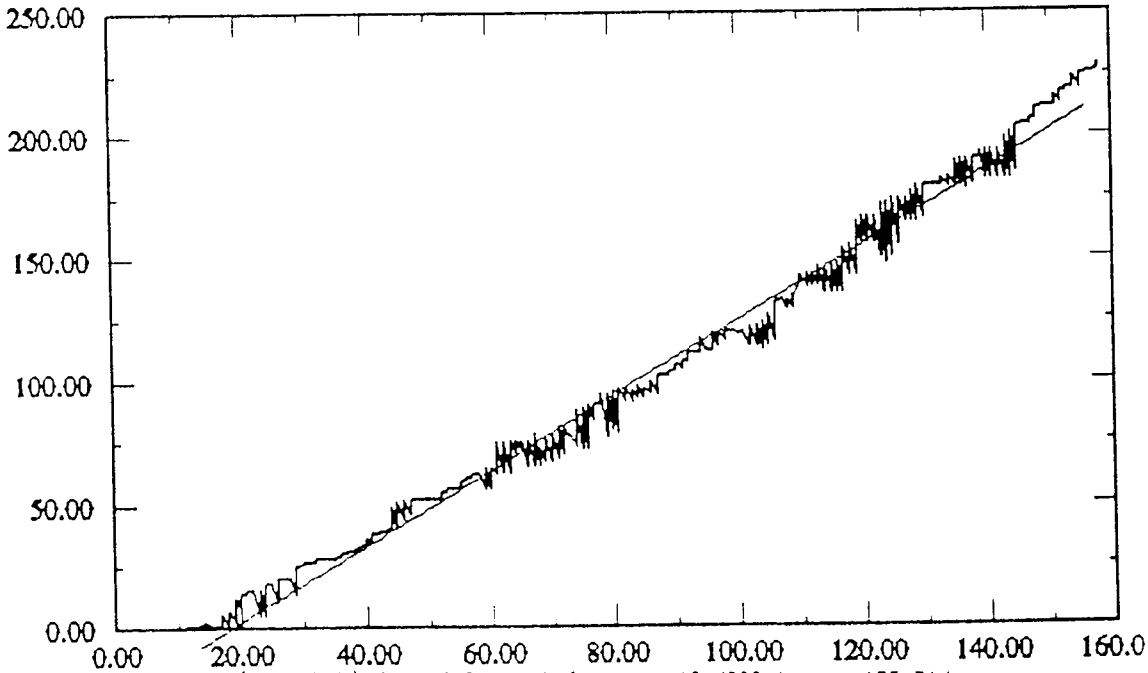

Linear (Y = aX+b) fit of Curve 1 from x = 13.4286 to x = 155.714:
a = 1.52919 +/- 0.00802865 b = -27.8192 +/- 0.793042 Chi-square=24899.8
Linear correlation coefficient: 0.993166; Probability of correlation: 1

Drain 7

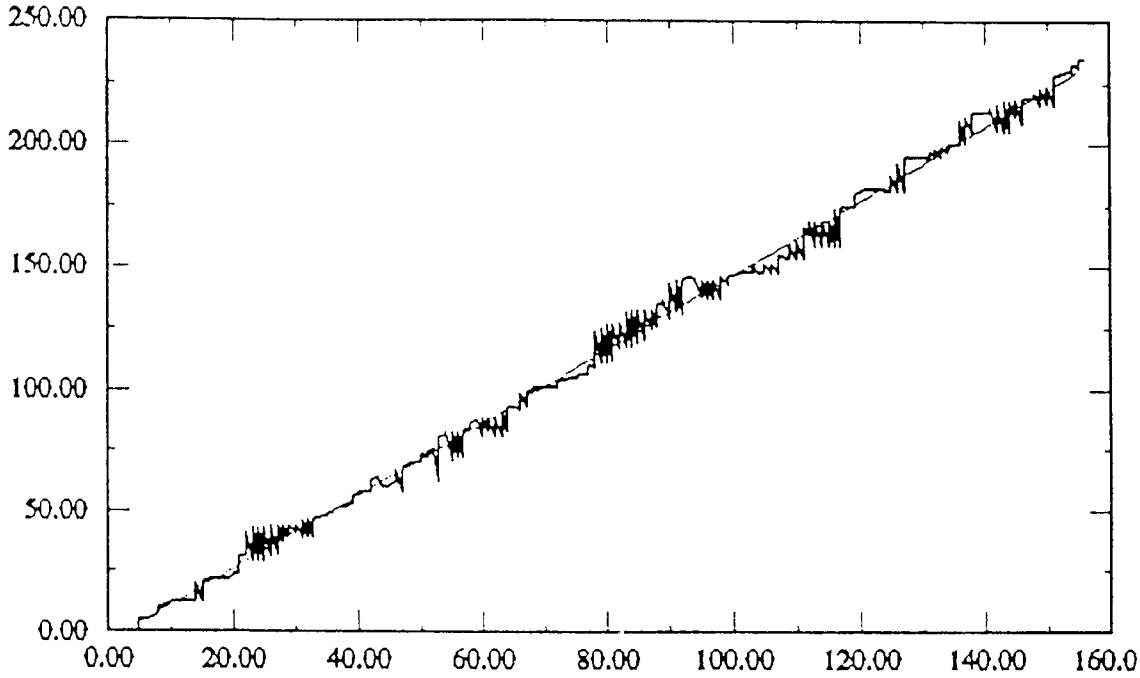

Linear (Y = aX+b) fit of Curve 1 from x = 5.14286 to x = 154.571:
a = 1.51054 +/- 0.0053328 b = -3.76386 +/- 0.488244 Chi-square=10858.8
Linear correlation coefficient: 0.997121; Probability of correlation: 1

Drain 8

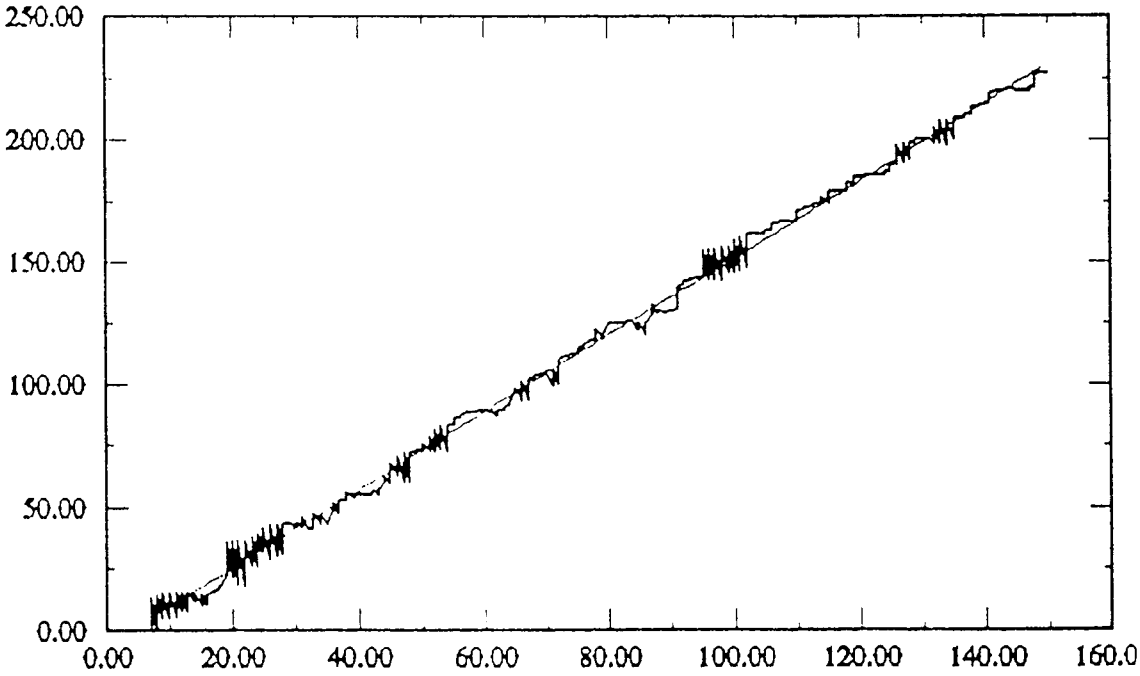

Linear (Y = aX+b) fit of Curve 1 from x = 8 to x = 148.857:
a = 1.57707 +/- 0.00517152 b = -5.7022 +/- 0.440389 Chi-square=7388.96
Linear correlation coefficient: 0.997915; Probability of correlation: 1

Drain 9

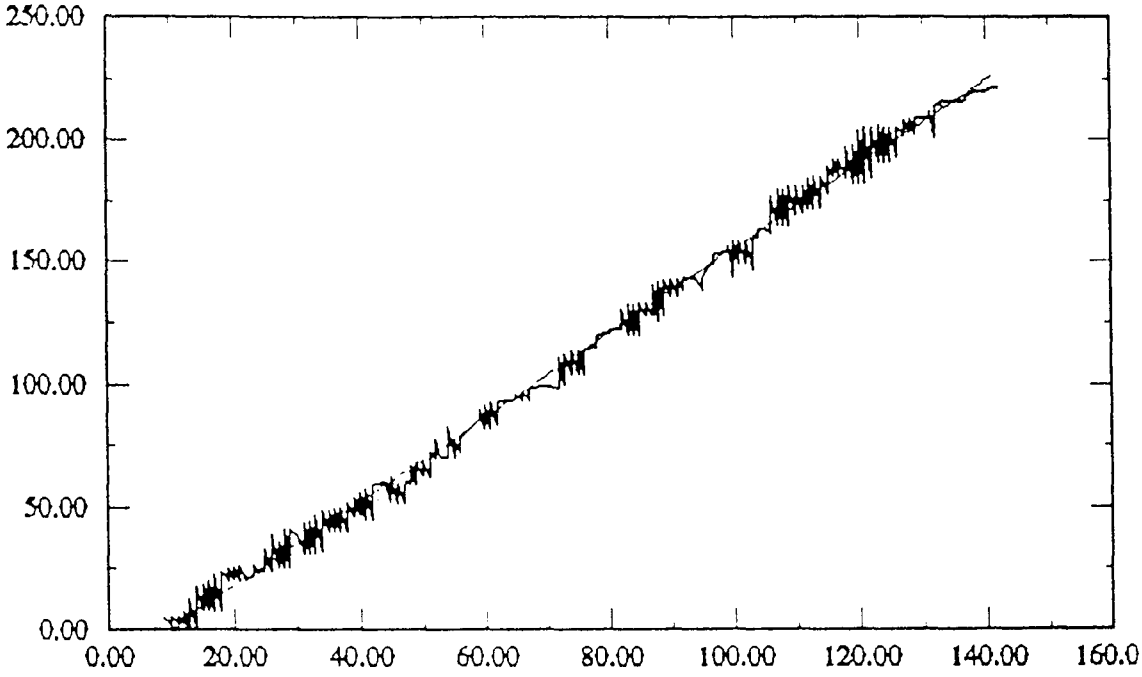

Linear (Y = aX+b) fit of Curve 1 from x = 10.2857 to x = 140.857:
a = 1.7205 +/- 0.00671644 b = -16.2284 +/- 0.569778 Chi-square=14068.7
Linear correlation coefficient: 0.99646; Probability of correlation: 1

Drain 10

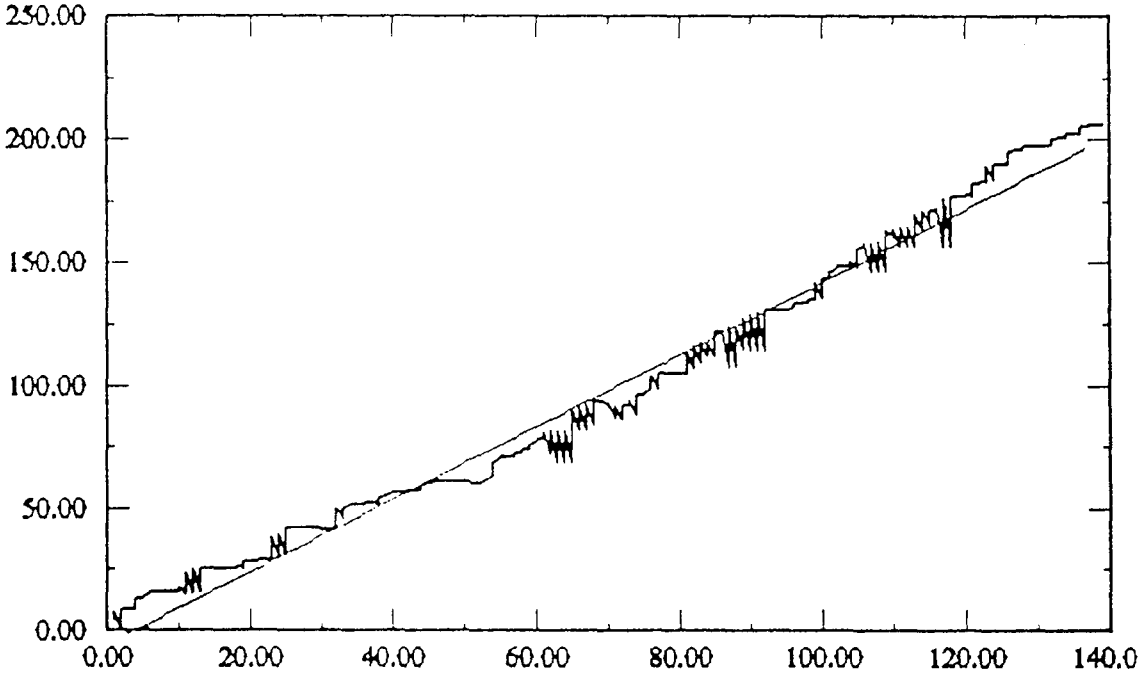

Linear (Y = aX+b) fit of Curve 1 from x = 2.5 to x = 136.5:
a = 1.47747 +/- 0.0112696 b = -5.3265 +/- 0.935978 Chi-square=21214.1
Linear correlation coefficient: 0.990028; Probability of correlation: 1

Drain 11

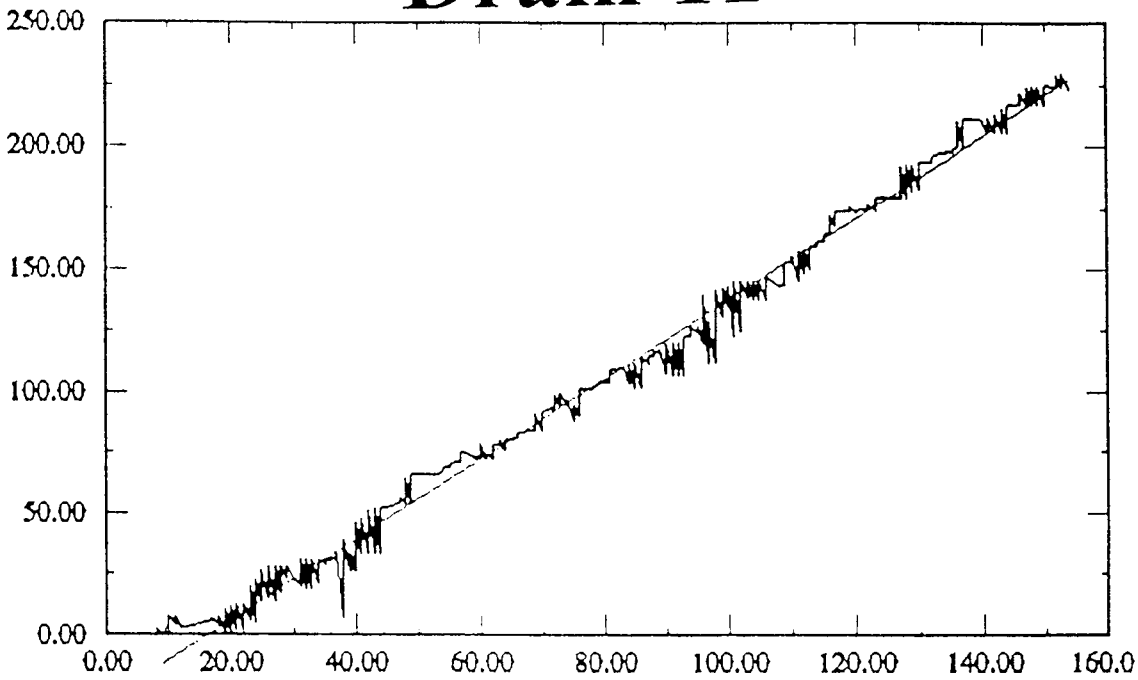

Linear (Y = aX+b) fit of Curve 1 from x = 9.14286 to x = 153.714:
a = 1.64898 +/- 0.00722062 b = -26.3094 +/- 0.672166 Chi-square=17442.8
Linear correlation coefficient: 0.995808; Probability of correlation: 1

Drain 12

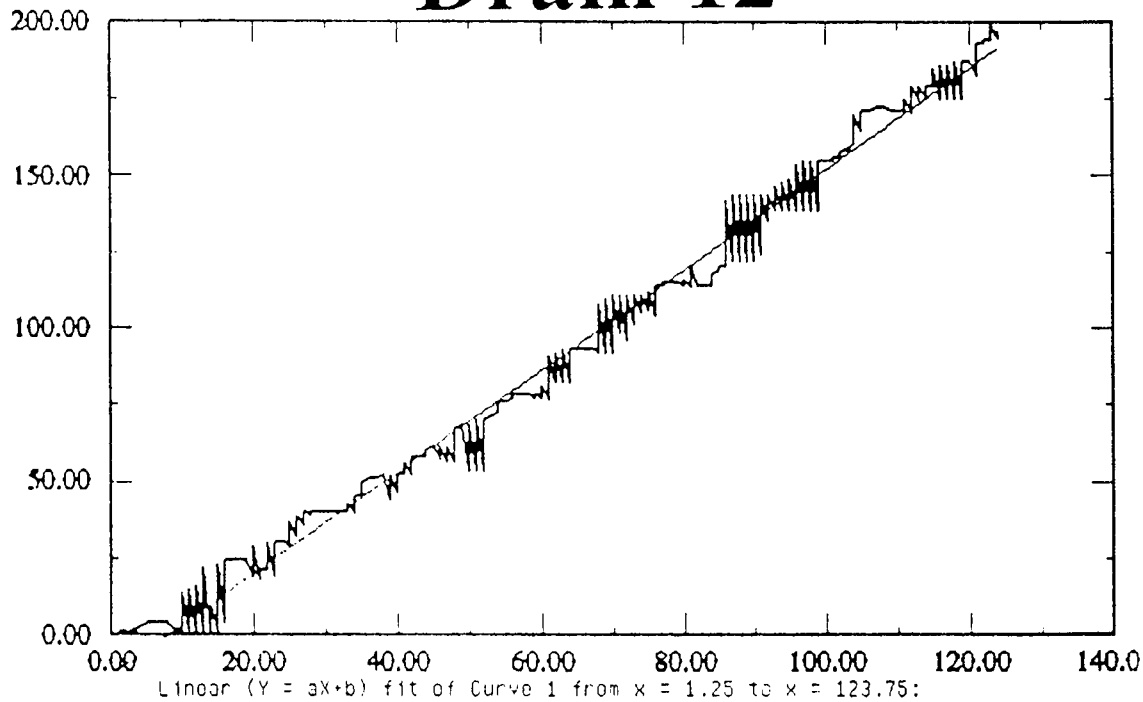

Linear (Y = aX+b) fit of Curve 1 from x = 1.25 to x = 123.75:
a = 1.6526 +/- 0.00913193 b = -12.9713 +/- 0.681696 Chi-square=15477.8
Linear correlation coefficient: 0.9939; Probability of correlation: 1

Drain 13

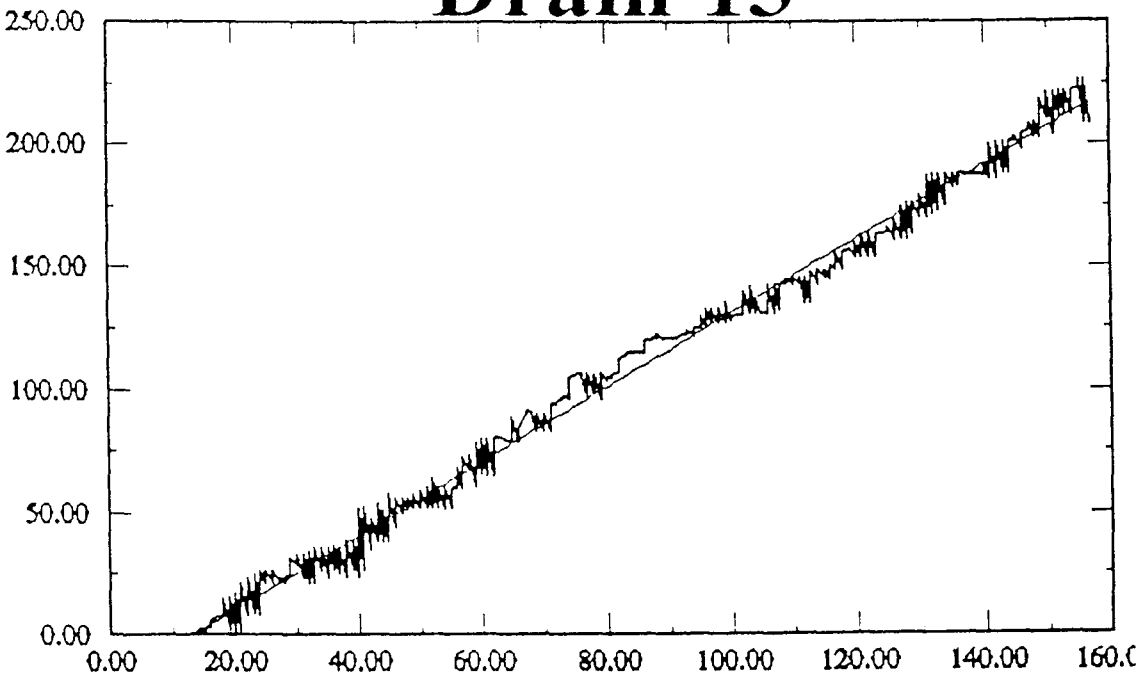

Linear (Y = aX+b) fit of Curve 1 from x = 12.8571 to x = 155.714:
a = 1.51261 +/- 0.00586658 b = -19.7458 +/- 0.543898 Chi-square=21501
Linear correlation coefficient: 0.995681; Probability of correlation: 1

Drain 14

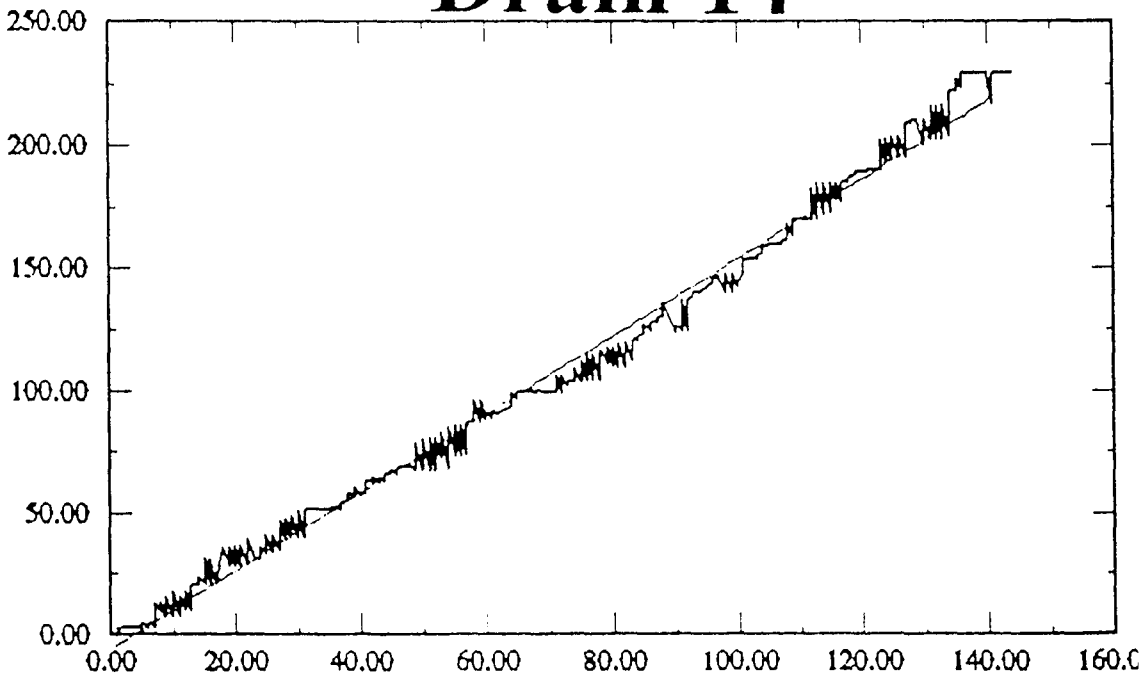

Linear (Y = aX+b) fit of Curve 1 from x = 0.571429 to x = 140.286:
a = 1.59869 +/- 0.00778809 b = -5.56376 +/- 0.640311 Chi-square=19030.6
Linear correlation coefficient: 0.994819; Probability of correlation: 1

Drain 15

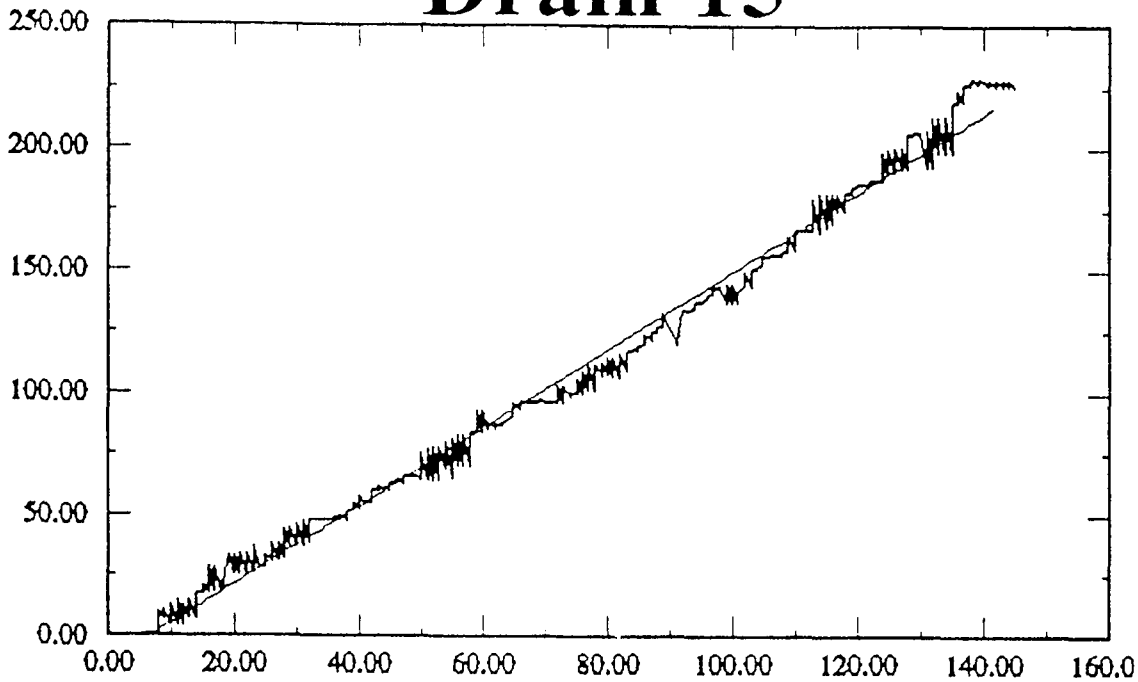

Linear (Y = aX+b) fit of Curve 1 from x = 8 to x = 141.429:
a = 1.60481 +/- 0.00789267 b = -10.4171 +/- 0.672278 Chi-square=18870.9
Linear correlation coefficient: 0.994792; Probability of correlation: 1

Drain 16

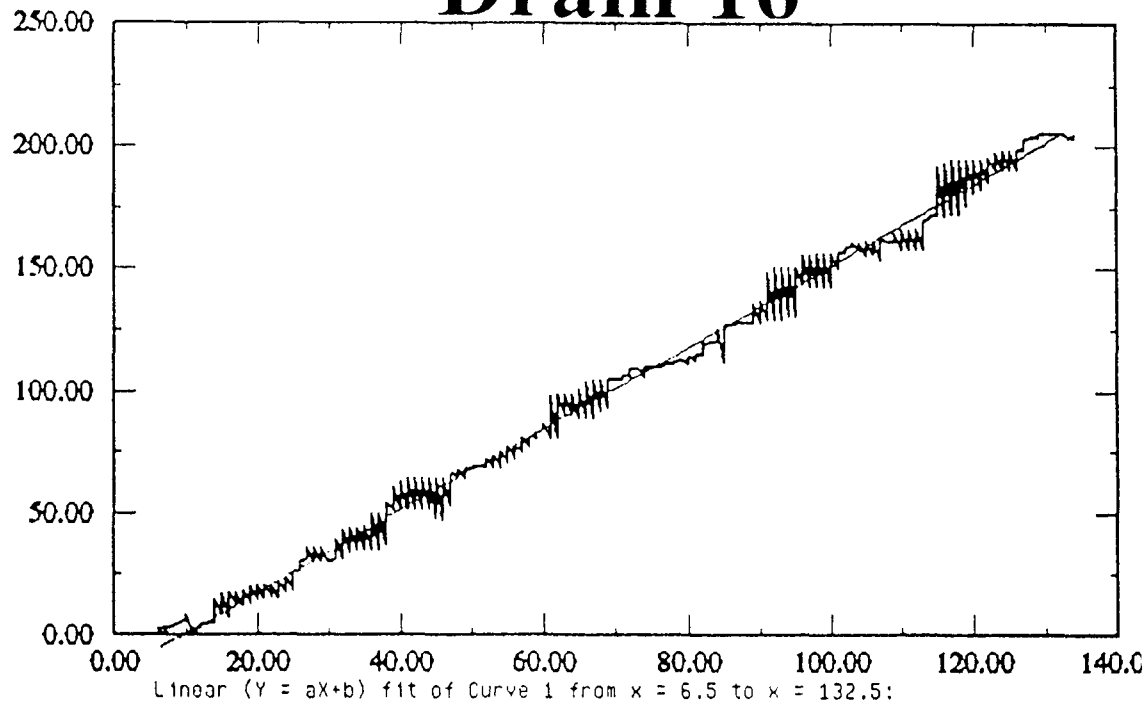

Linear (Y = aX+b) fit of Curve 1 from x = 6.5 to x = 132.5:
a = 1.67255 +/- 0.0075736 b = -15.6307 +/- 0.602773 Chi-square=16216.1
Linear correlation coefficient: 0.995176; Probability of correlation: 1

Drain 17

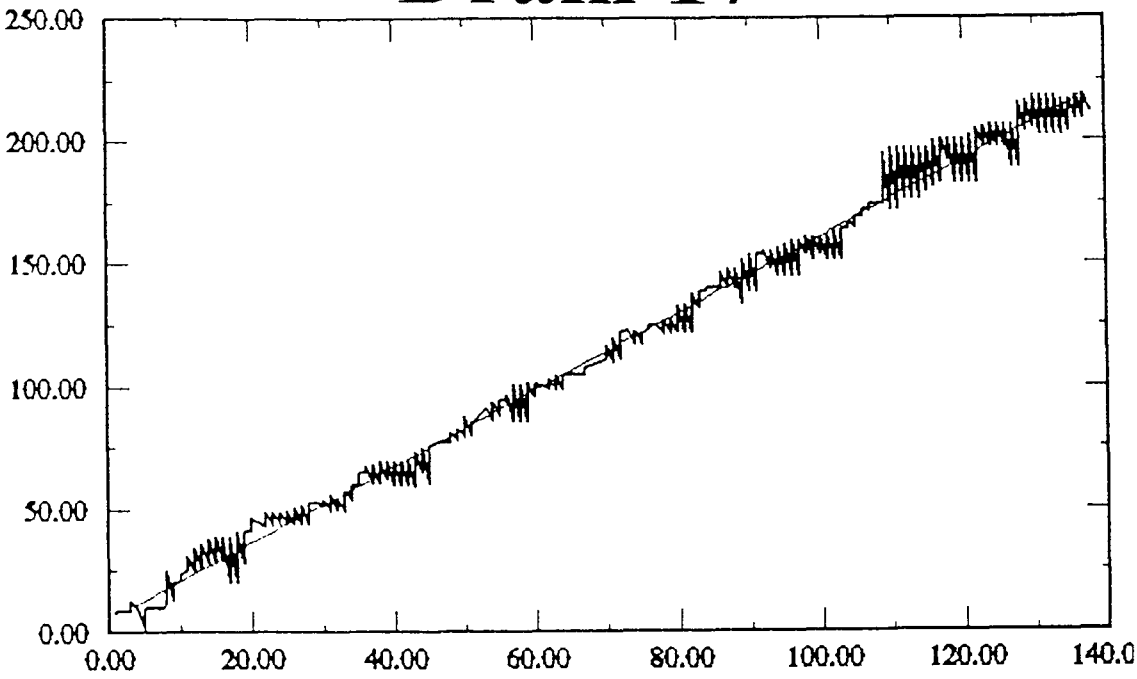

Linear (Y = aX+b) fit of Curve 1 from x = 3.75 to x = 136.25:
a = 1.55891 +/- 0.00711516 b = 5.57849 +/- 0.603122 Chi-square=19440.7
Linear correlation coefficient: 0.994853; Probability of correlation: 1

Drain 18

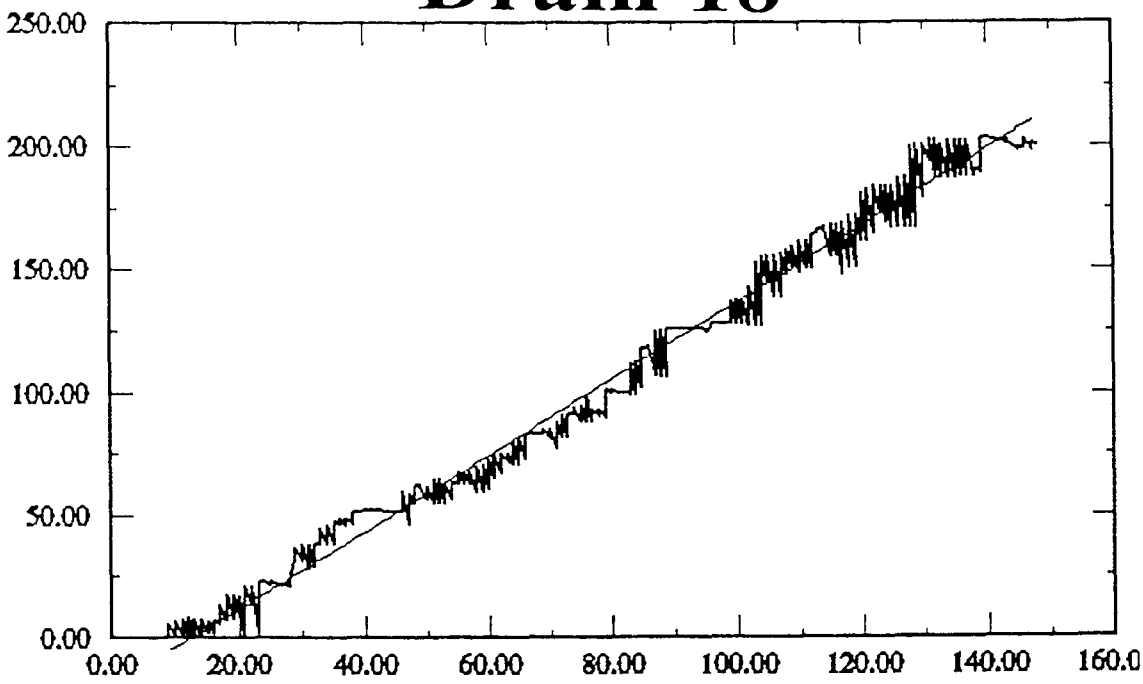

Linear (Y = aX+b) fit of Curve 1 from x = 9.14286 to x = 147.143:
a = 1.55868 +/- 0.00767803 b = -18.9232 +/- 0.714454 Chi-square=29884.7
Linear correlation coefficient: 0.993132; Probability of correlation: 1

Drain 19

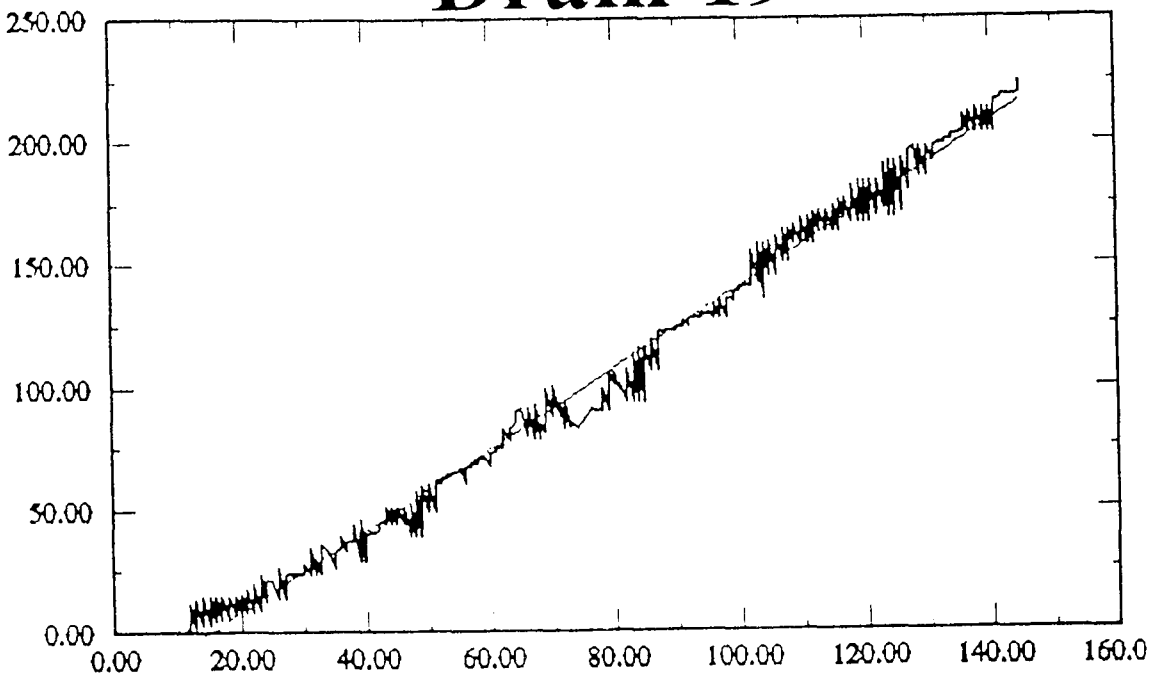

Linear (Y = aX+b) fit of Curve 1 from x = 12 to x = 144.571:
a = 1.66224 +/- 0.00763838 b = -24.6231 +/- 0.678756 Chi-square=22973.2
Linear correlation coefficient: 0.994689; Probability of correlation: 1

Drain 20

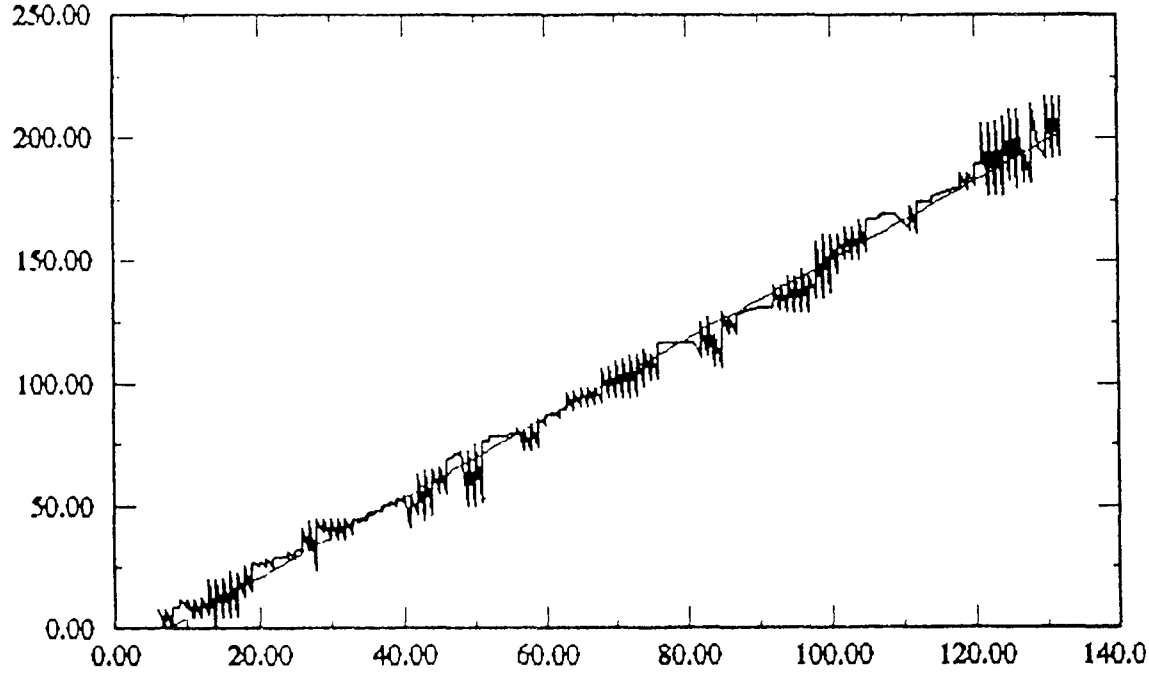

Linear (Y = aX+b) fit of Curve 1 from x = 6.75 to x = 131.5:
a = 1.61784 +/- 0.00924389 b = -11.1212 +/- 0.703649 Chi-square=24765.1
Linear correlation coefficient: 0.992543; Probability of correlation: 1

APPENDIX D

List of Experimental Apparatus

LIST OF EXPERIMENTAL APPARATUS

Vibratory Equipment:

Bruel and Kjaer Power Amplifier Type 2707
Bruel and Kjaer Vibration Exciter Control Type 1050
Bruel and Kjaer General Purpose Head Type 4812
Bruel and Kjaer Exciter Body Type 4801
Breul and Kjaer Accelerometer Type 4332
Bruel and Kjaer Charge Amplifier Type 2635
Bruel and Kjaer Accelerometer Calibrator Type 4291

Humidifying Equipment:

Crest Deluxe Ultrasonic Humidifier Model 16-103
Micronta LCD Twin Display Thermometer and Hygrometer Cat. No. 63-844

Video and Lighting Equipment:

Kodak EktaPro 1000 Monitor Model 08500003-001
Kodak EktaPro 1000 Processor
Kodak EktaPro 1000 Intensified Imager
Kodak EktaPro 1000 Intensified Imager Controller
Elicar V-HQ Macro MC 90mm f/2.5 O62 No. 611091
Mole-Richardson Co. Two-Light Molecool Type 4721

Other Equipment:

10' x 18' Plastic Drop Cloth
6' x 6' Clear Plastic Drop Cloth
1/8" Diameter Acrylic Spheres (Engineering Laboratories, NYC, N.Y.)
2-7/8" Diameter by 8" High Acrylic Cylinder
Three Acrylic Spheres, 3/4", 3/8" and 1/8" Diameter (Grewe Plastics, Newark, N.J.)

REFERENCES

1. A. M. Abouzeid and D. W. Fuerstenau, "Effect of Humidity on Mixing of Particulate Solids", *Ind. Eng. Chem. Process Des. Develop.* **11** (2) (1972) 296-301.

2. K. Ahmad and I. J. Smalley, "Observation of Particle Segregation in Vibrated Granular Systems", *Powder Tech.* **8**, (1973) 69-75.

3. D. Boland and D. Geldart, "Electrostatic Charging in Gas Fluidised Beds", *Powder Tech.* **5** (1971/1972) 289-297.

4. R. L. Brown, "The Fundamental Principles of Segregation", *J. Inst. Fuel* **13** (1939) 15-19.

5. R. L. Brown and J. C. Richards, Principles of Powder Mechanics, Vol. 10, New York, Pergamon Press, (1966).

6. R. N. Dave, "Robust Fuzzy Clustering Algorithms", *Second IEEE International Conference on Fuzzy Systems* **2**, (1993) 1281-1286.

7. J. Duran, J. Rajchenbach and E. Clement, "Arching Effect Model for Particle Size Segregation", *Physical Review Letters* **70** (16), (1993) 2431-2434.

8. M. D. Faiman and E. G. Rippie, "Segregation Kinetics of Particulate Solids Systems III", *J. of Pharm. Sci.* **54** (5) (1965) 719-722.

9. W. A. Gray, The Packing of Solid Particles, Chapman and Hall Ltd., London (1968).

10. P. K. Haff and B. T. Werner, "Computer Simulation of the Mechanical Sorting of Grains", *Powder Tech.* **46**, (1986) 239-245.

11. H. M. Jaeger, C. Liu and S. R. Nagel, "Relaxation at the Angle of Repose", *Physical Review* Letters **62**, (1989) 40-43.

12. R. Jullien, P. Meakin and A. Pavlovitch, "Three Dimensional Model for Particle-Size Segregation by Shaking", *Physical Review Letters* **69**, (1992) 640-643.

13. R. Jullien and P. Meakin, "A mechanism for particle size segregation in three dimensions", *Nature* **344** (1990) 425-427.

14. J. B. Knight, H. M. Jaeger and S. R. Nagel, "Vibration-Induced Size Separation in Granular Media: the Convection Connection", Preprint, *Phys. Rev. Lett.* (1993).

15. P. M. Lacey, "Development in the Theory of Particle Mixing", *J. App. Chem.* **4**, (1954) 257-269.

16. P. Meakin, "A Simple Two-Dimensional Model For Particle Segregation", *Physica A* **163** (1990) 733-746.

References Continued

17. J. L. Olsen and E. G. Rippie, "Segregation Kinetics of Particulate Solids Systems I", *J. of Pharm. Sci.* **53** (2) (1964) 147-150.

18. D.S. Parsons, "Particle Segregation in fine Powders by Tapping as Simulation of Jostling During transportation", *Powder Tech.* **13**, (1977) 269-277.

19. E. G. Rippie, J. L. Olsen and M. D. Faiman, "Segregation Kinetics of Particulate Solids Systems II", *J. of Pharm. Sci.* **53** (11) (1964) 11360-1363.

20. E. G. Rippie, M. D. Faiman and M. K. Pramoda, "Segregation Kinetics of Particulate Solids Systems IV", *J. of Pharm. Sci.* **56** (11) (1967) 1*47-150.*

21. A. Rosato, F. Prinz, K. J. Strandburg and R. Swedson, "Monte Carlo Simulation of Particulate Matter Segregation", *Powder Tech.* **49**, (1986) 59-69.

22. A. Rosato, K. J. Strandburg, F. Prinz, and R. Swedson, "Why the Brazil Nuts Are on Top: Size Segregation of Particulate Matter by Shaking", *Phys. Rev. Let.* **58** (10) (1987) 1038-1040.

23. A. D. Rosato, Y. Lan and D. T. Wang, "Vibratory particle size sorting in multi- component systems", *Powder Tech.* **66**, (1991) 149-160.

24. A. M. Scott and J. Bridgwater, "Interparticle percolation: a Fundamental Solids Mixing Mechanisms", *Ind. Eng. Chem. Fundam.* **14** (1), (1975) 22-26.

25. R. L. Shreve, "Sherman Landslide", *Science* **154**, (1966) 1639-1643.

26. B. Thomas, M. O. Mason, Y. A. Liu and A. M. Squires, "Identifying States in Shallow Vibrated Beds", *Powder Tech.* **57**, (1989) 267-280.

27. W. M. Visscher and M. Bolsterli, "Random Packing of Equal and Unequal Spheres in Two and Three Dimensions", *Nature* **239**, (1972) 504-507.

28. S. S. Weidenbaum, "Mixing of solids", *Adv. Chem. Eng.* **2**, (1958) 209.

29. J. C. Williams, "The Segregation of Powders and Granular Materials", *Fuel Soc.* **14** (1963) 29-34.

30. J. C. Williams, "The Segregation of Particulate Materials. A Review", *Powder Tech.* **15** (1976), 245-251.

32. J. C. Williams and R. Richardson, "The Continuous Mixing of Segregating Particles", *Powder Tech.* **33** (1982) 5-16.